

**Pharmacokinetics and Enterohepatic Recycling of CZ48, a  
Lactone-Stabilized Camptothecin: Effects of Nanosuspension  
Formulation**

A Dissertation Presented to the  
Faculty of the Department of Pharmacological and Pharmaceutical Sciences  
College of Pharmacy, University of Houston

In Partial Fulfillment of  
the Requirements for the Degree of  
Doctor of Philosophy

By

Yu Jin Kim

August 2017

**Pharmacokinetics and Enterohepatic Recycling of CZ48, a Lactone-Stabilized Camptothecin: Effects of Nanosuspension Formulation**

By

---

Yu Jin Kim

Approved By:

---

Diana S-L Chow, Ph.D.

---

Romi Ghose, Ph.D.

---

Ming Hu, Ph.D.

---

Erik Rytting, Ph.D.

---

Sai-Ching J Yeung, Ph.D., M.D.

---

F. Lamar Pritchard, Ph.D.

Dean, College of Pharmacy

## **Acknowledgements**

First and foremost, I would like to express my deepest and sincere gratitude to my advisor, Dr. Diana S-L Chow, for her continuous support, patience, and encouragement throughout my Ph.D. years. She motivated, guided, and inspired me to continuously move forward whenever I had problems with experimental design and data analysis. Her insight and wisdom made me grow professionally as well as personally. My time in Dr. Chow's lab was precious and memorable, and I was lucky to have her as my dissertation advisor. She will forever be my mentor in my career and life.

My deepest appreciation also goes to my dissertation committee: Drs. Romi Ghose, Ming Hu, Erik Rytting, and Sai-Ching J Yeung. I would never have been able to complete my dissertation without their advices, valuable inputs, and encouragements.

I would like to thank Drs. Xiaohui Li and Dong Dong for their research and efforts on previous CZ48 projects in Dr. Chow's lab.

I express my sincere appreciation to my labmates and colleagues: Dr. Lei Wu, Dr. Yang Wang, Dr. Stanley Hsiao, Dr. Daping Zhang, Mahua Sarkar, Nashid Farhan, Asma El-Zailik, Lorita Agu, Ashley Nguyen, Dr. Shufan Ge, Yu He, Guncha Taneja, Jian Zhou, Yifan Tu, and Katherine Shatzer, for their helps and advices. I would also like to thank all faculty, staff, and graduate students in the Department of Pharmacological and Pharmaceutical Sciences for their helps during my Ph.D. years.

Lastly, special thanks to my family for their unconditional support, encouragement, and love. They always believe my strength and potential, and their support was my precious energy to make this accomplishment.

## **Abstract**

CZ48, a lactone-stabilized camptothecin (CPT), is a topoisomerase 1 enzyme inhibitor. Its strong potential as an anticancer agent has been demonstrated against various types of human tumors with a lack of toxicity in human tumor-xenografted mice. In addition, previous preclinical pharmacokinetic (PK) studies implied potential enterohepatic recycling of CZ48 and CPT responsible for their sustained concentrations in plasma for 6 hr after an oral dose of CZ48 in co-solvent formulation. The prolonged exposure of a drug by enterohepatic recycling may significantly alter drug PK and pharmacological effects, and cause unpredictable toxicity by multiple dosing. Hence, it is critical to characterize the hepatic metabolism, biliary excretion and enterohepatic recycling using preclinical models in early stages of drug discovery and development. Moreover, nanosuspension (NS) of CZ48 has been formulated in our laboratory to overcome its poor water solubility. Thus, the overall objective of this project was to evaluate the impacts of NS on biodistributions of CZ48 and CPT in human tumor-xenografted mice, and biliary excretions and enterohepatic recycling in rats. Different biodistribution patterns of CZ48 were observed between co-solvent (CoS) and NS groups in tumor-xenografted mice; however, the pattern of CPT was similar between CoS and NS groups. The highest exposure of CPT was in the liver and the lowest was in the brain. The extent of CPT exposure in tumor was comparable with those in

kidney, spleen, and lung. Half-lives of CZ48 and CPT were 1.5 – 3.6 times increased in all tested organs and tumor. The prolonged exposure of CPT may offer a merit of NS for its antitumor activity as a topoisomerase 1 inhibitor of cell-cycle S-phase specific activity.

In enterohepatic recycling study, biliary secretions of CZ48 and CPT were confirmed mainly by their parent forms not conjugates. After an intravenous (IV) dose of CZ48-CoS, the percentages of dose recovered in bile were 0.19 % and 3.05 % for CZ48 and CPT, respectively, indicating more favorable biliary secretion of CPT than CZ48. NS did not significantly increase biliary excretions of CZ48 and CPT, with comparable  $AUC_{0-12h}$  ratios of CZ48 (or CPT) in bile to plasma (B/P) after an oral dose between CZ48-NS and CZ48-CoS. Enterohepatic recycling of CZ48 and CPT was minor, since their plasma concentration-time profiles and biliary secretions exhibited similar trends with or without interrupting the recycling. Our PK model adequately described plasma concentrations of CZ48 and CPT and biliary excretion of CPT when adopting compartments for enterohepatic recycling. In conclusion, this is the first report evaluating biliary excretions of CZ48 and CPT, and characterizing their enterohepatic recycling by employing *in vitro*, *in vivo*, and PK modeling approaches. Our findings on the metabolisms, biodistributions, biliary excretions, and enterohepatic recycling of CZ48 and CPT are significant, and has

enabled us to rationalize the clinical PK of CZ48 and CPT in the currently ongoing phase 1 clinical trials.

## Table of Contents

Acknowledgements.....	iii
Abstract.....	v
List of Tables.....	xiii
List of Figures.....	xv
List of Abbreviations.....	xviii
Chapter 1. Introduction and Literature Review.....	1
1.1 Introduction.....	1
1.2 Needs of New Camptothecin (CPT) Analogues.....	3
1.2.1 Limitations of CPT.....	3
1.2.2 Limitations of Topotecan and Irinotecan.....	6
1.3. CZ48 as an Anticancer Agent.....	9
1.3.1 Mechanism of Action of CZ48.....	9
1.3.2 Advantages of CZ48 over CPT.....	9
1.3.3 Needs of Formulations for CZ48.....	10
1.4 Nanoparticle Drug Delivery System for CPT.....	12
1.5 Enterohepatic Recycling.....	13
1.5.1 Components in Enterohepatic Recycling.....	17
1.5.1.1 Absorption of a Drug into the Portal Vein.....	17
1.5.1.2. Intestinal and Hepatic Metabolisms.....	17
1.5.1.3 Biliary Excretion.....	19
1.5.2 Current Experimental Approaches to Characterize Enterohepatic Recycling.....	23
1.5.2.1 Chemical Interruption of Enterohepatic Recycling.....	23
1.5.2.2 A Linked-Rat Model.....	24
1.5.2.3 Bile Duct-Intact vs. Bile Duct-Cannulated Rats... ..	27
Summary.....	28

Chapter 2. Hypotheses and Specific Aims.....	29
2.1 Central Hypothesis.....	29
2.2 Specific Aims.....	30
2.1.1 Aim 1.....	30
2.1.2. Aim 2.....	30
2.1.3. Aim 3.....	30
Chapter 3. Materials and Methods.....	32
3.1 Materials.....	32
3.1.1 Chemicals and Materials.....	32
3.1.2 Equipment and Apparatus.....	35
3.1.3 Surgical Instruments and Supplies.....	38
3.1.4 Animals.....	40
3.2. Methods.....	42
3.2.1 Preparation of Co-Solvent (CoS) Formulation .....	42
3.2.2 Preparation and Characterization of Nanosuspension Formulation.....	42
3.2.3 Organ Biodistribution Study Using Human Tumor-Xenografted Mice.....	43
3.2.3.1 Animal Study Protocol for Biodistribution Study.....	43
3.2.3.2 HPLC Assay for the Simultaneous Quantifications of CZ48 and CPT in Mouse Organs.....	44
3.2.3.2.1 Preparations of Standard Stock and Working Solutions of CZ48 and CPT.....	45
3.2.3.2.2 Biological Sample Preparation for HPLC Analysis.....	45
3.2.3.2.3 Analytical Conditions for HPLC Analysis.....	46
3.2.3.3 Pharmacokinetic and Statistical Analyses.....	46
3.2.4 <i>In Vitro</i> Phase 1 Metabolism of CPT.....	48

3.2.5 <i>In Vitro</i> Phase 2 Metabolism of CPT .....	49
3.2.6. UPLC-MS/MS Assay for the Simultaneous Quantifications of CZ48 and CPT in Rat Plasma and Bile.....	50
3.2.6.1 Preparations of Stock and Working Solutions of CZ48 and CPT.....	50
3.2.6.2 Biological Sample Preparations for a UPLC-MS/MS Analysis.....	50
3.2.6.3 Analytical Conditions for UPLC-MS/MS Analysis.....	51
3.2.6.4 Method Validation for UPLC-MS/MS Assay.....	59
3.2.6.4.1 Linearity and Sensitivity (Lower Limit of Quantification, LLOQ).....	59
3.2.6.4.2 Intra- and Inter-Day Accuracy and Precision.....	60
3.2.6.4.3 Extraction Recovery and Matrix Effect.....	60
3.2.6.4.4 Stability Tests.....	61
3.2.7 Biliary Excretions of CZ48 and CPT After an Intravenous Dose of CZ48-CoS.....	62
3.2.7.1 Surgical Procedure for Bile Duct-Cannulation.....	62
3.2.7.2 Animal Study Protocol.....	63
3.2.7.3 Pharmacokinetic Analysis.....	63
3.2.8 Biliary Excretions and Enterohepatic Recycling of CZ48 and CPT after an Oral Dose of CZ48.....	64
3.2.8.1 Animal Study Protocol for the Evaluation of Biliary Excretion.....	64
3.2.8.2 Animal Study Protocol for the Characterization of Enterohepatic Recycling.....	65
3.2.8.3 Pharmacokinetic (PK) and Statistical Analyses.....	66
3.2.9 The Population Pharmacokinetic (PK) Modeling for the Biliary Excretions of CZ48 and CPT.....	70
Chapter 4. Results.....	72
4.1 Biodistributions of CZ48 and CPT.....	72

4.1.1 Biodistributions of CZ48 from Co-S or NS in Tumor-Xenografted Mice.....	72
4.1.2 Biodistributions of CPT from Co-S or NS in Tumor-Xenografted Mice.....	78
4.1.3 Comparison of Biodistribution Patterns of CZ48 and CPT Between Healthy and Tumor-Xenografted Mice.....	82
4.2 Method Development and Validation Using UPLC- MS/MS.....	87
4.2.1 Linearity and Sensitivity.....	87
4.2.2 Intra- and inter-day Accuracy and Precision.....	95
4.2.3 Extraction Recovery and Matrix Effect.....	98
4.2.4 Stability Tests.....	101
4.3 Phase 1 Metabolism.....	103
4.4 Phase 2 Metabolism.....	103
4.5 Biliary Excretions of CZ48 and CPT after an IV Dose of CZ48-CoS.....	109
4.6 Biliary Excretions of CZ48 and CPT after an Oral Dose of CZ48-CoS or CZ48-NS.....	113
4.6.1 Characterization of CZ48 Nanosuspension (CZ48-NS).....	113
4.6.2 Comparison of Biliary Excretions of CZ48 and CPT Between Oral and IV Doses of CZ48-CoS.....	113
4.6.3 Comparison of Biliary Excretions of CZ48 and CPT after an Oral Dose of CZ48-CoS or CZ48-NS.....	120
4.7 Enterohepatic Recycling of CZ48 and CPT after an Oral Dose of CZ48-NS.....	127
4.8 Development of a Population Pharmacokinetic (PK) Model.....	133
Chapter 5. Discussion.....	155
5.1 Biodistributions of CZ48 and CPT in Tumor-Xenografted Mice.....	157
5.1.1 Biodistributions of CZ48 and CPT from CoS or NS in Tumor-Xenografted Mice.....	158

5.1.2 Biodistributions of CZ48 and CPT from Co-S or NS in Healthy or Tumor-Xenografted Mice.....	160
5.2 Method Development and Validation Using UPLC-MS/MS.....	163
5.3 Phase 1 and 2 Metabolisms of CPT.....	165
5.4 Biliary Excretions of CZ48 and CPT in SD Rats.....	167
5.4.1 Biliary Excretions of CZ48 and CPT after an IV Dose of CZ48-CoS.....	168
5.4.2 Biliary Excretions of CZ48 and CPT after an Oral Dose of CZ48-CoS.....	170
5.4.3 Comparison of Biliary Excretions of CZ48 and CPT Between IV and Oral Doses of CZ48-CoS.....	171
5.4.4 Impact of NS on the Biliary Excretions of CZ48 and CPT after an Oral Dose of CZ48.....	173
5.5 Enterohepatic recycling of CZ48 and CPT after an oral dose of CZ48-NS.....	174
5.6 Development of a Population PK Model.....	178
Chapter 6. Summary.....	184
6.1 Biodistributions of CZ48 and CPT in Tumor-Xenografted Mice.....	184
6.2 Method Development and Validation Using UPLC-MS/MS.....	185
6.3 Phase 1 and 2 Metabolisms of CPT.....	186
6.4 Biliary Excretions of CZ48 and CPT.....	186
6.5 Enterohepatic Recycling of CZ48 and CPT.....	188
6.6 PK Model for Biliary Excretions and Enterohepatic Recycling of CZ48 and CPT.....	188
Reference.....	192

## List of Tables

Table 1:	Mobile Phase Gradient Conditions.....	53
Table 2:	The MS/MS Parameters for Simultaneous Quantifications of CZ48 and CPT.....	54
Table 3:	Compound-Dependent Parameters for CZ48, CPT, and CZ44 (IS).....	55
Table 4:	Animal Study Design for Evaluation of Biliary Excretions of CZ48 and CPT and Characterization of Their Enterohepatic Recycling.....	68
Table 5:	Biodistribution Parameters of CZ48 from Co-S or NS in Tumor-Xenografted Mice (Mean $\pm$ SD, n=3).....	76
Table 6:	Biodistribution Parameters of CPT from Co-S or NS in Tumor-Xenografted Mice (Mean $\pm$ SD, n=3).....	80
Table 7:	Intra- and Inter-day Accuracies and Precisions of CZ48 and CPT in Rat Plasma (Mean $\pm$ SD).....	96
Table 8:	Intra- and Inter-day Accuracies and Precisions of CZ48 and CPT in Rat Bile (Mean $\pm$ SD).....	97
Table 9:	Extraction Recoveries and Matrix Effects of CZ48 and CPT in Rat Plasma (Mean $\pm$ SD).....	99
Table 10:	Extraction Recoveries and Matrix Effects of CZ48 and CPT in Rat Bile (Mean $\pm$ SD).....	100
Table 11:	Stability Tests for CZ48 and CPT in Rat Plasma (Mean $\pm$ SD)....	102
Table 12:	Phase 1 Metabolism of CPT in the <i>In Vitro</i> System.....	104
Table 13:	Phase 1 Metabolism of Testosterone in the <i>In Vitro</i> System.....	105
Table 14:	Phase 2 Metabolism of CPT in the <i>In Vitro</i> System.....	106
Table 15:	Phase 2 Metabolism of Genistein in the <i>In Vitro</i> System.....	107
Table 16:	Pharmacokinetic Parameters of CZ48 and CPT in Rat Plasma and Bile after an IV Dose of CZ48-CoS.....	112
Table 17:	AUC <sub>0-t</sub> of CZ48 and CPT in Plasma after an IV or Oral Dose of CZ48-CoS.....	118

Table 18:	Concentration Ratios of CZ48 (or CPT) in Bile to Plasma (CZ48-B/P or CPT-B/P) after Single IV or Oral Dose of CZ48-CoS (Mean $\pm$ SD).....	119
Table 19:	AUC <sub>0-12</sub> of CZ48 and CPT in Plasma and Bile after an Oral Dose of CZ48-CoS or CZ48-NS (Mean $\pm$ SD, n=3-7).....	122
Table 20:	AUC <sub>0-t</sub> of CZ48 and CPT in Plasma after an Oral Dose of CZ48-NS (Mean $\pm$ SD).....	130
Table 21:	Estimated Population PK Parameters of CZ48 and CPT after an Oral Dose of CZ48-CoS for Each Compartment in the PK Model Shown in Figure 34.....	137
Table 22:	Estimated Population PK Parameters of CZ48 and CPT after an Oral Dose of CZ48-NS for Each Compartment in the PK Model Shown in Figure 34.....	142
Table 23:	Final Population Parameter Estimates and the Results of Bootstrap for the CoS Group.....	147
Table 24:	Final Population Parameter Estimates and the Results of Bootstrap for the NS Group.....	148

## List of Figures

Figure 1:	Chemical Structures of CZ48 (a) and CPT (b), CZ44 (c, Internal Standard).....	2
Figure 2:	The Conversion from the Lactone Form of CPT to Its Carboxylate Form at pH 7.4.....	5
Figure 3:	Chemical Structures of Topotecan (a) and Irinotecan (b).....	8
Figure 4:	Enterohepatic Recycling after an Oral Administration of a Drug in Humans.....	16
Figure 5:	Drug Transporters Located in the Liver.....	22
Figure 6:	The Linked-Rat Model to Characterize Enterohepatic Recycling of Drugs.....	26
Figure 7:	Q1 (a) and Precursor Ion Mass Spectra (b) of CZ48.....	56
Figure 8:	Q1 (a) and Precursor Ion Mass Spectra (b) of CPT.....	57
Figure 9:	Q1 (a) and Precursor Ion Mass Spectra (b) of CZ44.....	58
Figure 10:	Experimental Design for the Interruption of Enterohepatic Recycling of CZ48 and CPT.....	69
Figure 11:	Concentration versus Time Profiles of CZ48 and CPT from Co-S or NS in Tumor-Xenografted Swiss Nude Mice (Mean $\pm$ SD, n=3 per Time Point for Each Formulation).....	74
Figure 12:	Comparison of Organ Exposure and Half-Life of CZ48 Between CoS and NS in Tumor-Xenografted Mice (Mean $\pm$ SD, n=3 for Each Formulation Group).....	77
Figure 13:	Comparison of Organ Exposure and Half-Life of CPT Between CoS and NS in Tumor-Xenografted Mice (Mean $\pm$ SD, n=3 for Each Formulation Group).....	81
Figure 14:	Organ Exposures (Dose Adjusted AUC <sub>0-∞</sub> ) of CZ48 and CPT in Healthy and Tumor-Xenografted Mice (n=3).....	85
Figure 15:	Comparison of Half-Lives of CZ48 and CPT after an IV Dose of CZ48-CoS or CZ48-NS between Healthy and Tumor-Xenografted Mice (n=3).....	86

Figure 16:	Representative Calibration Curves for the Linearities of CZ48 and CPT in Plasma.....	89
Figure 17:	Representative Calibration Curves for the Linearities of CZ48 and CPT in Bile.....	90
Figure 18:	Representative MRM Chromatograms of (a) Blank, (b) Zero Blank, and (c) Spiked CZ48 at 15.6 ng/ml in Rat Plasma.....	91
Figure 19:	Representative MRM Chromatograms of (a) Blank, (b) Zero Blank, and (c) Spiked CPT at 15.6 ng/ml in Rat Plasma.....	92
Figure 20:	Representative MRM Chromatograms of (a) Blank, (b) Zero Blank, and (c) Spiked CZ48 at 15.6 ng/ml in Rat Bile.....	93
Figure 21:	Representative MRM Chromatograms of (a) Blank, (b) Zero Blank, and (c) Spiked CPT at 15.6 ng/ml in Rat Bile.....	94
Figure 22:	Chromatograms of CPT and CPT-Sulfate Scanned with m/z 349.1/305.2 (Blue Peak) and m/z 429.1/349.1 (Red Peak), Respectively, after an Overnight Incubation.....	108
Figure 23:	Plasma Concentration-Time Profiles of CZ48 and CPT after an IV Dose of CZ48-CoS (Mean $\pm$ SD, n=3).....	110
Figure 24:	Cumulative Amounts of CZ48 and CPT in Bile after an IV Dose of CZ48-CoS (Mean $\pm$ SD, n=3).....	111
Figure 25:	Plasma Concentration-Time Profiles of CZ48 and CPT after a Single IV Dose or a Single Oral Dose of CZ48-CoS (Mean $\pm$ SD, n=3-7).....	116
Figure 26:	Amounts of CZ48 and CPT Secreted into Bile after a Single IV Dose or a Single Oral Dose of CZ48-CoS (Mean $\pm$ SD, n=3-7).....	117
Figure 27:	Plasma Concentration-Time Profiles of CZ48 and CPT after Single Oral Dose of CZ48-CoS or CZ48-NS (Mean $\pm$ SD, n=3-7).....	123
Figure 28:	Amounts of CZ48 and CPT Secreted into Bile after Single Oral Dose of CZ48-CoS or CZ48-NS (Mean $\pm$ SD, n=3-7).....	124
Figure 29:	Concentrations of CZ48 and CPT in Plasma and Bile from CoS and NS Formulations (Mean $\pm$ SD, n=3-7).....	125
Figure 30:	AUC <sub>0-12h</sub> Ratios (B/P) of CZ48 (a) and CPT (b) after a Single Oral Dose of CZ48-CoS or CZ48-NS (Mean $\pm$ SD).....	126

Figure 31:	Plasma Concentration-Time Profiles of CZ48 and CPT after Single Oral Dose of CZ48-NS with or without Interrupting Enterohepatic Recycling (Mean $\pm$ SD, n=3-6).....	129
Figure 32:	Amounts of CZ48 and CPT Secreted into Bile after Single Oral Dose of CZ48-NS with or without Interrupting Enterohepatic Recycling (Mean $\pm$ SD, n=3-6).....	131
Figure 33:	Concentration Ratios (B/P) of CZ48 and CPT after Single Oral Dose of CZ48-NS with or without Interrupting Enterohepatic Recycling (Mean $\pm$ SD, n=3-6).....	132
Figure 34:	The Population PK Model Structure Describing Pharmacokinetics of CZ48 and CPT in Plasma and Bile.....	136
Figure 35:	Diagnostic Plots for CZ48 and CPT after an Oral Dose of CZ48-CoS.....	138
Figure 36:	Diagnostic Plots for CZ48 and CPT after an Oral Dose of CZ48-NS.....	143
Figure 37:	Visual Predictive Check Plots for CZ48 and CPT from the CoS Group.....	149
Figure 38:	Visual Predictive Check Plots for CZ48 and CPT from the NS Group.....	152

## List of Abbreviations

AUC	Area Under the Curve
B/P	Concentration Ratio of CZ48 (or CPT) in Bile to Plasma
CI	Confidence Interval
CL	Clearance
CL <sub>b</sub>	Biliary Clearance
CoS	Co-solvent formulation
CPT	Camptothecin
CV %	Coefficient of Variation Percent (%)
CWRES	Conditional Weighted Residuals
CZ48	Comptothecin-20(S)-O-propionate hydrate
DMPK	Drug Metabolism and Pharmacokinetics
DMSO	Dimethylsulfoxide
DV	Dependent Variable
FA	Formic Acid
F-108	Pluronic® F-108

FOCE ELS	First Order Conditional Estimation Extended Least Squares
GI Tract	Gastrointestinal Tract
HPLC	High-Performance Liquid Chromatography
IACUC	Institutional Animal Care and Use Committee
IPRED	Individual Predicted Estimates
IS	Internal Standard
IV	Intravenous
LLOQ	Low Limit of Quantification
MDR	Multidrug Resistance
MeOH	Methanol
MRP	Multidrug Resistance Associated Proteins
NADPH	Nicotinamide Adenine Dinucleotide Phosphate
NCI	National Cancer Institute
NS	Nanosuspension formulation with particle size of 200 nm
NSCLC	Non-Small Cell Lung Cancer
PAPS	Adenosine 3'-phosphate 5'-phosphosulfate lithium salt hydrate

PBS	Phosphate-Buffered Saline
PEG 400	Polyethylene Glycol 400
P-gp	P-glycoprotein
PK	Pharmacokinetics
PRED	Population Predictions
QQ IWRES	Quantile-Quantile Plot of the Individual Weighted Residuals
QC	Quality Control
RES	Reticuloendothelial System
RLM	Rat Liver Microsomes
SPE	Solid Phase Extraction
SULT	Sulfotransferase
TAD	Time After Dose
Tw-80	Tween 80
UDPGA	Uridine 5'-Diphosphoglucuronic Acid Triammonium Salt
UGT	UDP-Glucuronosyltransferase
UPLC-MS/MS	Ultra-Performance Liquid Chromatography-Tandem Mass Spectrometer

UV

Ultraviolet

VPC

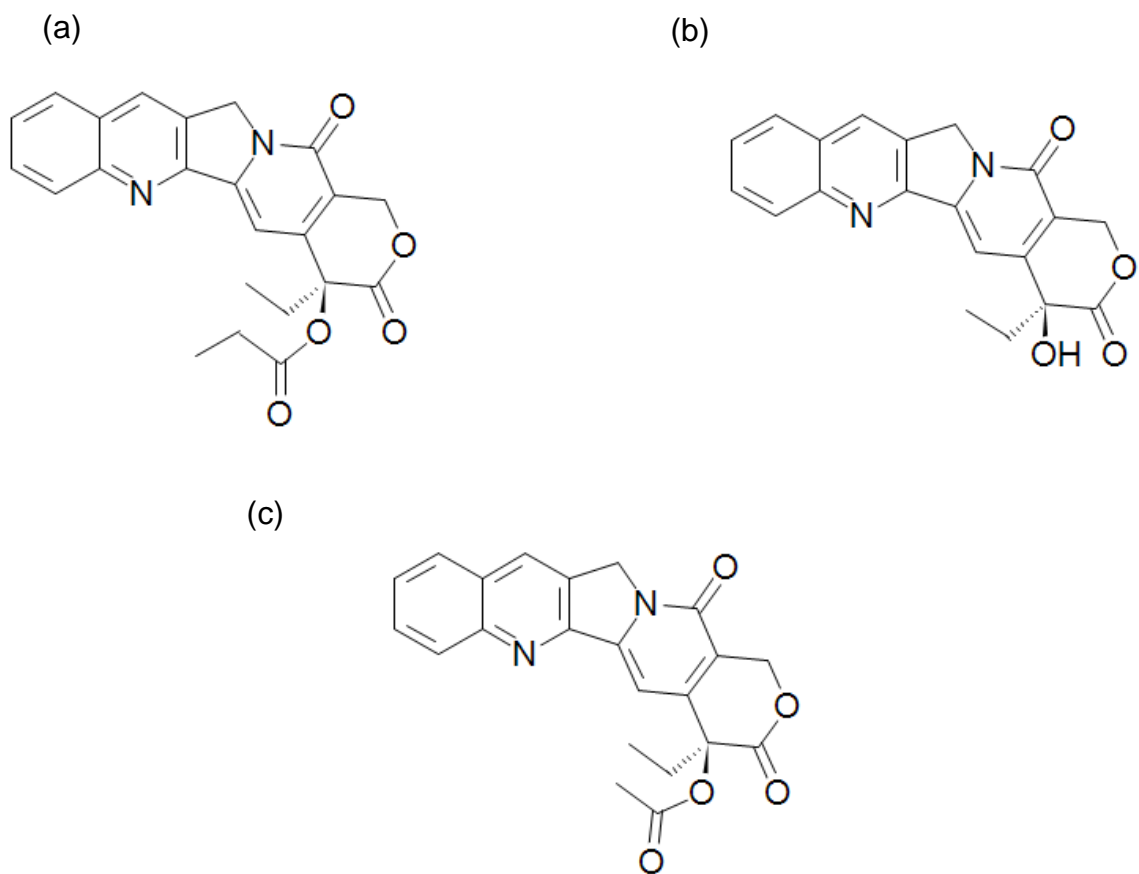
Visual Predictive Check

## **Chapter 1. Introduction and Literature Review**

### **1.1 Introduction**

Crystalline camptothecin-20-O-propionate hydrate (CZ48) is a prodrug of camptothecin (CPT). CZ48 and CPT are classified as topoisomerase-1 enzyme inhibitors. As a potential anticancer agent, CZ48 was synthesized in 1995 at the CHRISTUS Stehlin Foundation for Cancer Research in Houston (currently Cao Pharmaceuticals Inc., Friendswood, TX). To enhance the lactone stability, the chemical structure of CZ48 was modified by removing a hydrogen bonding, but adding an acyl substituent near a lactone ring of CPT (1, 2). In 2014, a phase 1 clinical trial was terminated in patients with solid tumors or lymphoma after an oral administration of CZ48 in a capsule form. The second phase 1 clinical trial has been recently initiated using micronized CZ48.

Figure 1. Chemical Structures of CZ48 (a) and CPT (b), CZ44 (c, Internal Standard)



## 1.2 Needs of New Camptothecin (CPT) Analogues

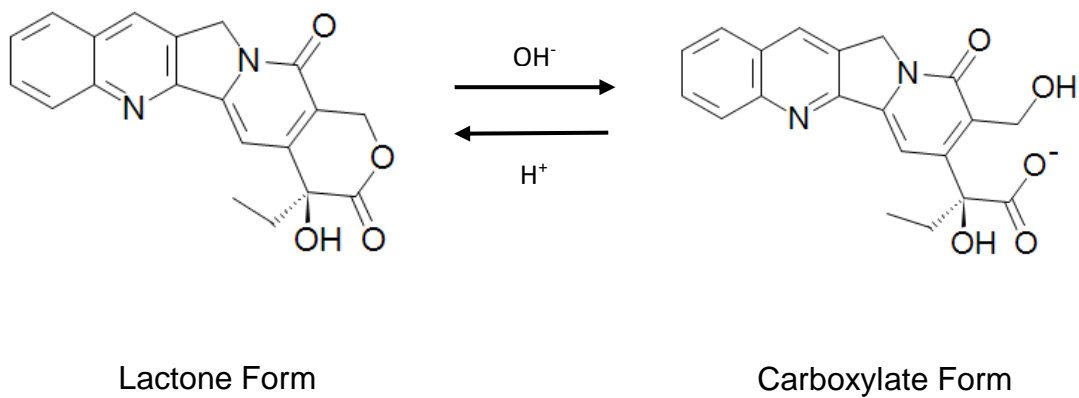
### 1.2.1 Limitations of CPT

CPT is a natural alkaloid originally extracted from the Chinese trees, *Camptotheca acuminata*, in the late 1960s (3). Due to the poor water solubility of CPT, a water-soluble sodium salt form of CPT (Na-CPT) was used in its phase 1 clinical trials in the early 1970s. However, CPT induced severe and unpredictable toxicity, particularly hemorrhagic cystitis (4, 5), so that the clinical trials were terminated in the early phase. Later, studies demonstrated that the lactone ring of CPT is required for its antitumor activity. However, the lactone ring of CPT is susceptible to spontaneous reversible hydrolysis at physiological pH 7.4 (Figure 2). The lactone ring predominates at acidic pH condition (pH < 4), but the ring is opened and converted to an inactive carboxylate form at neutral and alkaline pH (6).

Although CPT showed severe toxicity in early phase 1 clinical trials, strong antitumor activities of CPT against various types of tumors including colon, lung, breast, stomach, ovary, and malignant melanoma have been demonstrated using human tumor xenografts in nude mice (7). Hence, there have been efforts to understand its mechanism of actions and pharmacology, as well as synthesize more water-soluble CPT derivatives for future clinical uses. To date, two CPT

derivatives, topotecan and irinotecan, were approved by the U.S. Food and Drug Administration (FDA) and have been used for clinical purposes.

Figure 2. The Conversion from the Lactone Form of CPT to Its Carboxylate Form at pH 7.4



### 1.2.2 Limitations of Topotecan and Irinotecan

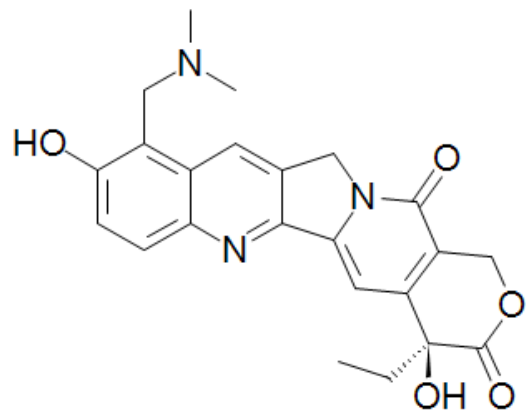
Topotecan (Hycamtin<sup>®</sup>, Smith-Kline Beecham Pharmaceuticals, Philadelphia, PA) is a water soluble semisynthetic CPT derivative with a basic *N,N*-dimethylaminomethyl functional group at C-9. Topotecan is a second-line therapy in advanced ovarian cancer and small cell lung carcinoma. The recommended dose regimen of topotecan is 1.5 mg/m<sup>2</sup> as a 30-min IV infusion, daily for 5 days, repeated every 21 days (8-10). A predominant elimination route of topotecan is renal excretion after its conversion to the carboxylate form. About 30-50 % of the administered dose was recovered as an unchanged drug in the urine (9, 11). Hepatic metabolism by cytochrome P450 enzymes does not seem to be a major elimination pathway of topotecan (12). Oral bioavailability was 30-40 % in humans (13, 14). One of the limitations of topotecan was its favorable conversion to inactive carboxylate form at physiological pH. To decrease the pH of the dose, a formulation has been introduced by containing tartaric acid in the IV infusion of topotecan. Another limitation of topotecan is a moderate response rate, which was 2-37% in phase 2 trials of topotecan in small cell lung cancer (9, 15).

Irinotecan (Camptosar<sup>®</sup>, Pharmacia and Upjohn Co., Kalamazoo, MI) is a water-soluble prodrug of SN-38 (7-ethyl-10-hydroxy analogue of CPT). It is used in the treatment of advanced colorectal cancer, both as the first-line therapy in

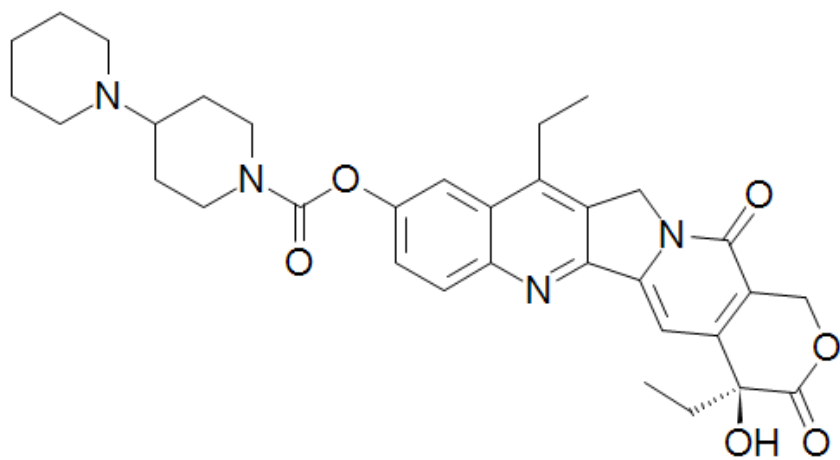
combination with 5-fluorouracil (5-FU) and as a salvage treatment in 5-FU refractory diseases. The approved administration of irinotecan in the U.S. is 125 mg/m<sup>2</sup> given as a 90-min IV infusion once weekly for 4 of 6 weeks (16). The response rates in phase 2 trials conducted in Japan, U.S. and France were in the range of 10-35% for the single agent therapy in patients with previously treated and untreated metastatic colorectal cancer, including those with 5-FU-resistant tumors (9, 17, 18). The major elimination routes of irinotecan are metabolism and biliary excretions. The limitation of irinotecan is a low conversion to its active form, SN-38. The AUC of SN-38 was about 4% of that of irinotecan (9, 16).

Figure 3. Chemical Structures of Topotecan (a) and Irinotecan (b)

(a)



(b)



### **1.3. CZ48 as an Anticancer Agent**

#### **1.3.1 Mechanism of Action of CZ48**

CZ48 is a prodrug of CPT. In contrast to CPT, CZ48 does not directly bind to topoisomerase-1 enzymes. Thus, the biotransformation from CZ48 to CPT is required for the antitumor activity of CZ48. CZ48 is converted to CPT by esterase. Topoisomerase-1 enzymes covalently bind to double-stranded DNA, which reduces torsional stress of supercoiled DNA and creates a single-strand break. Once the torsional strain is relieved, topoisomerase-1 enzymes rejoin the cleaved strand of DNA and are dissociated from the relaxed double helix. The mechanism of action of CPT starts when it binds to the interface between topoisomerase-1 enzymes and double-stranded DNA. The ternary complexes (CPT-Topoisomerase-1 enzymes-DNA) inhibit the relegation step in the cleavage/relegation of topoisomerase-1 enzymes, and result in the accumulation of single-stranded DNA, leading to cell death (19-22).

#### **1.3.2 Advantages of CZ48 over CPT**

A lactone stability makes CZ48 a promising camptothecin derivative. The lactone stability of CZ48 was demonstrated in mouse blood showing the majority of molecules stayed intact as the lactone form in blood circulation, with a small

fraction of CZ48 metabolized into CPT (23). In addition, preclinical studies have demonstrated the strong antitumor activity of CZ48 against various types of human tumors (24). In their study, the biological effectiveness of CZ48 was evaluated using Swiss nude mice xenografted with 21 different human tumor cell lines, including bladder, breast, colon, lung, melanoma, pancreatic, and desmoplastic small round cell tumor. CZ48 was highly effective against 19 different human tumor cell lines with a lack of toxicity. The effective doses required to achieve positive response rates were varied between 100 and 1000 mg/kg/d depending on the types of tumors.

### **1.3.3 Needs of Formulations for CZ48**

In the first phase 1 clinical trials in patients with solid tumor and lymphoma, CZ48 was delivered orally in a capsule form. Results from the clinical trials indicated that the concentration level of CZ48 in the blood was lower than expected, which was due to more active biotransformation of CZ48 in the human liver than that in tumor-xenografted mice (25). To improve oral absorption of CZ48, a micronized CZ48 in a capsule form is used in the current phase 1 clinical trials. In addition, CZ48 has a poor aqueous solubility, which is only 52 ng/ml in PBS at pH 7.4 (26).

The development of formulations for CZ48 is a potential approach to overcome these limitations. Among different types of formulations, nanosuspension has been selected to improve the poor water-solubility of CZ48 in our laboratory. Nanosuspension formulation has been widely used for a poorly water-soluble drug. The advantages of nanosuspensions over other formulations include simple manufacturing, long-term stability, and flexible modification of particle characteristics, such as charges and particle size (27, 28). Moreover, nanosuspensions can be applied to various dosing routes in a wide range of dose. The reduction of particle size increases the surface area of particles, which results in the increased dissolution rate, and thus bioavailability. In particular, the sustained release of CZ48 was achieved using nanosuspension developed in our laboratory, and its sustained release characteristics were demonstrated in our *in vitro* release studies in PBS and human plasma, and *in vivo* biodistribution studies using healthy Swiss nude mice (29).

CPT (active moiety of CZ48) and CPT derivatives are S-phase specific cell cycle compounds, so that the mechanism of action for topoisomerase 1 enzyme inhibitors (CPT and CPT derivatives) suggests prolonged exposures of the inhibitors are optimal for their antitumor efficacy (30). Hence, nanosuspension is a

reasonable approach to enhance poor water solubility of CZ48 and to achieve the prolonged exposure of CPT converted from the sustained release of CZ48 from nanosuspension. The efficacy of nanosuspension with the particle size of 200 nm was previously demonstrated in tumor-xenografted mice with subcutaneous inoculation of non-small cell lung carcinoma (NSCLC) H460 cells (29). In the efficacy study, three different IV doses, 5, 25, and 50 mg/kg, were given twice weekly for 4 weeks, a total of eight doses. The suppression of tumor growth, increase of survival duration and median survival (the period when half of the animals are alive) were evaluated. At the low dose (5 mg/kg), no significant suppression of tumor growth was observed. On the contrary, the highest tumor growth suppression was observed at the high dose (50 mg/kg), but it caused animal death (2 out of 10) after the first dose, which might be due to toxicity. Significant tumor growth suppression and prolonged duration of median survival without significant body weight loss were observed with the treatment of NS at 25 mg/kg, which supported the further development of CZ48-NS for potential future antitumor therapy.

#### **1.4 Nanoparticle Drug Delivery System for CPT**

To date, several nanoformulations have been introduced for CPT. The biodistribution of CPT loaded solid lipid nanoparticles (SLN) coated with poloxamer

188 was evaluated in C57BL/6J mice (31). The area under curve (AUC) and mean residence time (MRT) of CPT were significantly increased in all tested organs, especially for brain, blood, heart, lung, and liver. Since the increase of AUC of CPT in brain was the highest among tested organs, SLN may be advantageous for anticancer agents that target brain, but have difficulty of crossing the blood brain barrier. *In vitro* results indicated that the sustained release of CPT from SLN was achieved by showing half-life values longer than 20 h in the different pH conditions (pH 3.5, 5.5, and 7.4) at 37°C. Another study developed hydrophobically modified glycol chitosan nanoparticles for CPT (CPT-HGC), which showed prolonged blood circulation and high accumulation of CPT in tumors in human breast cancer xenografted nude mice (32). In addition, there is an *in vitro* study showing cyclodextrin nanoparticles increased the stability of CPT against hydrolysis (33).

### **1.5 Enterohepatic Recycling**

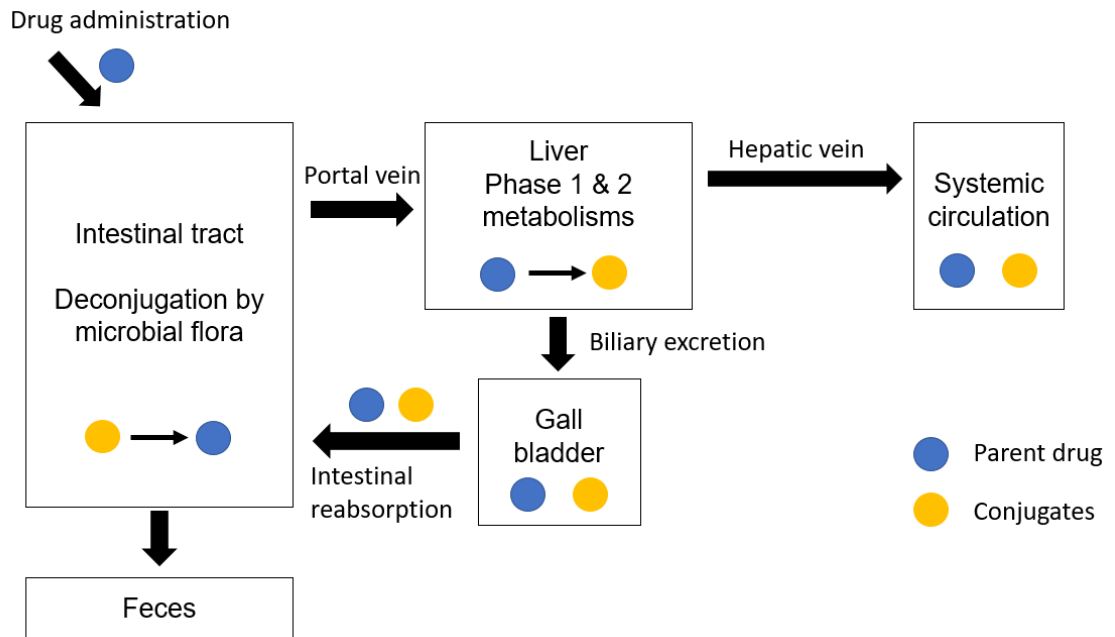
Enterohepatic recycling is the circulation of a drug and/or its conjugates from the liver to bile, followed by deconjugation of conjugates by  $\beta$ -glucuronidases in the intestine, and its reabsorption into the intestine, transporting back to the liver (Figure 4). Oral and intestinal absorptions, hepatic conjugation, biliary excretions, reabsorption into the liver, and intestinal deconjugation are critical factors that influence enterohepatic recycling. If a drug undergoes enterohepatic recycling,

double or multiple peaks are observed in the oral pharmacokinetic plasma profile of the drug with a long half-life and low clearance. Also, the drug is favorably secreted into the bile with or without its conjugates (34). The extended drug residence time in the systemic circulation due to enterohepatic recycling may significantly alter pharmacokinetics and pharmacological effects of a drug, which may result in unpredictable toxicity by sustained drug concentrations at higher levels. Thus, it is a prerequisite to characterize enterohepatic recycling of a drug in the early drug discovery and development process using preclinical models.

In particular, preclinical pharmacokinetic plasma profiles of CZ48 and CPT implied their enterohepatic recycling (35). Plasma concentration-time profiles were established after a single oral or intravenous dose of CZ48 in co-solvent formulation in Sprague Dawley (SD) rats. After an oral dose, sustained concentrations and multiple peaks of CPT were observed up to 6 hr post dose in the plasma profiles. On the contrary, their concentrations were rapidly declined within 3 hr after an intravenous dose. CZ48 concentrations were also sustained with multiple peaks in its oral pharmacokinetic profile. The prolonged drug concentration in plasma with multiple peaks is one of the unique observations when a drug undergoes enterohepatic recycling. Hence, we proposed that the

sustained concentrations of CZ48 and CPT in oral pharmacokinetic plasma profiles are due to enterohepatic recycling.

Figure 4. Enterohepatic Recycling after an Oral Administration of a Drug in Humans



[This figure was drawn based on Roberts et al., 2002 (34)]

## **1.5.1 Components in Enterohepatic Recycling**

### **1.5.1.1 Absorption of a Drug into the Portal Vein**

The drug amount available for enterohepatic recycling depends on the extent of drug absorption from the gastrointestinal tract (GI) into the portal blood. Oral absorption of a drug is affected by several factors, such as physicochemical properties of a drug in GI (solubility and pKa), dissolution properties of a drug formulation, drug metabolism by the gut wall and gut microflora, and physiological conditions (pH of lumen, gastric emptying time, intestinal transit time, blood flow, the presence of food, etc.) (34, 36). Some highly lipophilic drugs such as cyclosporin, naftifine, and probucol, bypass the portal circulation, but are absorbed via the intestinal lymph system and circulated via the thoracic duct back into the systemic circulation (34, 37).

### **1.5.1.2. Intestinal and Hepatic Metabolisms**

The expression level of drug metabolizing enzymes in the intestine is relatively lower than that in the liver. But both phase 1 and 2 metabolisms occur in the gut wall and influence a drug transport across membranes and enterohepatic recycling (34, 38). The phase 1 metabolisms occurred in the gut wall are oxidation, C-hydroxylation, N-dealkylation, O-dealkylation, deamination, S-oxidation,

desulfuration, decarboxylation, and hydroxamate reduction. The phase 2 metabolisms in the gut wall include esterification, ether formation, sulfation, glutathione conjugation, glycine conjugation, *N*-acetylation, *O*-acetylation, and *O*-methylation.

Liver is a major site for phase 1 and 2 metabolisms of many drugs, responsible for biotransformation or biliary excretion to eliminate toxic chemicals. The liver is composed of two types of epithelial cells, hepatocytes and cholangiocytes. In hepatocytes, drugs, metabolites, and hormones are absorbed from the blood and secreted into the bile. Cholesterol is converted to bile acids only in hepatocytes, and bile acids are secreted into the bile through canalicular membrane. Cholangiocytes are responsible for drug transport between blood and bile as well as bile formation (39).

The CYP superfamily is responsible for the most common phase 1 metabolism in the liver. Glucuronidation is the most common phase 2 metabolism, and most drug and endogenous glucuronides are secreted into the bile and can undergo enterohepatic recycling. Drug conjugates by phenol sulfotransferase and cytosolic glutathione *S*-transferase (GST) can also undergo enterohepatic recycling. Hydrophilic conjugates have difficulty of backdiffusing across the sinusoidal barrier,

which result in longer residence time and accumulation in the hepatocyte if diffusion is their main transport way, and then become subjected to biliary excretion (34).

After the reabsorption of drugs and/or conjugates from bile to the intestine, the conjugates may be deconjugated by  $\beta$ -glucuronidase in gut microflora, which may re-enter the portal vein and liver for enterohepatic recycling. In humans,  $\beta$ -glucuronidase activities are 0.02 and 0.9  $\mu\text{mol}$  of substrate degraded/h/g content in the proximal and distal regions of small intestine, respectively (34, 38).

### **1.5.1.3 Biliary Excretion**

Biliary excretion of a drug depends on several factors, such as drug properties (polarity, molecular size, etc.) and transporter activities expressed in sinusoidal and canalicular membranes.

The minimum molecular weight of drugs required for significant biliary excretion in rats is approximately 325 (40). The threshold molecular weight of drugs secreted into the bile in humans is estimated to be 500-600 Da (39, 40). However, the molecular weights of more than 45 molecules that undergo enterohepatic recycling

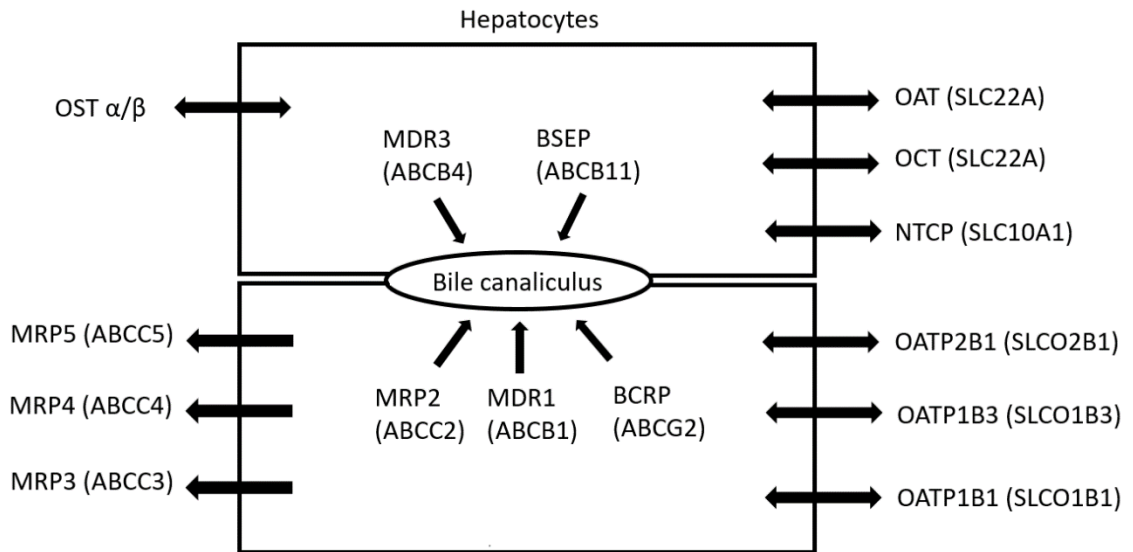
were in the range of 290 to 1300 Da (39). Along with molecular weight of a drug, polarity is another factor that may affect biliary excretion of a drug. Polar molecules are generally secreted into the bile (40). However, molecular weight and polarity of drugs are not sole requirements to predict biliary excretion and enterohepatic recycling of drugs.

Biliary excretions of anionic compounds including glutathione S-conjugates are mediated by multidrug resistance associated proteins 2 (MRP2) (41). MRP2 plays a role in transporting many drug conjugates including glucuronides, sulfates, and glutathiones (34, 42), which may undergo enterohepatic recycling.

P-glycoprotein (P-gp) is exclusively expressed on the canalicular membrane of hepatocytes. Class 1-P-gp from the MDR1 gene plays a role in the secretion of hydrophobic, cationic, and metabolites, whereas class 2-P-gp from the MDR3 gene is associated with phospholipid transport (34, 41). It has been studied that irinotecan, SN-38, and glucuronides of SN-38 are excreted into the bile and intestine via P-gp, MRP2, and BCRP (43-45). On the contrary, MRP1, MRP3, and MRP6 transport drugs and metabolites from hepatocytes into the sinusoids, which minimize their potential enterohepatic recycling (34, 46). There are multiple

influx/efflux transporters located in hepatocytes and enterocytes, and involved in biliary excretion and enterohepatic recycling of a drug (Figure 5) (36, 45).

Figure 5. Drug Transporters Located in the Liver



[This figure was drawn based on Chandra and Brouwer, 2004 (47), and Köck and Brouwer, 2012 (45)]

BCRP: Breast Cancer Resistance Protein

BSEP: Bile Salt Export Pump

OAT: Organic Anion Transporter

OATP: Organic Anion Transporting Polypeptide

OCT: Organic Cation Transporter

OST: Organic Solute Transporter

MDR: Multidrug Resistance

MRP: Multidrug Resistance-associated Protein

NTCP: Sodium-Taurocholate Cotransporting Polypeptide

## **1.5.2 Current Experimental Approaches to Characterize Enterohepatic Recycling**

### **1.5.2.1 Chemical Interruption of Enterohepatic Recycling**

It has been known that co-administration of activated charcoal or neomycin interrupts enterohepatic recycling of drugs by binding to the drugs and preventing them from reabsorption into the intestine. Activated charcoal was simultaneously administered to rats via oral gavage after an IV dose of dioscin to characterize enterohepatic recycling (48). The enterohepatic recycling of apixaban was also characterized after co-administration of activated charcoal (suspended in water) via oral gavage to bile-duct cannulated dogs at different time points post IV infusion or oral dose of [<sup>14</sup>C] apixaban, and activated charcoal was also administered to bile duct-cannulated rats via implanted duodenal catheters before and after the [<sup>14</sup>C] apixaban dosing (49). Neomycin was used to interrupt enterohepatic recycling of mestranol and estradiol, and their results indicated that biliary excretions were efficient and the enterohepatic recycling of mestranol and estradiol metabolites was reduced after co-administration of neomycin (50). However, there is no clue whether activated charcoal or neomycin binds to CZ48 and/or CPT, and interrupts their recycling. To adopt activated charcoal or neomycin for the interruption of enterohepatic recycling of CZ48 and CPT, it is necessary to evaluate

the interaction between CZ48 (or CPT) and activated charcoal (or neomycin) using *in vitro* system.

#### **1.5.2.2 A Linked-Rat Model**

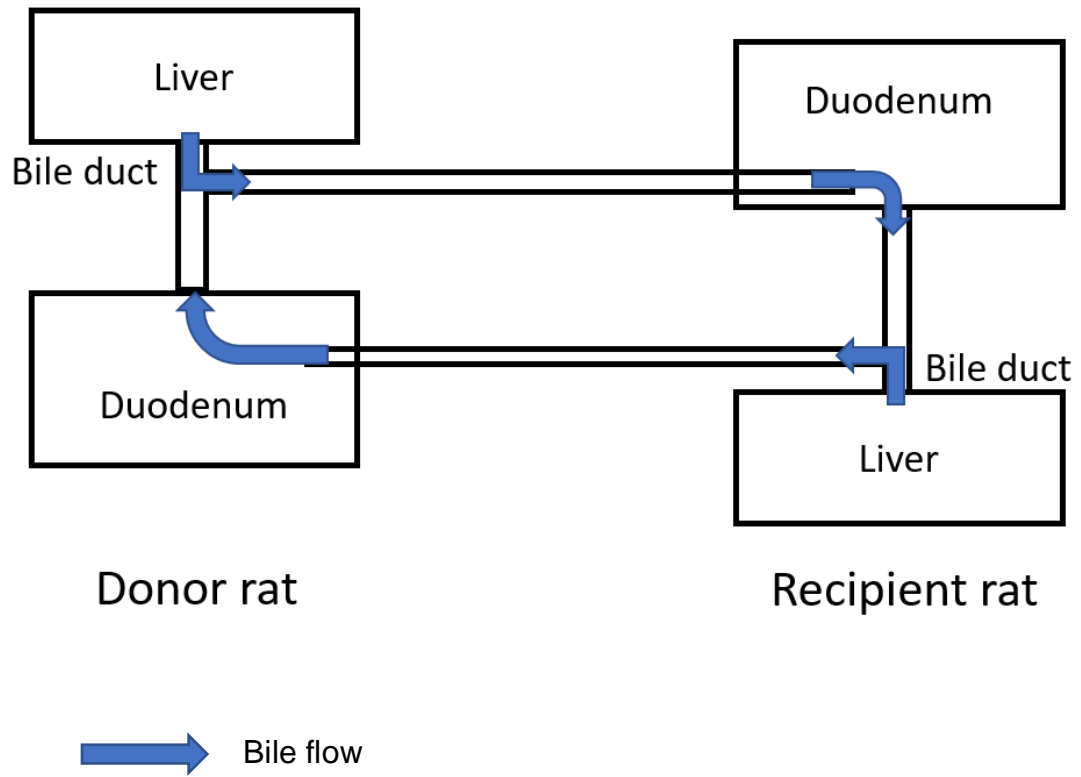
A linked-rat model is employed to characterize enterohepatic recycling of drugs (36, 39). The linked-rat model is designed as shown in Figure 6. Two rats, a donor rat and a recipient rat, are surgically linked and used as one set of the model. Bile from the liver in the donor rat flows to the bile duct in the duodenum of the recipient rat. To balance a fluid loss, bile from the liver in the recipient rat flows to the bile duct in the duodenum of the recipient rat. The donor rat receives a test drug and a recipient rat receives bile from the donor rat. If a drug is recycled, a drug concentration in plasma from the donor rat will decline due to the interruption of enterohepatic recycling, but a drug concentration in plasma from the recipient rat will increase by absorbing a drug from the bile of the donor rat.

The enterohepatic recycling of resveratrol was characterized by using the linked-rat model (51). In the study, resveratrol was administered orally to the donor rats and concentrations of resveratrol and its glucuronide in plasma were measured. In the bile duct-intact rats, plasma concentration was increased between 4 and 8 hr

post dose, and an elimination half-life of resveratrol was prolonged due to enterohepatic recycling. However, in the linked-rat model, the plasma concentrations of resveratrol and its glucuronide were decreased in the donor rat due to the interruption of recycling. On the contrary, there was a significant increase in the plasma concentrations of resveratrol and its glucuronide over the 4 to 8 hr time period. The linked-rat model was also employed to characterize enterohepatic recycling of other drugs (52-54).

However, limitations of this model are: (1) two rats with similar body weight are needed for one set, (2) animals are not free to move during experiments, and (3) the model is surgically complicated.

Figure 6. The Linked-Rat Model to Characterize Enterohepatic Recycling of Drugs



[The figure was drawn based on Gao et al., 2014 (39)]

### **1.5.2.3 Bile Duct-Intact vs. Bile Duct-Cannulated Rats**

There are previous studies using bile duct-intact and bile duct-cannulated rats to measure the influence and extent of enterohepatic recycling of drugs by comparing plasma concentration-time profiles and pharmacokinetic parameters between non-cannulated and bile duct-cannulated rats. Bile duct-intact and bile duct-cannulated rats were employed to evaluate biliary excretion and characterize enterohepatic recycling of morphine-3-glucuronide after the direct administration of the metabolite (55). There are studies showing negligible biliary excretion and enterohepatic recycling of cosalane after an IV administration of cosalane, since no significant differences of  $AUC_{0-\infty}$ , clearance (CL), and elimination half-life of the drug were observed between normal and bile duct-cannulated rats (56).

It is an efficient model to characterize enterohepatic recycling of drugs, since drug reabsorption into the intestine can be completely interrupted during experiments by collecting bile continuously from bile duct-cannulated rats. On the contrary, bile is completely intact in the bile duct-intact rats, so that drug recycling is completely protected during experiments.

## Summary

This survey of the literature illustrates a strong potential of CZ48, a prodrug of CPT, as an anticancer agent. Its strong antitumor activity against various types of human tumors and lactone stability have been demonstrated *in vivo* and *in vitro* studies, respectively. Preclinical pharmacokinetic studies (35) implied enterohepatic recycling of CZ48 and CPT. Enterohepatic recycling may significantly alter pharmacokinetics and pharmacological effects of drugs by extending their half-lives. Hence, it is required to characterize the recycling of CZ48 and CPT using a preclinical animal model. Along with several factors affecting enterohepatic recycling (hepatic metabolism and biliary excretion), sustained drug release characteristics of nanosuspension may also impact potential enterohepatic recycling of CZ48 and CPT, which need to be thoroughly investigated.

## **Chapter 2. Hypotheses and Specific Aims**

### **2.1 Central Hypothesis**

The overall objective for this project is to evaluate the impact of nanosuspension formulation on the biodistribution and enterohepatic recycling of CZ48 and CPT. For the biodistribution study, we hypothesize that the organ exposures of CZ48 and CPT are sustained in human tumor xenograft in nude mice due to the sustained release of CZ48 from nanosuspension. For the study of enterohepatic recycling, we hypothesize that CZ48 and CPT are secreted into the bile in a sustained manner and increased amounts of CZ48 and CPT are available for enterohepatic recycling for a prolonged time due to the sustained release of CZ48 from nanosuspension. We propose that the exposure of CPT, the active moiety of CZ48, is prolonged in the systemic circulation and organs (liver) by a sustained drug release characteristic of nanosuspension, which increases the extent of enterohepatic recycling of CPT.

## **2.2 Specific Aims**

### **2.1.1 Aim 1**

To characterize biodistribution patterns of CZ48 and CPT from nanosuspension formulation (200 nm) in human tumor xenograft mouse model induced with inoculation of non-small cell lung carcinoma (NSCLS) H460 cell line.

We hypothesized that exposures of CZ48 and CPT in organs and tumor cells will be sustained by nanosuspension formulation in the human tumor xenograft mouse model.

### **2.1.2. Aim 2**

To characterize enterohepatic recycling of CZ48, CPT, and/or potential conjugates using a rat model.

We hypothesize that CZ48 and CPT undergo enterohepatic recycling with their conjugates.

### **2.1.3. Aim 3**

To evaluate the effect of nanosuspension formulation on the enterohepatic recycling of CZ48, CPT and/or conjugates.

We hypothesize that increased drug amounts are available for enterohepatic recycling due to the sustained release of CZ48 from nanosuspension and a prolonged exposure of CZ48 in the liver.

## Chapter 3. Materials and Methods

### 3.1 Materials

#### 3.1.1 Chemicals and Materials

- 0.9 % sodium chloride injection USP grade was purchased from Martin Surgical Supplies (Houston, TX, USA), and used to flush bile duct- and jugular vein-cannulas in pharmacokinetic studies.
- Acetic acid LC-MS grade was purchased from Fluka<sup>®</sup> Analytical (St. Louis, MO, USA) to adjust pH of mobile phase in LC-MS/MS assay.
- Acetonitrile LC-MS grade (EMD Millipore, Billerica, MA, USA) was used in the preparation of mobile phase for the HPLC and LC-MS/MS assays, the extraction of CZ48 and CPT from biological matrices, and the preparation of a solution for *in vitro* metabolism study.
- CPT was purchased from Selleck Chemicals (Houston, TX, USA), and used to prepare a calibration curve for HPLC and LC-MS/MS assays as well as to investigate its *in vitro* metabolism.
- CZ48 and CZ44 (internal standard) were kindly provided by Cao Pharmaceuticals (Friendswood, TX, USA).
- Dimethylsulfoxide (DMSO) analytical grade (Fluka<sup>®</sup> Analytical, St. Louis, MO, USA) was used to prepare stock solutions of CZ48, CPT, and CZ44, and a constituent of the co-solvent formulation.

- Double distilled water was produced by a Milipore Milli-Q system (Billerica, MA, USA).
- Ethanol (Pure 200 Proof, EMD, Gibbstown, NJ, USA) was used to prepare CZ48 co-solvent formulation.
- Formic acid LC-MS grade was purchased from Fluka<sup>®</sup> Analytical (St. Louis, MO, USA) to adjust pH of solutions in solid phase extraction process.
- Glacial acetic acid (J.T. Baker Chemical Co., Phillipsburg, NJ, USA) was used to adjust the pH of the mobile phase in HPLC assay.
- Glass beads (0.5 – 0.75, 0.75 – 1, 1 – 1.3  $\mu\text{m}$ ) were purchased from Glenmills (Clifton, NJ, USA), and used in the preparation of CZ48 nanosuspension formulations.
- Glucose-6-phosphate dehydrogenase (from Baker's Yeast, type XV), D-glucose-6-phosphate sodium salt, B-nicotinamide adenine dinucleotide ( $\geq$  98%), and magnesium chloride hexahydrate (99%) (Sigma Aldrich, St. Louis, MO, USA) were used in the phase 1 metabolism studies.
- Heparin sodium injection USP grade was purchased from Martin Surgical Supplies (Houston, TX, USA), and used to heparinize micro-centrifuge tubes for blood collections and to flush a jugular vein cannula in pharmacokinetic studies.

- Isoflurane USP (Henry Schein, Melville, NY, USA) and urethane (Sigma Aldrich, St. Louis, MO, USA) were used as short-term and long-term anesthesia, respectively, in pharmacokinetic studies.
- Methanol LC-MS grade (EMD Millipore, Billerica, MA, USA) was used in the solid phase extraction process.
- Potassium phosphate monobasic and potassium phosphate dibasic (BDH Chemicals, Merck Co. Inc. Kenilworth, NJ, USA) were used to prepare a phosphate buffer (pH 7.4).
- Pluronic F-108 (F-108, BASF Corporation, NJ, USA) was used to prepare CZ48 nanosuspension formulation.
- Polyethylene glycol 400 (PEG 400) (Avantor Performance Materials, Center Valley, PA, USA) was used to prepare CZ48 co-solvent formulation.
- Pooled Sprague Dawley (SD) rat plasma was purchased from Equitech-Bio Inc. (Kerrville, TX, USA) and used to prepare calibrators in UPLC-MS/MS assay.
- Pooled male SD rat liver microsomes and pooled male SD rat liver S9 fractions were purchased from Life Technologies (Carlsbad, CA, USA), which were used in phase 2 metabolism studies.
- Pooled male SD rat liver microsomes were purchased from Sekisui XenoTech, LLC (Kansas City, KS, USA), which were used in phase 1 metabolism studies.

- Sodium chloride 99% (ACROS Organics, Geel, Belgium) was dissolved in double distilled water to prepare normal saline solution used for the tissue homogenization process.
- Tween 80 (Tw-80) was purchased from PCCA (Houston, Texas, USA), and used to prepare CZ48 nanosuspension formulation.
- Uridine 5'-Diphosphoglucuronic acid triammonium salt (UDPGA), adenosine 3'-phosphate 5'-phosphosulfate lithium salt hydrate (PAPS), saccharolactone, alamethicin, and magnesium chloride ( $MgCl_2$ ) were purchased from Sigma-Aldrich (St. Louis, MO, USA), and used in the *in vitro* phase 2 metabolism studies.
- Water LC-MS grade (EMD Millipore, Billerica, MA, USA) was used in the preparation of mobile phase for LC-MS/MS assay.

### **3.1.2 Equipment and Apparatus**

- Balance (Mettler New Classic MF, Mettler-Toledo International Inc., Greifensee, Switzerland) was used for weighing purposes.
- Beckman Coulter Microfuge 22R Refrigerated Microcentrifuge was used in sample preparations.

- Brookhaven ZetaSizer with Zeta Plus Particle Sizing software Ver.3.85 (Brookhaven Instrument Corporation, NY, USA) was used to measure particle size, polydispersity index, and zeta potential of nanoformulations.
- Empower 2 software (Waters Corp, Milford, MA, USA) was used to operate HPLC system, and to acquire, process, report, and manage chromatographic information.
- Eppendorf pipettes (Hamburg, Germany) with three different sizes, 1-10  $\mu$ l, 10-200  $\mu$ l, and 100-1000  $\mu$ l were used in sample preparation.
- GraphPad Prism 7 was used for data analysis and graphic presentation.
- HPLC system with 515 HPLC pumps, 717 plus autosampler, and 2475 multi  $\lambda$  fluorescence detector was used for sample analysis in biodistribution studies.
- HPLC system with 515 HPLC pumps, 717 plus autosampler, and 2996 photodiode array detector was used for sample analysis in *in vitro* metabolism studies.
- MedChem Designer 3.0 (SimulationsPlus Inc., Lancaster, CA, USA) was used to draw chemical structures.
- Microsoft excel (Microsoft corp., Seattle, WA, USA) was used for data analysis.
- Pipette-aid controller (Drummond Scientific, Broomall, PA, USA) was used in delivering liquids for sample preparation.
- pH meter (VWR Handheld pH meter, VWR international, Radnor, PA, USA) was used to measure the pH of mobile phase.

- Phoenix<sup>®</sup> WinNonlin<sup>®</sup> 6.4 (Certara USA Inc., Princeton, NJ, USA) was used for individual pharmacokinetic (PK) analysis.
- Phoenix<sup>®</sup> Non-Linear Mixed Effects (NLME)<sup>™</sup> 1.3 (Certara USA Inc., Princeton, NJ, USA) was used to develop and validate a population PK model.
- RStudio<sup>®</sup> 1.0.153 (RStudio Inc. Boston, MA, USA) was used to test normal distribution of collected data in the biodistribution and pharmacokinetic studies.
- Small animal anesthesia machine (EZ-150C Classic, EZ System Corp. Palmer, PA, USA) was used in animal studies.
- Sonication bath (VWR<sup>®</sup> Ultrasonic cleaners, VWR international, Radnor, PA, USA) was used in entire projects.
- Speedisk 48 positive pressure processor (Mallinckrodt Baker Inc., Philipsburg, PA, USA) extraction apparatus was used for solid phase extraction of analytes from bile samples.
- Tissue tearor (model 985370, Biospec Products Inc., Bartlesville, OK, USA) was used to homogenize tissue samples in biodistribution studies.
- Ultra-performance liquid chromatography (UPLC) with the API 3200 and 5500 Q Trap triple quadrupole mass spectrometers (AB SCIEX, Framingham, MA, USA) were used for simultaneous quantifications of CZ48 and CPT in biological samples.
- Vortex mixer (Vortex-Genie 2, Scientific Industries, Inc., Bohemia, NY, USA) was used in sample preparation.

- Water bath (VWR water bath, VWR international, Radnor, PA, USA) was used in the *in vitro* metabolism studies.

### **3.1.3 Surgical Instruments and Supplies**

- Alcohol wipes (Webcol® Alcohol Preps, Kendall Healthcare Products Co., Mansfield, MA, USA) were used in pharmacokinetic studies.
- Cotton swabs (Q-tips, 6 inch) (Tyco Healthcare Group LP., Mansfield, MA, USA) were used to prepare heparinized micro-centrifuge tubes.
- Gastric gavage blunt needle (20-gauge, 2.5 inch, curved, ball-end; Harvard Apparatus Inc., Holliston, MA, USA) was used for oral administration of CZ48 in rats.
- HPLC glass vials (2ml; Waters Corp, Milford, MA, USA) were used for sample analysis using HPLC in biodistribution and *in vitro* metabolism studies.
- Microcentrifuge tubes (1.5 mL; VWR international, Radnor, PA, USA) were used for collecting, storing, and preparing pharmacokinetic samples.
- Needles (22 and 23G, sterile for single use) were purchased from Becton, Dickinson and Company (Franklin Lakes, NJ) and used in pharmacokinetic studies.
- Pipettes with different sizes (5, 10, and 25 ml) were purchased from VWR international (Radnor, PA, USA) and used in sample preparation.

- Pipette tips with different sizes (1-10  $\mu$ l, 10-200  $\mu$ l, and 100-1000  $\mu$ l) were purchased from VWR international (Radnor, PA, USA) and used for measuring and delivering samples and solutions.
- Polyethylene tubing (PE-10 and PE-50) was purchased from Instech Laboratories Inc. (Plymouth Meeting, PA, USA) and used for bile duct cannulation in SD rats and for the extension of cannulas to collect bile conveniently.
- Polypropylene tubes (10 and 50 ml) were purchased from VWR international (Radnor, PA, USA).
- Polypropylene conical inserts with spring were purchased from VWR international (Radnor, PA, USA) and used in sample analysis using HPLC.
- Rat jacket was purchased from Braintree Scientific Inc. (Braintree, MA, USA) and used in pharmacokinetic studies.
- Scintillation glass vials with caps with foil liner were purchased from VWR international (Radnor, PA, USA).
- Stainless steel tubing port plugs and connectors (22G and 23G) were purchased from Braintree Scientific Inc. (Braintree, MA, USA) and used in pharmacokinetic studies.
- Surgical absorbent pads (VWR international, Radnor, PA, USA) were used in pharmacokinetic studies.

- Syringes (1 and 5 ml) were purchased from Becton, Dickinson and Company (Franklin Lakes, NJ, USA) and used in pharmacokinetic studies.
- Syringe filter (0.45 µm, HPLC certified) were used to filter CZ48 co-solvent formulation.
- UPLC vials and black caps (9mm Thread, PTFE/Sil) were purchased from Chrom Tech Inc. (Apple Valley, MN, USA) and used in sample analysis using UPLC-MS/MS.
- Waters ACQUITY UPLC BEH Shield RP18 column (2.1 mm × 50 mm, 130 Å, 1.7 µm, Waters, Milford, MA, USA) was used in sample analysis using UPLC-MS/MS.
- Waters Oasis HLB extraction cartridges (Waters, Milford, MA, USA) were used in the solid phase extraction process.
- XTerra® RP8 column (5 µm, 4.6×150 mm, Waters Corp., Milford, MA) was used in sample analysis using HPLC-fluorescence.

#### **3.1.4 Animals**

- Male Sprague Dawley rats (250-300 g) with or without bile duct- or jugular vein-cannulation were purchased from Envigo (Indianapolis, IN, USA) and used for pharmacokinetic studies.

- Bile duct-cannulation for a pharmacokinetic study after an intravenous administration of CZ48 in a co-solvent formulation was conducted under guidance of research fellows in Dr. Ming Hu's laboratory.
- Preparation of human tumor xenograft in Swiss nude mice for the biodistribution study was conducted at the former CHRISTUS Stehlin Foundation for Cancer Research in Houston (currently Cao Pharmaceuticals, Friendswood, TX)

## **3.2. Methods**

### **3.2.1 Preparation of Co-Solvent (CoS) Formulation**

CZ48 in CoS (CZ48-CoS) was prepared in the mixture of DMSO, PEG 400, and ethanol (2:2:1, v/v/v) at 2 mg/ml for the biodistribution study using human tumor xenograft mouse model and an intravenous pharmacokinetic study using Sprague Dawley (SD) rats. Ten mg/ml of CZ48-CoS was prepared for oral pharmacokinetic studies using SD rats. CZ48-CoS was filtered through a 0.45  $\mu\text{m}$  syringe filter before dosing.

### **3.2.2 Preparation and Characterization of Nanosuspension Formulation**

Nanosuspension (CZ48-NS) with the particle size of 200 nm was prepared by the media milling method described in (29, 57). The mixture of CZ48 (5.9 % by wt), two stabilizers (Tw-80 and F-108) and distilled water were placed in a 7 ml of a scintillation vial. The ratio of Tw-80 and CZ48 was 0.1:1 (w/w) and that of F-108 and CZ48 was 0.28:1 (w/w). One gram of three different sizes of glass beads (0.5-0.75: 0.75-1: 1-1.3  $\mu\text{m}$ , 1:1:1) were added into the mixture as milling agents. The mixture was stirred at 1,600 rpm for 24 hr. Particle size, polydispersity index, and zeta potential of CZ48-NS were measured by Zetapals (Brookhaven Instruments, Holtsville, NY).

### **3.2.3 Organ Biodistribution Study Using Human Tumor-Xenografted Mice**

#### **3.2.3.1 Animal Study Protocol for Biodistribution Study**

All experiments were conducted in accordance with approved animal protocols from the Institutional Animal Care and Use Committee (IACUC) at the University of Houston and the CHRISTUS Stehlin Foundation for Cancer Research (Currently Cao Pharmaceuticals Inc., Friendswood, TX). Male Swiss athymic nude mice (25 – 30 g) were provided from the CHRISTUS Stehlin Foundation for Cancer Research. Mice were maintained in individually ventilated cages under standard laboratory conditions (12-hour light/dark cycle, temperature of ~73 °F, humidity of 40 – 55 %), and allowed free access to food and water. Athymic Swiss nude mouse was selected because human tumors can be xenografted, and it is a well-established animal model for human cancer research.

For human tumor-xenografted mouse model, non-small cell lung carcinoma (NSCLC) H460 cells were cultured and prepared for the biodistribution study at the CHRISTUS Stehlin Foundation for Cancer Research. NSCLC H460 tumor cells were subcutaneously injected into the Swiss nude male mice. When the estimated tumor volume is approximately 100 mm<sup>3</sup> (approximately 8-10 days after being injected with the NSCLC H460 cells), mice were considered to be ready for the biodistribution study. If a mouse lost more than 15% of its body weight, it was

sacrificed. The tumor-xenografted mice were randomly divided into control and treatment groups (9 mice per group).

Five mg/kg of CZ48-CoS (control) or 25 mg/kg of CZ48-NS (treatment) was intravenously (IV) administered to tumor-xenografted mice through the tail vein. Mice were sacrificed under anesthesia using Avertin (tribromoethanol and amyl alcohol) based on the CHRISTUS Stehlin Foundation Standard Operating Procedure for mouse anesthesia. Tumor cells and tested organs including liver, kidneys, lung, brain, heart, and spleen were harvested after the whole body was flushed by normal saline. The tested organs (n=3 at each time point) were harvested at 0.5, 2, and 4 hr after a single IV dose of CZ48-CoS or CZ48-NS. Tumor samples (n=3) were collected at the same time points after the last IV dose of CZ48-CoS or CZ48-NS in twice weekly regimen for 4 weeks.

### **3.2.3.2 HPLC Assay for the Simultaneous Quantifications of CZ48 and CPT in Mouse Organs**

CZ48 and CPT in tissues and tumor harvested from tumor-xenografted mice were simultaneously quantified by following the same sample extraction and analytical methods employed for the biodistribution study using healthy mice (29).

### **3.2.3.2.1 Preparations of Standard Stock and Working Solutions of CZ48 and CPT**

Stock solutions of CZ48, CPT and CZ44 (IS) were prepared in DMSO at the concentration of 1 mg/ml. For calibrators, the stock solutions were diluted with 50% of acetonitrile in distilled water.

### **3.2.3.2.2 Biological Sample Preparation for HPLC Analysis**

Mouse organs and tumor were precisely weighed and homogenized by adding 0.2-1 mL of normal saline depending on the weight of organs and tumor. Five hundred  $\mu\text{L}$  of acetonitrile including internal standard (IS, CZ44) was added into 100  $\mu\text{L}$  of organ or tumor homogenate samples. After vortexing for 1-2 min, the samples were centrifuged at 17,968  $\times g$  for 20 min. Supernatant was evaporated under the air and residue was reconstituted with 100  $\mu\text{L}$  of the mixture of 0.1 % acetic acid in water and acetonitrile (50:50, v/v). The reconstituted samples were injected into the high-performance liquid chromatography (HPLC) with a fluorescence detector for analysis.

### **3.2.3.2.3 Analytical Conditions for HPLC Analysis**

Homogenized organ samples were analyzed by HPLC consisted of the Waters 2475 multi  $\lambda$  fluorescence detector, two Waters 515 HPLC pumps, and the Waters 717 plus autosampler (Waters Corp., Milford, MA). Chromatographic separations were achieved by using XTerra<sup>®</sup> RP8 (5  $\mu$ m, 4.6 $\times$ 150 mm). Mobile phase consisted of 0.1% acetic acid in distilled water (pH 5.3) (A) and acetonitrile (B), and was eluted at the flow rate of 1.2 ml/min in the following gradient condition: 80% of A (0-1 min), 80% to 78% of A (1-15 min), 78% of A to 55% of A (15-25 min), 55% of A to 20% of A (25-30 min), 20% of A to 0% of A (30-31 min), 0% of A to 80% of A (31-32 min), and 80% of A (32-34 min). The excitation and emission wavelengths were 360 and 455 nm, respectively. Calibration curves were freshly prepared on the day of analysis and constructed at a linear range of 1.88 (LLOQ) – 800 ng/ml for CZ48 and CPT.

### **3.2.3.3 Pharmacokinetic and Statistical Analyses**

Concentration versus time profiles were constructed to characterize the biodistribution patterns of CZ48 and CPT in each organ and tumor. In case of the biodistribution study, destructive sampling was used since each animal contributed to a single observation in the concentration-time profiles. Thus, mean concentrations from three rats at each sampling time point were used to establish

the concentration-time profiles and calculate the area under the curve ( $AUC_{0-4h}$ ).  $AUC_{0-4h}$  was calculated by using the linear trapezoidal rule. In order to statistically compare  $AUC_{0-4h}$  values of CZ48 and CPT between co-solvent (CoS) and nanosuspension (NS) groups, standard deviations of the  $AUC_{0-4h}$  values were calculated by following the Bailer's method (58). To contrast  $AUC_{0-4h}$  values between CoS and NS groups, the t-distribution test was performed. The normality of the data was tested using RStudio (Boston, MA). When  $P < 0.05$ ,  $AUC_{0-4h}$  values of CZ48 or CPT were statistically different between CoS and NS groups. Half-lives of CZ48 and CPT were calculated using a linear regression method from the concentration-time profiles. Slopes of the linear regression lines were used to conduct a statistical comparison between CoS and NS groups. When  $P < 0.05$ , slopes between the two formulation groups were considered statistically different.

### **3.2.4 *In Vitro* Phase 1 Metabolism of CPT**

Phase 1 metabolism of CPT was evaluated by following a slightly modified procedure described in Ackley et al., 2004 (59). CPT was incubated in rat liver microsomes (final concentration: 0.5 mg/ml) with a cofactor, nicotinamide adenine dinucleotide phosphate (NADPH), for 0, 2, and 4 hr. Testosterone was selected as a positive control. NADPH was prepared by mixing the following solutions; 3.3 mM of glucose-6-phosphate, 1.3 mM of  $\beta$ -nicotinamide adenine dinucleotide phosphate (NADP), 0.4 U/ml of glucose 6-phosphate dehydrogenase, and 3.3 mM of magnesium chloride hexahydrate ( $\text{MgCl}_2 \cdot 6\text{H}_2\text{O}$ ), at the same volume ratio (1:1:1:1, v/v/v/v). One hundred mM potassium phosphate buffer was prepared at pH 7.4. The mixture of 271  $\mu\text{l}$  of potassium phosphate buffer and 8  $\mu\text{l}$  of liver microsomes was pre-incubated at 37 °C water bath for 5 min. Three  $\mu\text{l}$  of CPT (or testosterone) at the concentration of 5 mM was added into the mixture. To start a reaction, 18  $\mu\text{l}$  of NADPH was added into the mixture. During the reaction, the mixture was placed at 37°C water bath. To terminate the reaction, 150  $\mu\text{l}$  of a stop solution (94% acetonitrile + 6% acetic acid) was added into the mixture at designated time points. The mixture was vortexed briefly and centrifuged at 17,968 xg for 20 min. A supernatant was injected into the HPLC with UV. Mobile phase was the mixture of distilled water, acetonitrile, and methanol, 50:25:25, v/v/v, and flowed at 0.8 ml/min for 15 min.

### **3.2.5 *In Vitro* Phase 2 Metabolism of CPT**

Phase 2 metabolisms of CPT by two major phase 2 metabolizing enzymes, UDP-glucuronosyltransferases (UGTs) and sulfotransferases (SULTs), were evaluated as described in Yang et al., 2012 (60). Uridine 5'-Diphosphoglucuronic Acid Triammonium Salt (UDPGA) and Adenosine 3'-phosphate 5'-phosphosulfate lithium salt hydrate (PAPS) were used as cofactors for glucuronidation and sulfation, respectively. Genistein was selected as a positive control in this study. Potassium phosphate buffer at pH 7.4 and the mixed solution (solution A) containing MgCl<sub>2</sub> (0.88 mM), saccharolactone (4.4 mM), and alamethicin (0.022 mg/ml) were prepared. For the glucuronidation reaction, potassium phosphate buffer, solution A, and rat liver microsomes were incubated with 10 μM of CPT (or genistein) in 37 °C water bath for 0, 2 hr, and overnight for CPT and 0, 15, and 30 min for genistein. The glucuronidation reaction was started by adding UDPGA (3.5 mM) into the mixture. For the sulfation, CPT (or genistein) was added to the same mixture condition, but PAPS (0.1 mM) was added to rat S9 fractions. To terminate the reactions, 50 μl of the stop solution (94% of acetonitrile and 6% of acetic acid) was added to the mixture. The collected samples were centrifuged at 17,968 xg for 20 min, and the supernatant was analyzed for CPT (or genistein) and metabolite(s) using UPLC-UV or UPLC-MS/MS (API 3200). The same mobile phases and analytical conditions were used as described in Section 3.2.6.

### **3.2.6. UPLC-MS/MS Assay for the Simultaneous Quantifications of CZ48 and CPT in Rat Plasma and Bile**

#### **3.2.6.1 Preparations of Stock and Working Solutions of CZ48 and CPT**

Stock solutions of CZ48, CPT and CZ44 (IS) were prepared in DMSO at the concentration of 1 mg/ml. To prepare calibrators, the stock solutions were diluted with acetonitrile.

#### **3.2.6.2 Biological Sample Preparations for a UPLC-MS/MS Analysis**

The protein precipitation method was employed to extract CZ48 and CPT from rat plasma. Five hundred  $\mu$ l of acetonitrile with 1% formic acid (FA) was added to plasma. FA was used for preserving the lactone stability of CPT during extraction. The samples were vortexed for 1-2 min and centrifuged at 17,968  $\times$ g for 20 min. The supernatant was evaporated under the air for dryness. The residue was reconstituted with 100  $\mu$ l of the mixture of 0.1% acetic acid in water and 0.1% acetic acid in acetonitrile (50:50, v/v). The reconstituted samples were centrifuged at 17,968  $\times$ g for 20 min and 10  $\mu$ l of the supernatant was injected into the UPLC-MS/MS system.

The solid phase extraction (SPE) method was used for extracting CZ48 and CPT from rat bile. Waters Oasis HLB columns were pre-conditioned with 1 ml of methanol, followed by 1 ml of water. Fifty  $\mu$ l of bile samples was mixed with 900  $\mu$ l of 0.1% FA in water, and loaded into the pre-conditioned columns. The columns were washed with 1 ml of water and 1 ml of 40% methanol in water. CZ48, CPT, and IS were eluted with 1 ml of 90% methanol in water with 1% FA. The eluted samples were evaporated under the air to dryness, and the residue was reconstituted with 100  $\mu$ l of the mixture of 0.1% acetic acid in water and 0.1% acetic acid in acetonitrile (50:50, v/v). The samples were centrifuged at 17,968  $\times$ g for 20 min and 10  $\mu$ l of the supernatant was injected into the UPLC-MS/MS system for analysis.

### **3.2.6.3 Analytical Conditions for UPLC-MS/MS Analysis**

The UPLC with the API 3200 Q Trap triple quadrupole mass spectrometer was used to simultaneously quantify CZ48 and CPT in plasma and bile samples. Waters ACQUITY UPLC BEH Shield RP18 column (2.1 mm  $\times$  50 mm, 130 Å, 1.7  $\mu$ m) was used for chromatographic separation. Mobile phase consisting of 0.1% acetic acid in water (A) and 0.1% acetic acid in acetonitrile (B) were given in a gradient elution at a flow rate of 0.45 ml/min as shown in Table 1. Temperatures of column and autosampler were maintained at 30 °C and 10 °C, respectively. The

MS/MS parameters for CZ48, CPT, and CZ44 (IS) were shown in Table 2. The transitions and compound dependent parameters for CZ48, CPT, and CZ44 (IS) were shown in Table 3. Q1 and precursor ion mass spectra of CZ48, CPT, and IS were presented in Figure 7, 8, and 9. Detection was performed in the positive ion and multiple reaction monitoring (MRM) modes. The API 5500 Q Trap triple quadrupole mass spectrometer was additionally used to simultaneously quantify CZ48 and CPT in plasma when a higher sensitivity is required in oral pharmacokinetic studies. The API 5500 was performed in the same UPLC and MS/MS conditions except the curtain gas and ion source gas 1 as shown in Table 2.

Table 1. Mobile Phase Gradient Conditions

Time (min)	Mobile Phase	
	A (%)	B (%)
Initial	90	10
0.5	80	20
1.5	70	30
2.5	65	35
4.5	45	55
5	10	90
5.5	10	90
6	90	10
7	90	10

Mobile Phases: 0.1 % acetic acid in water (A) and 0.1 % of acetic acid in acetonitrile (B)

Table 2. The MS/MS Parameters for Simultaneous Quantifications of CZ48 and CPT

	API 3200	API 5500
Curtain gas (psi)	10	20
ionspray voltage (V)	5500	5500
Temperature (°C)	550	550
Collision gas	High	High
Ion source gas 1 (psi)	10	20
Ion source gas 2 (psi)	40	40

Table 3. Compound-Dependent Parameters for CZ48, CPT, and CZ44 (IS)

Compound	Q1 (m/z)	Q3 (m/z)	DP (V)	CEP (V)	CE (V)	CXP (V)	EP (V)
CZ48	405.1	331.2	85	23	35	3.5	10
CPT	349.1	305.2	80	24	28	3.95	10
CZ44	391.1	303.3	87	27	34	4.2	10

DP: Declustering potential

CEP: Collision cell entrance potential

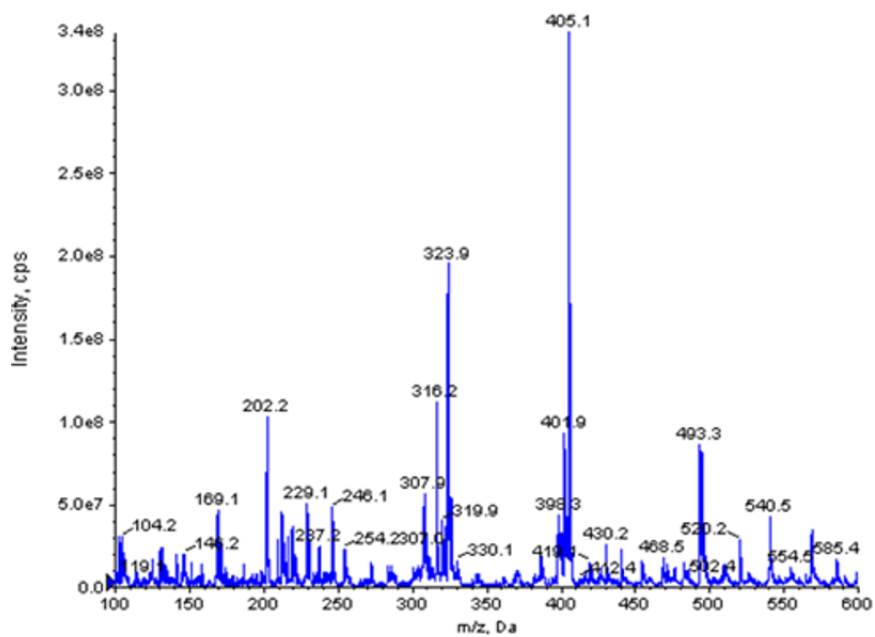
CE: Collision energy

CXP: Collision cell exit potential

EP: Entrance potentials

Figure 7. Q1 (a) and Precursor Ion Mass Spectra (b) of CZ48

(a)



(b)

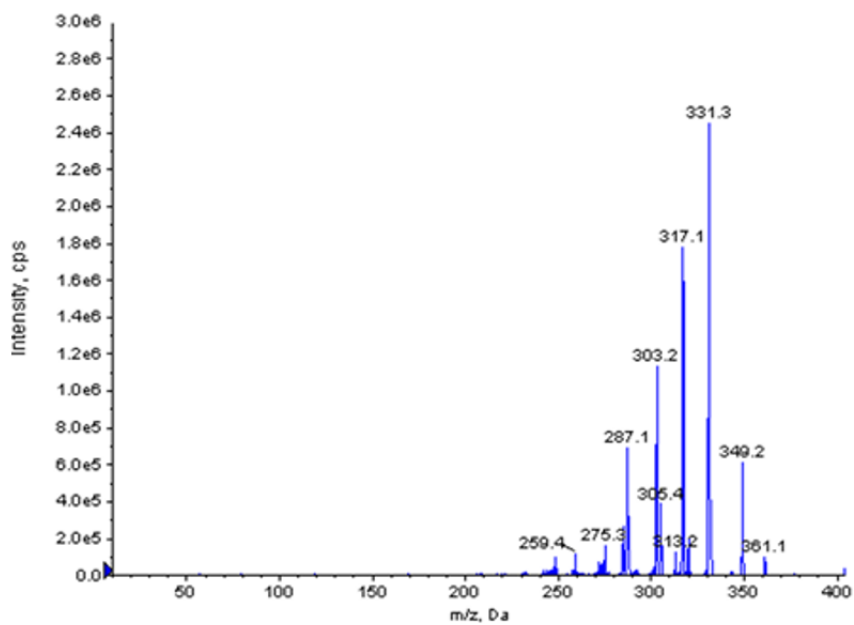
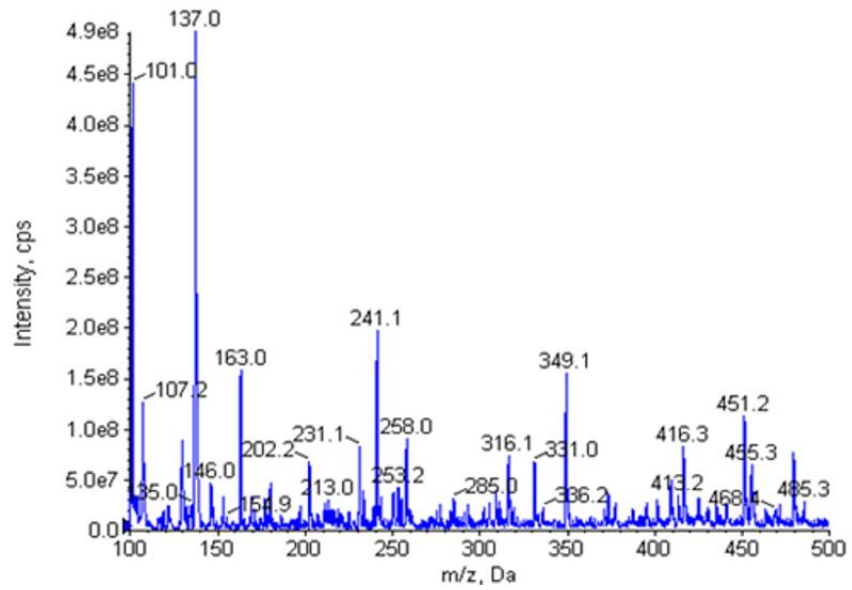


Figure 8. Q1 (a) and Precursor Ion Mass Spectra (b) of CPT

(a)



(b)

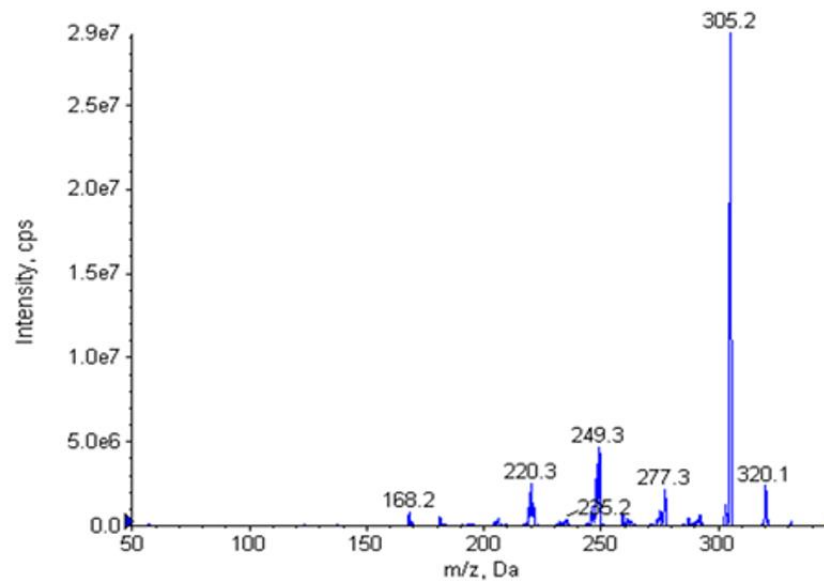
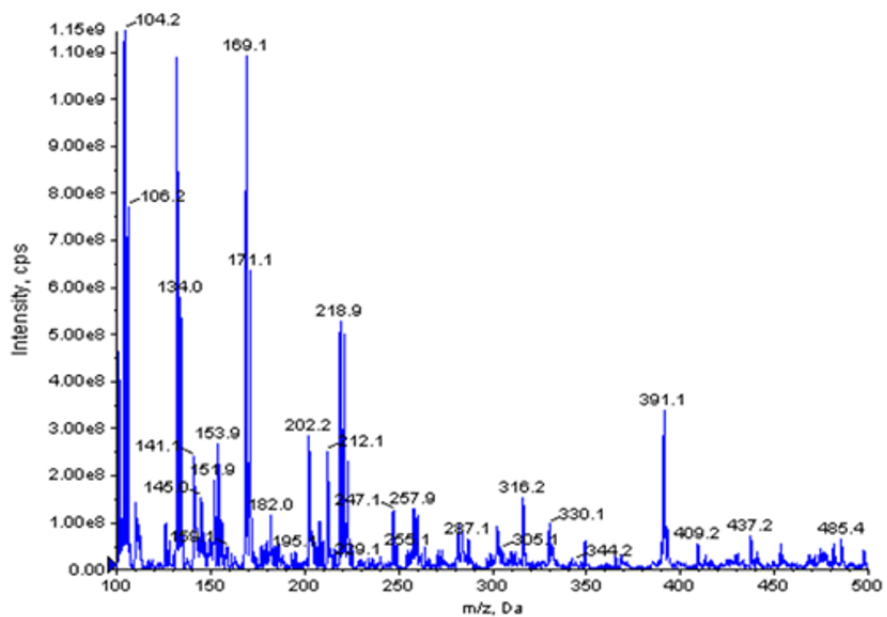
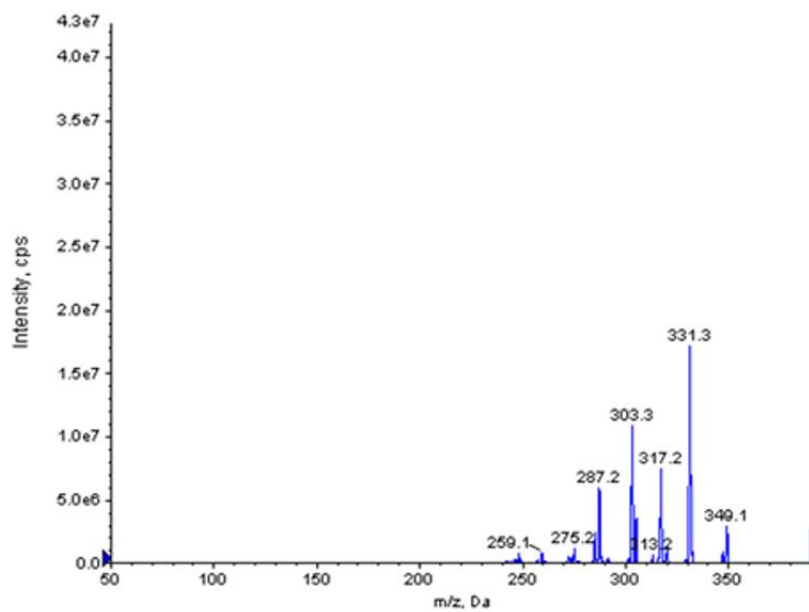


Figure 9. Q1 (a) and Precursor Ion Mass Spectra (b) of CZ44

(a)



(b)



#### **3.2.6.4 Method Validation for UPLC-MS/MS Assay**

The developed method was validated using the API 3200 system by following the US Food and Drug Administration (FDA) Guidance for Industry: Bioanalytical Method Validation (2013) (61). The validation included linearity, intra- and inter-day accuracy and precision, extraction recovery, matrix effect, short-term stability, and long-term stability for rat plasma. The method for rat bile was partially validated including linearity, intra- and inter-day accuracy and precision, extraction recovery, and matrix effect. In the validation process, stock solutions of CZ48 and CPT were freshly prepared on the day of analysis. Blank and zero blank rat or bile samples were included in each analysis.

##### **3.2.6.4.1 Linearity and Sensitivity (Lower Limit of Quantification, LLOQ)**

The linear ranges of calibration curves for CZ48 and CPT were 0.98 (LLOQ) – 1000 ng/ml in plasma and 3.9 (LLOQ) – 1000 ng/ml in bile. The linearity was evaluated on 3 separate days. Due to a low concentration of CPT in rat plasma after an oral dose of CZ48-CoS or CZ48-NS, the API 5500 system was employed to achieve the required higher sensitivity. In this system, the linear ranges of calibration curves were 0.98 (LLOQ) – 250 ng/ml for CZ48 and 0.45 (LLOQ) – 250 ng/ml for CPT in plasma.

#### **3.2.6.4.2 Intra- and Inter-Day Accuracy and Precision**

Accuracy and Precision were evaluated at three quality control (QC) concentrations of CZ48 and CPT (2, 40, and 800 ng/ml) in plasma and two QC concentrations of CZ48 and CPT (10 and 800 ng/ml) in bile (n=6 at each concentration). The accuracy and precision values were calculated as shown below.

$$\text{Accuracy (\%)} = (\text{Mean observed concentration}^*) / (\text{Nominal concentration}) \times 100 \quad (\text{Eq. 1})$$

$$\text{Precision} = \text{Relative standard deviation (R.S.D)} \quad (\text{Eq. 2})$$

\* The mean observed concentration was calculated using a calibration curve.

#### **3.2.6.4.3 Extraction Recovery and Matrix Effect**

The extraction recoveries and matrix effects of CZ48 and CPT were evaluated at three QC concentrations (2, 40, and 800 ng/ml, n=6 for each concentration) in plasma and two QC concentrations (10 and 800 ng/ml, n=6 for each concentration) in bile. The recovery was calculated by comparing the peak area ratio of pre-extracted CZ48 (or CPT) to IS in plasma (or bile) with the ratio of post-extracted analytes to IS in plasma (or bile). The matrix effect was evaluated by comparing the peak area of post-extracted analytes in plasma (or bile) with the peak area of analytes in neat solution.

#### **3.2.6.4.4 Stability Tests**

Stability tests included bench-top (short-term), 3 cycles of freeze and thaw, processed stability in autosampler, and long-term stability at three QC concentrations of CZ48 and CPT, 2, 40, and 800 ng/ml, in plasma. The bench-top stability was evaluated by placing QC samples at room temperature for 4 hr. The freeze and thaw stability was evaluated after 3 cycles of freeze-thaw by completely thawing QC samples at room temperature and re-freezing them at -80 °C. The processed stability was evaluated by placing QC samples in an autosampler at 10 °C for 24 hr after extraction and reconstitution processes. For the long-term stability, QC samples were kept in a -80 °C freezer for 3 months. After each storage condition and period, QC concentrations of CZ48 and CPT were calculated by constructing calibration curves freshly prepared on the day of analysis. The observed concentrations were compared with nominal QC concentrations, and relative errors were calculated.

### **3.2.7 Biliary Excretions of CZ48 and CPT After an Intravenous Dose of CZ48-CoS**

#### **3.2.7.1 Surgical Procedure for Bile Duct-Cannulation**

All experiments were conducted in accordance with an approved animal protocol from the IACUC at the University of Houston. Male Sprague Dawley (SD) rats (250 – 300 g) with jugular vein-cannulation were purchased from the Envigo (Indianapolis, IN). Rats (n=3) were maintained in individually ventilated cages under standard laboratory conditions (12-hour light/dark cycle), and allowed free access to food and water. Bile duct-cannulation was performed by a graduate student in Dr. Ming Hu's laboratory based on an approved animal protocol in his laboratory from the IACUC at the University of Houston. The rats were anesthetized by intramuscular injection of 50 % (w/v) urethane solution. Half of the dose (2 gram/kg body weight) of urethane was used to maintain anesthesia throughout the experiments for collecting bile. Bile duct-cannulation was performed when rats are completely under the anesthetic plane. The rats were placed on the heating pads and the skin was sterilized with alcohol swabs. The abdominal skin was held upwards approximately 3 cm and a deep incision (1 cm) was made on the very bottom part of the rat abdominal skin. Four to five cm long incision was made and duodenum region of the small intestine was found under the stomach. Bile duct was separated by removing surrounding fatty tissues. A PE-

10 tube was inserted in bile duct after making a small cut with a microvascular scissor. Bile was collected into a microcentrifuge tube.

### **3.2.7.2 Animal Study Protocol**

A single dose of CZ48-CoS was intravenously administered to bile duct-cannulated SD rats (n=3) at 5 mg/kg through a jugular vein (Group A in Table 4). Blood was withdrawn through the tail vein at 15, 30, 45 min, 1, 2, 3, 4 and 6 hr post-dose. Bile was collected at 30-min intervals through a cannula inserted into bile duct. Plasma was collected after centrifugation of blood at 4 °C at 9,168 xg for 10 min. Bile samples were weighted and the volume of bile was calculated by assuming the density of bile is 1 g/ml. All plasma and bile samples were stored at -80 °C until analysis. CZ48 and CPT in plasma and bile samples were quantified by using the developed and validated analytical method using UPLC-MS/MS as described in the section 3.2.6.

### **3.2.7.3 Pharmacokinetic Analysis**

PK parameters of CZ48 and CPT, such as  $AUC_{0-6h}$ ,  $t_{1/2}$ , and clearance (CL), were estimated based on 1-compartment model using Phoenix<sup>®</sup> WinNonlin (6.4) software. Biliary clearance ( $CL_b$ ) was calculated as follows:

$$CL_b = A_b / AUC_{0-6h, plasma} \quad (\text{Eq. 3})$$

$A_b$ : Cumulative amount of CZ48 or CPT secreted into the bile for 6 hr.

$AUC_{plasma}$ : Area under the curve in plasma concentration-time profile of CZ48 or CPT for 6 hr.

### **3.2.8 Biliary Excretions and Enterohepatic Recycling of CZ48 and CPT after an Oral Dose of CZ48**

#### **3.2.8.1 Animal Study Protocol for the Evaluation of Biliary Excretion**

All experiments were conducted in accordance with an approved animal protocol from the IACUC at the University of Houston. Male SD rats (230 – 280 g) with bile duct-cannulation were purchased from the Envigo (Indianapolis, IN). Rats were maintained in individually ventilated cages under standard laboratory conditions (12-hour light/dark cycle), and allowed free access to food and water. Rats were randomly divided into two groups for a CZ48-CoS (n=7) or CZ48-NS (n=3) dosing.

A single oral dose (25 mg/kg) of CZ48-CoS (Group B in Table 4) or CZ48-NS (Group C in Table 4) was administered to bile duct-cannulated SD rats via oral gavage. Rats were anesthetized using inhalation of isoflurane to collect blood and bile samples. Blood samples of 300  $\mu$ l were withdrawn through the tail vein at 15,

30 min, 1, 2, 4, 6, 8, and 12 hr post-dose. Bile (~100 µl) was intermittently collected for 2-10 min depending on the bile flow rate of each rat at 1, 2, 3, 4, 5, 6, 8, 10, and 12 hr. Plasma was collected after the centrifugation of blood sample at 4 °C at 9,168 xg for 10 min. Bile samples were weighted and the volume of bile was calculated by assuming the density of bile is 1 g/ml. All plasma and bile samples were stored at -80 °C until analysis. CZ48 and CPT in plasma and bile samples were quantified by using the developed and validated analytical method using UPLC-MS/MS as described in the section 3.2.6.

#### **3.2.8.2 Animal Study Protocol for the Characterization of Enterohepatic Recycling**

All experiments were conducted in accordance with an approved animal protocol from the IACUC at the University of Houston. Male SD rats (230 – 280 g) with or without bile duct-cannulation were purchased from the Envigo (Indianapolis, IN). Bile duct-cannulated rats were maintained in individual ventilated cages and rats without surgery were maintained in combined cages (2 rats per cage) under standard laboratory conditions (12-hour light/dark cycle). Rats were allowed free access to food and water. Rats were randomly divided into experimental groups, Group D (6 rats with bile duct-cannulation) and Group E (4 rats without bile duct-cannulation) shown in Table 4.

To characterize enterohepatic recycling of CZ48 and CPT, CZ48-NS was orally administered in a single dose at 25 mg/kg to bile duct-cannulated or bile duct-intact SD rats. Enterohepatic recycling was experimentally interrupted or not by collecting bile in three different ways, intermittently (Group C in Table 4), continuously (Group D in Table 4), or without collecting bile (Group E in Table 4). In Group C, bile was intermittently collected from bile duct-cannulated rats for 2-10 min (n=3) depending on the bile flow rate of each rat. Thus, bile circulation and drug recycling were existed during experiments, but only interrupted when bile samples were collected at designated time points. In Group D, bile was continuously collected from bile duct-cannulated rats (n=6), which interrupted drug reabsorption into the intestine (Figure 10). As a consequence, enterohepatic recycling of CZ48 and CPT was completely interrupted during experiments. In Group E, bile was not collected since bile duct-intact rats (n=4) were used. Bile circulation and enterohepatic recycling were completely protected during experiments.

### **3.2.8.3 Pharmacokinetic (PK) and Statistical Analyses**

AUC<sub>0-t</sub> after an oral dose of CZ48 were estimated based on the trapezoidal rule (non-compartment analysis). To compare the biliary excretions of CZ48 and CPT among different dosing and formulation groups, concentrations or AUC<sub>0-t</sub> ratios of

CZ48 (or CPT) in bile to plasma (B/P) were calculated. For the statistical analysis, normality of data was evaluated using Shapiro-Wilk Normality test in RStudio® 1.0.153. The ratios were statistically compared between IV and oral dosing groups or between CoS and NS groups at  $P < 0.05$  using Student's t-test or nonparametric test (Mann-Whitney test).

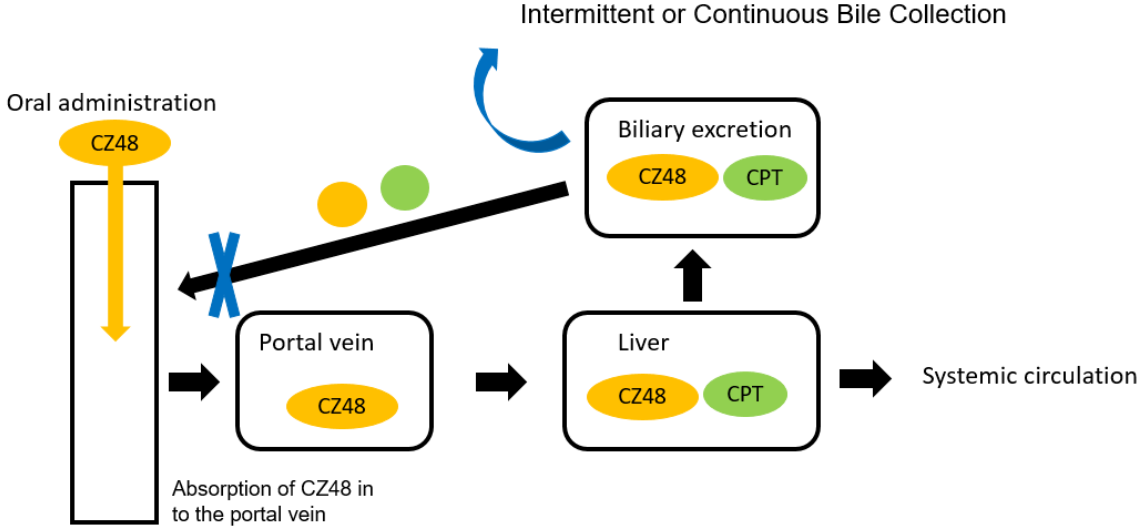
Table 4. Animal Study Design for Evaluation of Biliary Excretions of CZ48 and CPT and Characterization of Their Enterohepatic Recycling

	Group				
	A	B	C	D	E
Formulations	CoS	CoS	NS	NS	NS
Dosing Routes	Intravenous	Oral	Oral	Oral	Oral
Bile Duct in Rats	Cannulated	Cannulated	Cannulated	Cannulated	Intact
Bile Collections	Continuous	Intermittent	Intermittent	Continuous	No
Entero-hepatic Recycling	No	Yes	Yes	No	Yes

CoS: Co-solvent formulation

NS: Nanosuspension formulation (200 nm)

Figure 10. Experimental Design for the Interruption of Enterohepatic Recycling of CZ48 and CPT



### **3.2.9 The Population Pharmacokinetic (PK) Modeling for the Biliary Excretions of CZ48 and CPT**

A population PK model was established to describe biliary excretions of CZ48 and CPT using *in vivo* PK data collected from Group B and C in Table 4. By comparing model parameters between Group B and C, the impacts of nanosuspension on PK and biliary excretions of CZ48 and CPT were evaluated. Pharsight Phoenix Non-Linear Mixed Effects (NLME)<sup>TM</sup> 1.3 software was employed to establish the population PK model. The error model was multiplicative, and First Order Conditional Estimation Extended Least Squares (FOCE ELS) was used for population PK modeling. For the model estimation, Coefficient of Variation (CV) % of estimated parameters and the quality of diagnostic goodness of fit plots including the Dependent Variable (DV) versus Individual Predicted Estimates (IPRED), DV versus Population Predictions (PRED), Conditional Weighted Residuals (CWRES) versus Time After Dose (TAD), and Quantile-Quantile Plot of the Individual Weighted Residuals (QQ IWRES) were monitored and compared. The developed population PK model was validated in two procedures, bootstrapping and Visual Predictive Check (VPC), using Phoenix NLME. Bootstrapping (resampling technique) was performed by creating 145-200 bootstrap replicates from original data, and median, lower 2.5 %, and the upper 97.5 % values were calculated for each PK parameter. In addition, VPC plots were presented to illustrate observed data (concentrations of CZ48 in plasma and CPT

in plasma and bile) with predictive median and 90 % percentile interval derived from 1,000 simulations.

## Chapter 4. Results

### 4.1 Biodistributions of CZ48 and CPT

Biodistributions of CZ48 and CPT were characterized in six mouse organs including liver, kidney, spleen, lung, brain, and heart, which were harvested from human tumor-xenografted mice after a single IV dose of CZ48 in co-solvent (CoS) at 5 mg/kg or nanosuspension (NS) at 25 mg/kg. Tumor cells were also collected after the last IV dose of CZ48-CoS or CZ48-NS in twice weekly regimen for 4 weeks.

#### 4.1.1 Biodistributions of CZ48 from Co-S or NS in Tumor-Xenografted Mice

The concentration versus time profiles of CZ48 in the tested organs and tumor were shown in Figure 11.  $AUC_{0-4h}/Dose$  and half-life values of CZ48 from Co-S or NS were presented in Table 5.

After a CZ48-CoS dosing, the organ exposure ( $AUC_{0-4h}/Dose$ ) of CZ48 was the highest in the lung, which was  $1462.96 \pm 231.41$  [(ng\*h/g)/(mg/kg)]. The lowest exposure was observed in the brain ( $86.92 \pm 5.05$  [(ng\*h/g)/(mg/kg)]). The CZ48 exposures were intermediate in the liver, kidney, heart, spleen, and tumor, which were  $813.03 \pm 50.14$ ,  $566.26 \pm 50.37$ ,  $469.75 \pm 20.35$ ,  $357.97 \pm 55.16$ , and  $263.25$

$\pm 27.46$  [(ng\*h/g)/(mg/kg)], respectively. CZ48 from CoS was highly exposed in the following order: lung, liver, kidney, heart, spleen, tumor, and brain (Figure 12). Half-lives of CZ48 from CoS were about 0.6 – 0.8 hr in the tumor and tested organs.

After a CZ48-NS dosing, the exposure of CZ48 was significantly increased in the liver and spleen. In the liver and spleen, the CZ48 exposures were  $19171.15 \pm 1800.63$  and  $5755.31 \pm 653.85$  [(ng\*h/g)/(mg/kg)], respectively, which were approximately 23.6- and 16.1-fold of those from Co-S ( $813.03 \pm 50.14$  and  $357.97 \pm 55.16$  [(ng\*h/g)/(mg/kg)]). The CZ48 exposures were  $1052.41 \pm 161.02$ ,  $394.22 \pm 40.60$ ,  $237.87 \pm 29.39$ ,  $26.93 \pm 0.93$ , and  $116.44 \pm 4.11$  [(ng\*h/g)/(mg/kg)] in lung, kidney, heart, brain, and tumor, respectively, in the NS group, which were significantly decreased from CoS. CZ48 from NS was highly exposed in the following order: liver, spleen, lung, kidney, heart, tumor, and brain (Figure 12). Half-lives of CZ48 from NS were between 1.03 – 1.97 hr, which were about 1.5 – 2.8 times extended by NS as compared to those by Co-S (0.58 – 0.75 hr). Due to the sustained release of CZ48 from NS, prolonged exposures of CZ48 were observed in all tested organs and tumor. As shown in Figure 11, CZ48 concentrations in the NS group declined slowly and blood level was sustained, but the concentrations in the CoS group decreased more rapidly.

Figure 11. Concentration versus Time Profiles of CZ48 and CPT from Co-S or NS in Tumor-Xenografted Swiss Nude Mice (Mean  $\pm$  SD, n=3 per Time Point for Each Formulation)

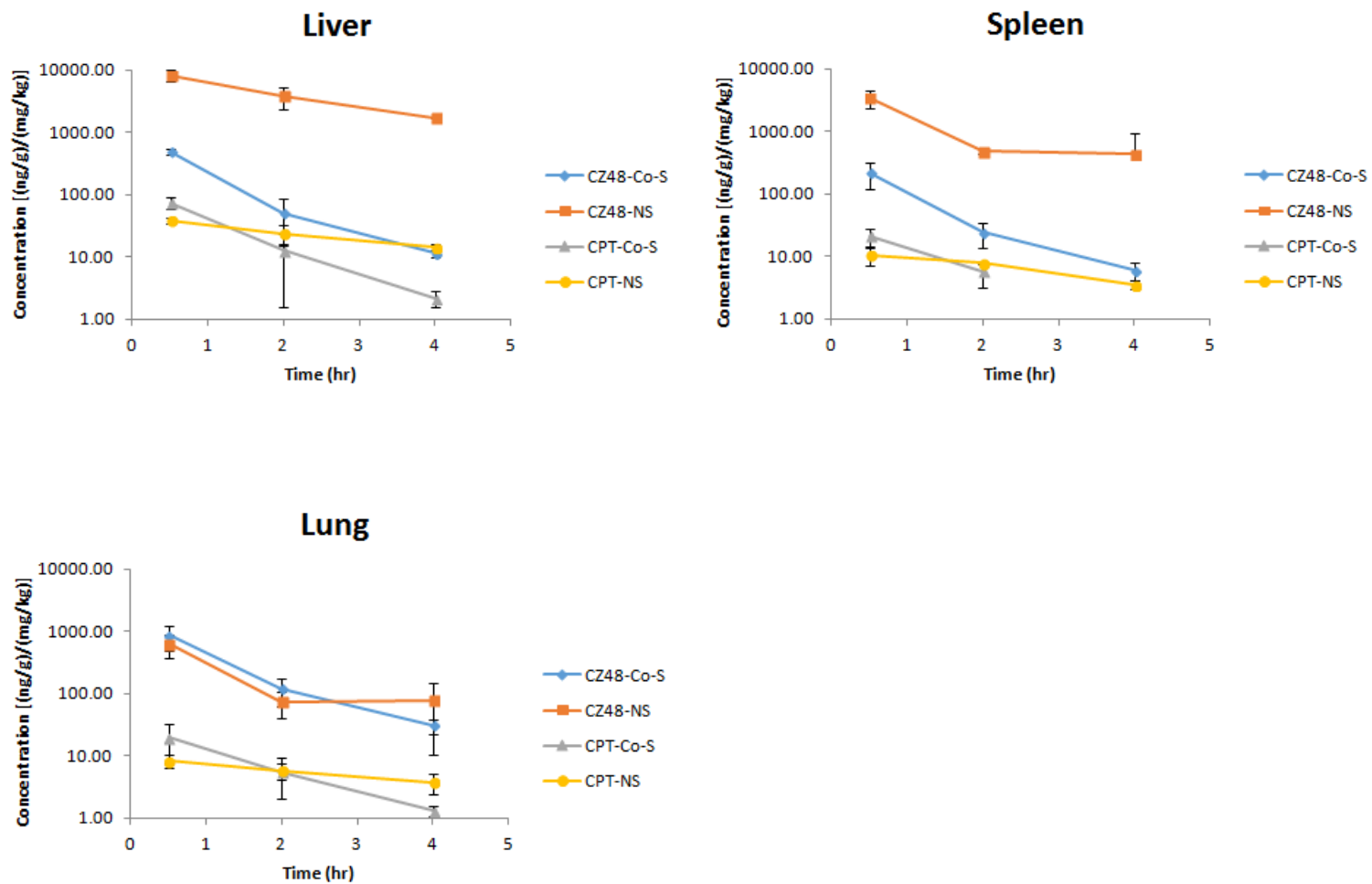


Figure 11 (Cont). Concentration versus Time Profiles of CZ48 and CPT from Co-S or NS in Tumor- Xenografted Swiss Nude Mice (Mean  $\pm$  SD, n=3 per Time Point for Each Formulation)

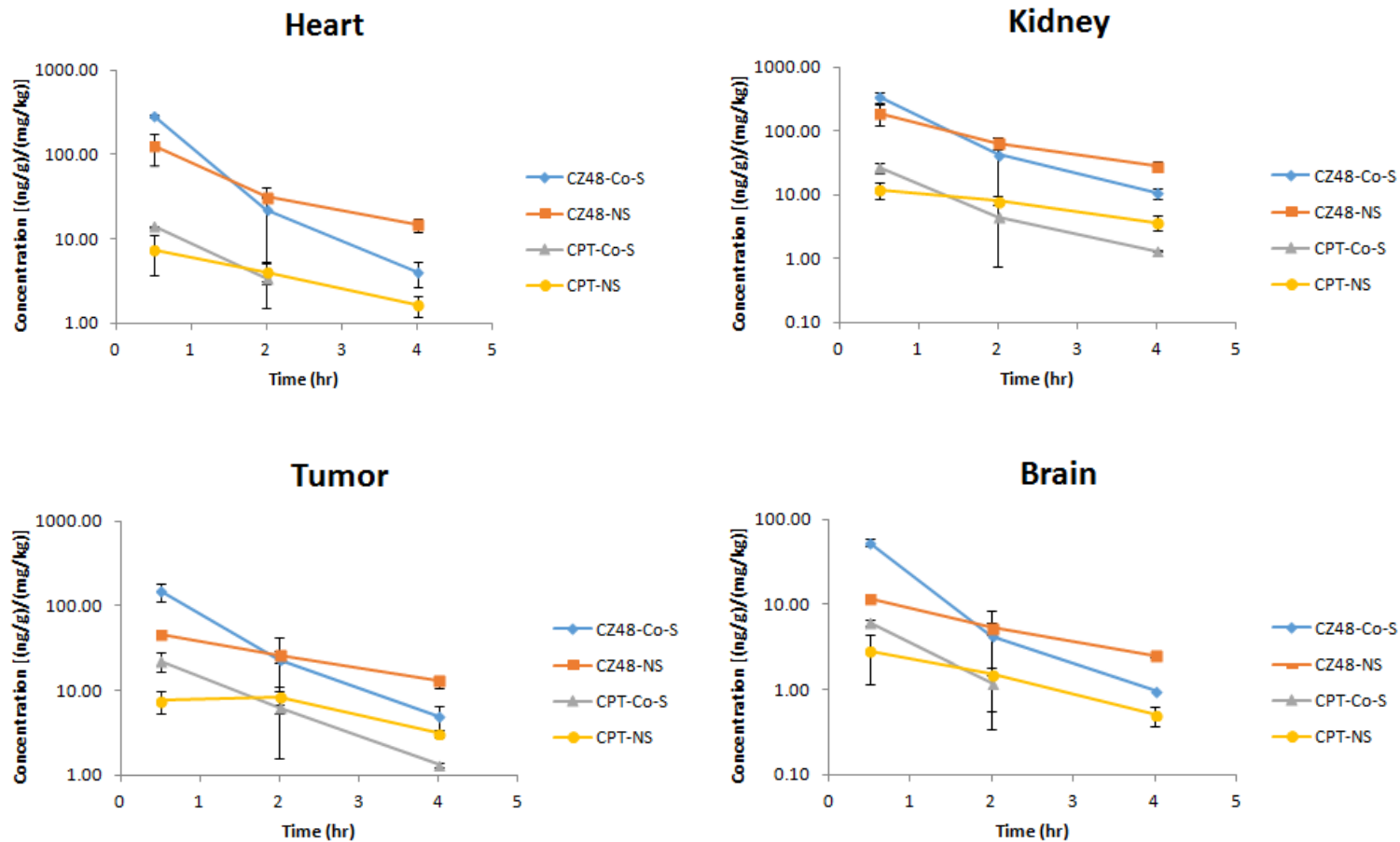


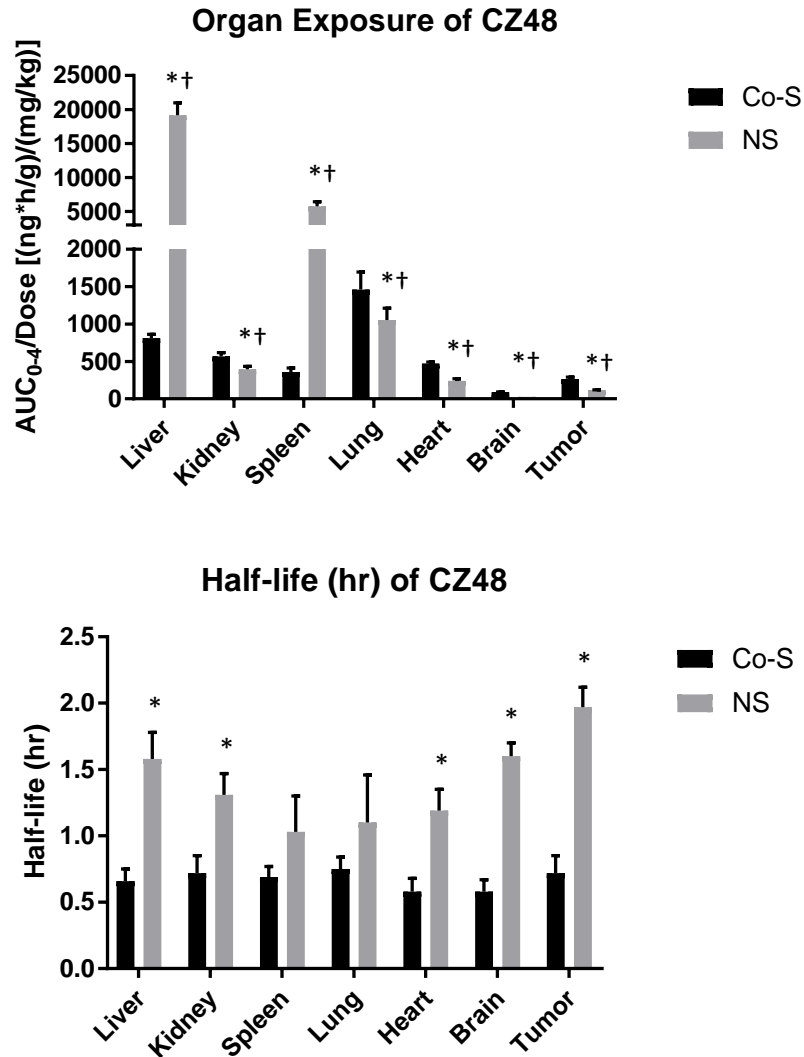
Table 5. Biodistribution Parameters of CZ48 from Co-S or NS in Tumor-Xenografted Mice (Mean  $\pm$  SD, n=3)

CZ48						
	AUC <sub>0-4h</sub> (ng*h/g)/(mg/kg)			Half-life (hr)		
	CoS	NS	NS/ CoS	CoS	NS	NS/ CoS
Liver	813.03 $\pm$ 50.14	19171.15 $\pm$ 1800.63 *†	23.58	0.66 $\pm$ 0.09	1.58 $\pm$ 0.20 *	2.39
Spleen	357.97 $\pm$ 55.16	5755.31 $\pm$ 653.85 *†	16.08	0.69 $\pm$ 0.08	1.03 $\pm$ 0.27	1.49
Lung	1462.96 $\pm$ 231.41	1052.41 $\pm$ 161.02 *†	0.72	0.75 $\pm$ 0.09	1.10 $\pm$ 0.36	1.47
Kidney	566.26 $\pm$ 50.37	394.22 $\pm$ 40.60 *†	0.70	0.72 $\pm$ 0.13	1.31 $\pm$ 0.16 *	1.82
Heart	469.75 $\pm$ 20.35	237.87 $\pm$ 29.39 *†	0.51	0.58 $\pm$ 0.10	1.19 $\pm$ 0.16 *	2.05
Tumor	263.25 $\pm$ 27.46	116.44 $\pm$ 4.11 *†	0.44	0.72 $\pm$ 0.13	1.97 $\pm$ 0.15 *	2.74
Brain	86.92 $\pm$ 5.05	26.93 $\pm$ 0.93 *†	0.31	0.58 $\pm$ 0.09	1.60 $\pm$ 0.10 *	2.76

AUC<sub>0-4h</sub>/Dose: Parameters were significantly different between CoS and NS groups in each organ and tumor when P<0.05 (\*) or P<0.0073 (†, Bonferroni adjusted). t-distribution test

t<sub>1/2</sub>: \* Parameters were significantly different between CoS and NS groups in each organ and tumor (P<0.05)

Figure 12. Comparison of Organ Exposure and Half-Life of CZ48 Between CoS and NS in Tumor-Xenografted Mice (Mean  $\pm$  SD, n=3 for Each Formulation Group)



AUC<sub>0-4h</sub>/Dose: Parameters were significantly different between Co-S and NS groups in each organ and tumor when P<0.05 (\*) or P<0.0073 (†, Bonferroni adjusted). t-distribution test

t<sub>1/2</sub>: \* Parameters were significantly different between Co-S and NS groups in each organ and tumor (P< 0.05)

#### 4.1.2 Biodistributions of CPT from Co-S or NS in Tumor-Xenografted Mice

The concentration versus time profiles of CPT in the tested organs and tumor were shown in Figure 11.  $AUC_{0-4h}/Dose$  and half-life values of CPT from Co-S or NS were represented in Table 6.

After a CZ48-CoS dosing, the exposure ( $AUC_{0-4h}/Dose$ ) of CPT was the highest in the liver, which was  $131.26 \pm 14.26$  [(ng\*h/g)/(mg/kg)]. The lowest exposure of CPT was observed in the brain ( $10.29 \pm 0.81$  [(ng\*h/g)/(mg/kg)]). The CPT exposures were  $46.16 \pm 4.82$ ,  $43.02 \pm 5.78$ ,  $37.91 \pm 7.85$ ,  $36.76 \pm 5.30$ , and  $24.42 \pm 2.30$  [(ng\*h/g)/(mg/kg)] in kidney, tumor, lung, spleen, and heart, respectively. CPT from CZ48-CoS was exposed in the decreasing order as follows: liver, kidney, tumor, lung, spleen, heart, and brain. Half-lives of CPT in the CoS group were about 0.6 – 0.9 hr in tumor and all tested organs.

After a CZ48-NS dosing, the CPT exposure was the highest in the liver ( $104.54 \pm 9.34$  [(ng\*h/g)/(mg/kg)]) and the lowest ( $6.90 \pm 0.96$  [(ng\*h/g)/(mg/kg)]) in the brain (Table 6 and Figure 13). The CPT exposures were  $33.53 \pm 2.41$ ,  $31.04 \pm 2.09$ ,  $28.06 \pm 2.09$ ,  $24.80 \pm 2.23$ , and  $18.40 \pm 2.44$  [(ng\*h/g)/(mg/kg)] in kidney, spleen, tumor, lung, and heart, respectively, which were significantly decreased by NS

compared to those in the Co-S group, about 65 – 84 % of those in the CoS group. CPT from CZ48-NS was exposed in a decreasing order as follows: liver, kidney, spleen, tumor, lung, heart, and brain. Similar to CZ48, a prolonged exposure of CPT was achieved by the sustained release of CZ48 from NS. Half-lives of CPT from NS were 1.47 – 2.93 hr, which were significantly increased (2.3 – 3.6 times) by NS in all tested organs and tumor than those by CoS (0.64 – 0.92 hr). As shown in Figure 11, CPT concentrations were more rapidly decreased after a CZ48-CoS dosing, so that concentrations at 4 hr post dose were not detectable (under LLOQ) in spleen, heart, and brain. However, the slopes of concentration-time profiles of CPT after a CZ48-NS dosing were declined slowly, so that CPT from CZ48-NS stayed in organs and tumor for a prolonged period of time.

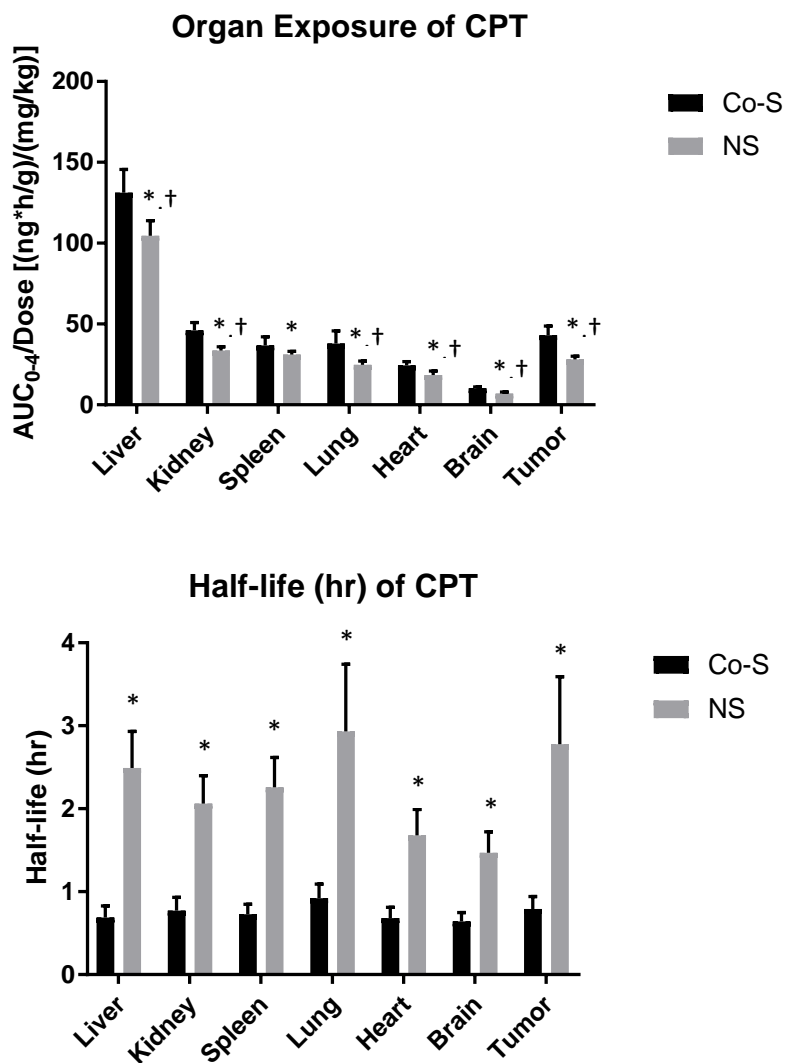
Table 6. Biodistribution Parameters of CPT from Co-S or NS in Tumor-Xenografted Mice (Mean  $\pm$  SD, n=3)

CPT						
	AUC <sub>0-4h</sub> (ng*h/g)/(mg/kg)			Half-life (hr)		
	CoS	NS	NS/ CoS	CoS	NS	NS/ CoS
Liver	131.26 $\pm$ 14.26	104.54 $\pm$ 9.34 *†	0.80	0.69 $\pm$ 0.14	2.49 $\pm$ 0.44 *	3.61
Kidney	46.16 $\pm$ 4.82	33.53 $\pm$ 2.41 *†	0.73	0.77 $\pm$ 0.16	2.06 $\pm$ 0.34 *	2.68
Spleen	36.76 $\pm$ 5.30	31.04 $\pm$ 2.09 *	0.84	0.73 $\pm$ 0.12	2.26 $\pm$ 0.36 *	3.10
Tumor	43.02 $\pm$ 5.78	28.06 $\pm$ 2.09 *†	0.65	0.79 $\pm$ 0.15	2.78 $\pm$ 0.81 *	3.52
Lung	37.91 $\pm$ 7.85	24.80 $\pm$ 2.23 *†	0.65	0.92 $\pm$ 0.17	2.93 $\pm$ 0.81 *	3.18
Heart	24.42 $\pm$ 2.30	18.40 $\pm$ 2.44 *†	0.75	0.68 $\pm$ 0.13	1.68 $\pm$ 0.31 *	2.47
Brain	10.29 $\pm$ 0.81	6.90 $\pm$ 0.96 *†	0.67	0.64 $\pm$ 0.11	1.47 $\pm$ 0.25 *	2.30

AUC<sub>0-4h</sub>/Dose: Parameters were significantly different between CoS and NS groups in each organ and tumor when P<0.05 (\*) or P<0.0073 (†, Bonferroni adjusted). t-distribution test

t<sub>1/2</sub>: \* Parameters were significantly different between CoS and NS groups in each organ and tumor (P<0.05)

Figure 13. Comparison of Organ Exposure and Half-Life of CPT Between CoS and NS in Tumor-Xenografted Mice (Mean  $\pm$  SD, n=3 for Each Formulation Group)



AUC<sub>0-4h</sub>/Dose: Parameters were significantly different between Co-S and NS groups in each organ and tumor when P<0.05 (\*) or P<0073 (†, Bonferroni adjusted). t-distribution test

t<sub>1/2</sub>: \* Parameters were significantly different between Co-S and NS groups in each organ and tumor (P< 0.05)

### **4.1.3 Comparison of Biodistribution Patterns of CZ48 and CPT Between Healthy and Tumor-Xenografted Mice**

Biodistribution patterns of CZ48 and CPT in healthy Swiss nude mice were previously evaluated after the same IV dose of CZ48-CoS or CZ48-NS (29). Six tested organs were collected till 12 hr post IV dose (n=4) in healthy mice (29), and till 4 hr post IV dose in tumor-xenografted mice (n=3).  $AUC_{0-\infty}/Dose$  values were used to compare organ exposures of CZ48 and CPT between the two mouse models.

The biodistribution patterns were similar between healthy and tumor-xenografted mice. After an IV dose of CZ48-CoS, CZ48 was highly distributed into lung, liver, and kidney, and the exposures were comparable between healthy and tumor xenografted mice. The CZ48 exposures ( $AUC_{0-\infty}/Dose$ ) were 1038.38, 690.54, and 604.57 [(ng\*h/g)/(mg/kg)] in lung, liver, and kidney in healthy mice, and 1496.54, 824.02, and 577.40 [(ng\*h/g)/(mg/kg)] in tumor-xenograft mice, respectively. CPT was highly distributed in the liver, as compared to other organs (Figure 14). The exposures of CPT in the liver were 99.03 and 133.43 [(ng\*h/g)/(mg/kg)] in healthy and tumor-xenografted mice, respectively, which indicated its comparable exposures between the mouse models. The exposures of CPT were comparable between healthy and tumor-xenografted mice in other tested organs. The CPT

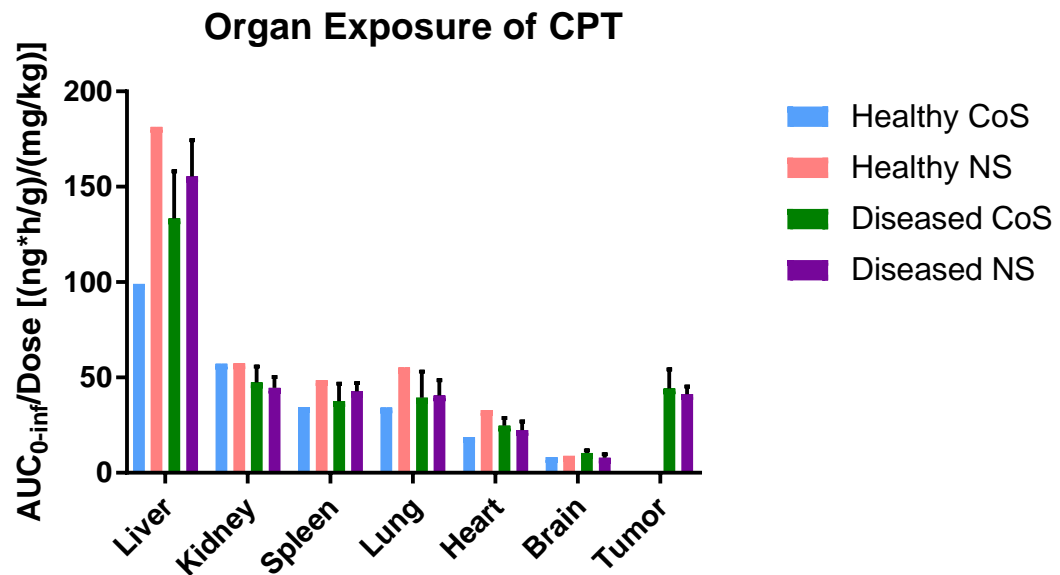
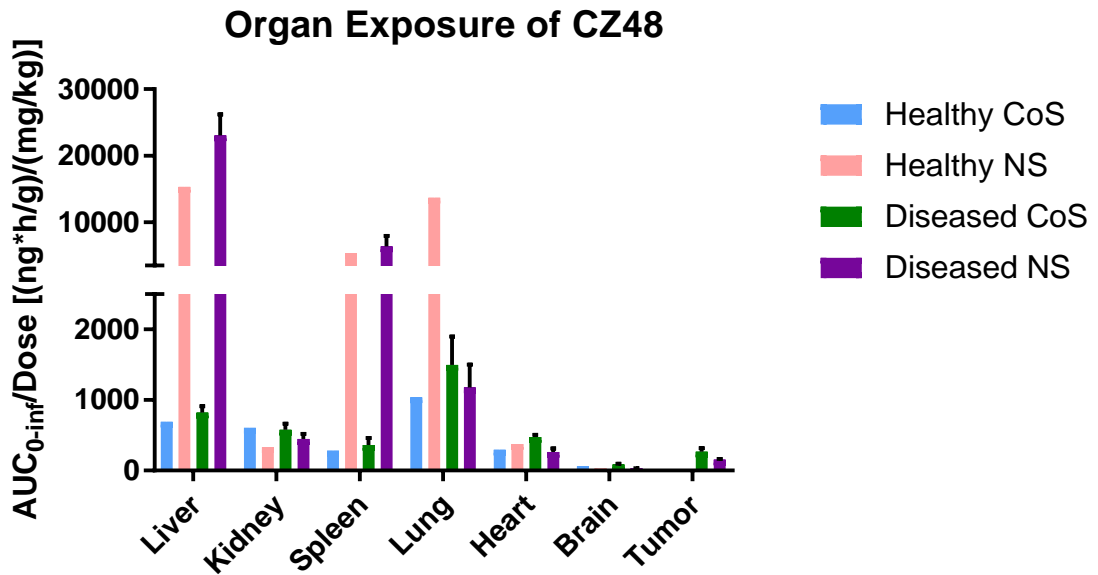
exposures were 57.25, 34.34, 34.18, 18.75, and 8.25 [(ng\*h/g)/(mg/kg)] in kidney, spleen, lung, heart, and brain in healthy mice, and 47.38, 37.53, 39.50, 24.80, and 10.42 [(ng\*h/g)/(mg/kg)] in tumor-xenografted mice, respectively.

NS remarkably increased the exposures of CZ48 in the liver and spleen in both healthy and tumor-xenografted mice. The CZ48 exposures from NS in the liver were 15324.07 and 23073.8 [(ng\*h/g)/(mg/kg)] in healthy and tumor-xenografted mice, respectively, which were approximately 22.2 and 28.0 times of those from CoS (690.54 and 824.02 [(ng\*h/g)/(mg/kg)] in healthy and tumor-xenografted mice, respectively). In other organs (except in lung), the CZ48 exposures were comparable between CoS and NS groups in both mouse models as shown in Figure 14. In the liver, the exposure of CPT from CZ48-NS was 181.38 [(ng\*h/g)/(mg/kg)], which was approximately 1.8 times of that from CZ48-CoS, 99.03 [(ng\*h/g)/(mg/kg)], in healthy mice. However, the CPT exposures were comparable in the liver in tumor-xenografted mice, which were 133.43 and 155.48 [(ng\*h/g)/(mg/kg)] in the CoS and NS groups, respectively. As shown in Figure 14, the CPT exposures were comparable in other tested organs between healthy and tumor-xenografted mice.

Half-lives of CZ48 and CPT were compared between healthy and tumor-xenografted mice (Figure 15). Half-lives of CZ48 in the NS group were 1.96 – 38.21 and 1.03 – 1.60 hr in healthy and tumor-xenografted mice, respectively, which were about 1.76 – 19.11 and 1.49 – 2.76 times of those in the CoS group (0.62 – 2.00 and 0.58 – 0.75 hr in healthy and tumor-xenografted mice, respectively). Half-life of active moiety, CPT, was also extended by NS. The half-lives of CPT from CZ48-NS were 2.99 – 7.28 and 1.47 – 2.93 hr in healthy and tumor-xenografted mice, respectively, which were approximately 2.81 – 9.45 and 2.30 – 3.61 times of those from CZ48-CoS (0.68 – 1.48 and 0.64 – 0.92 in healthy and tumor-xenografted mice, respectively). Prolonged exposures of CZ48 and CPT by NS in all tested organs in both healthy and tumor-xenografted mice supported the merit of NS for the effective antitumor activity of CPT after an IV dose of CZ48-NS. Half-lives of CZ48 and CPT were more dramatically increased by NS in healthy mice (1.76 – 19.11 times) than those in tumor xenografted mice (1.49 – 3.61 times).

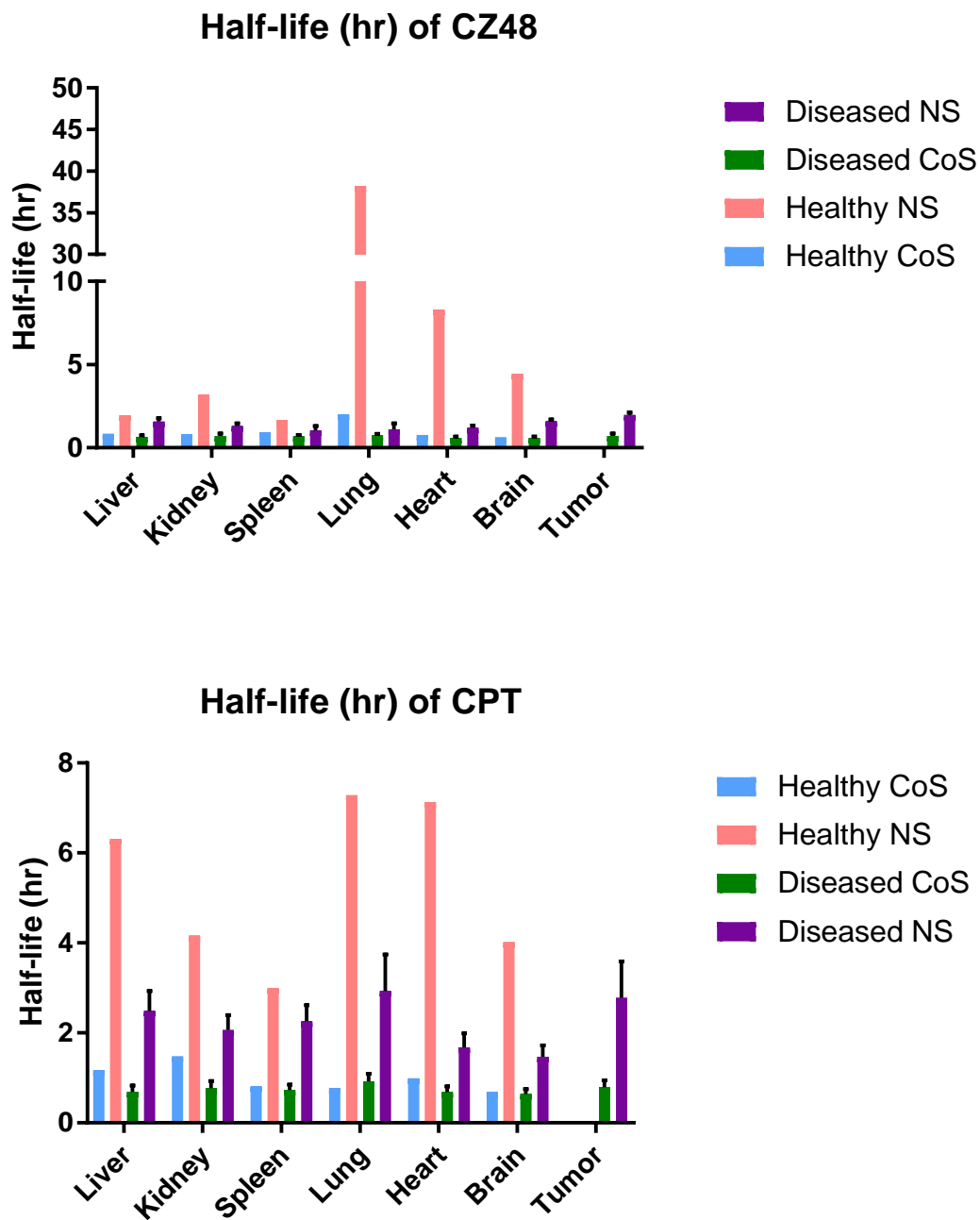
One remarkable discrepancy between healthy and tumor-xenografted mice was observed in the biodistribution pattern of CZ48 in lung. The CZ48 exposure was highly increased 13.2 times by NS in the lung of healthy mice. On the contrary, the exposure was unaffected by NS in tumor-xenografted mice.

Figure 14. Organ Exposures (Dose Adjusted  $AUC_{0-\infty}$ ) of CZ48 and CPT in Healthy and Tumor-Xenografted Mice (n=3)



- Data from healthy mice (29)

Figure 15. Comparison of Half-Lives of CZ48 and CPT after an IV Dose of CZ48-CoS or CZ48-NS between Healthy and Tumor-Xenografted Mice (n=3)



- Data from healthy mice (29)

## **4.2 Method Development and Validation Using UPLC-MS/MS**

The UPLC-MS/MS assay was developed for the simultaneous quantifications of CZ48 and CPT in rat plasma and bile. This analytical method using UPLC-MS/MS provides: (1) rapid and accurate analyses of CZ48 and CPT, (2) simple extraction procedure with good extraction recoveries of CZ48 and CPT with preserving lactone stability of CPT during the extraction process, and (3) no significant matrix effect. As compared to a previous analytical method using HPLC with a fluorescence detector (10 and 5 ng/ml for CZ48 and CPT in mouse plasma, respectively, (62)), the method using UPLC-MS/MS provides a higher sensitivity with lower LLOQs, 0.98 ng/ml for CZ48 and CPT in rat plasma.

### **4.2.1 Linearity and Sensitivity**

Calibration curves were constructed by plotting the peak area ratios of CZ48 (or CPT) to IS versus nominal concentrations. A linearity of the calibration curves was evaluated on three separate days. The linearity ranges of the curves for both CZ48 and CPT were 0.98 (LLOQ) – 1,000 ng/ml in plasma (Figure 16) and 3.9 (LLOQ) – 1,000 ng/ml in bile (Figure 17). Correlation coefficients were greater than 0.99 on 3 separate days. No significant interferences were observed at the retention times of CZ48, CPT and IS in chromatograms. The retention times of CZ48, CPT, and IS were at 3.4, 2.0, and 2.8 min, respectively. Chromatograms for blank, zero

blank, and CZ48 and CPT spiked at 15.6 ng/ml in plasma and bile are shown in Figures 18, 19, 20, and 21. The accuracy and precision of the LLOQs (n=6) did not deviate 7% in plasma and 18% in bile.

Figure 16. Representative Calibration Curves for the Linearities of CZ48 and CPT in Plasma

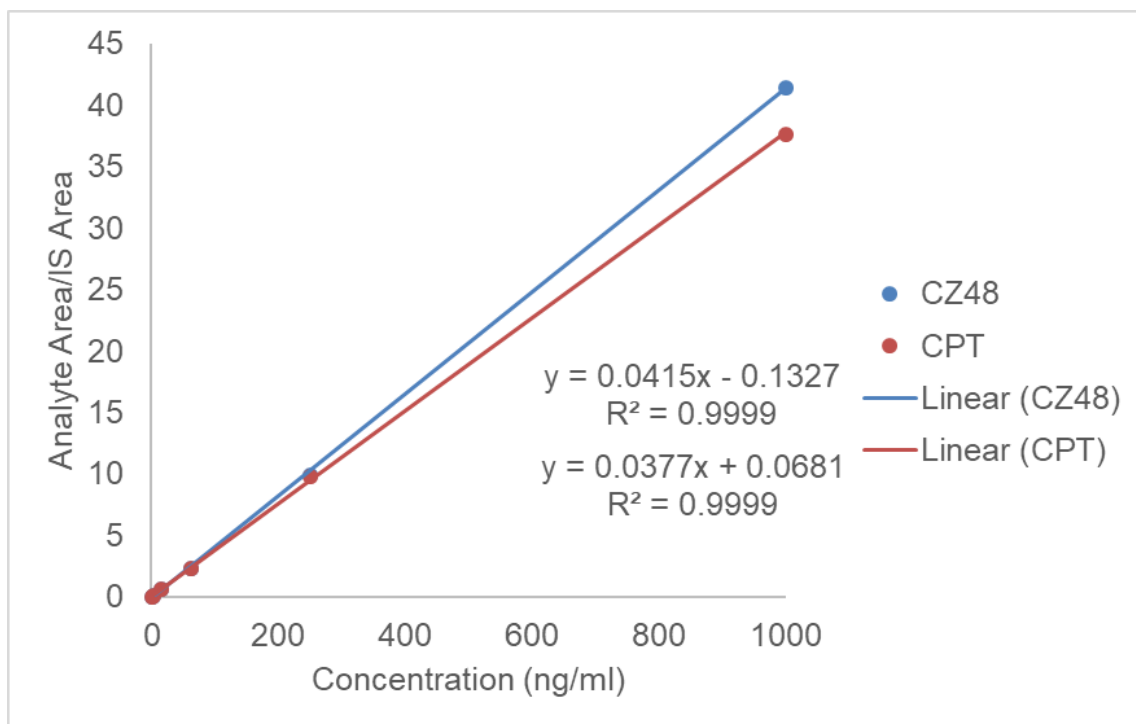


Figure 17. Representative Calibration Curves for the Linearities of CZ48 and CPT in Bile

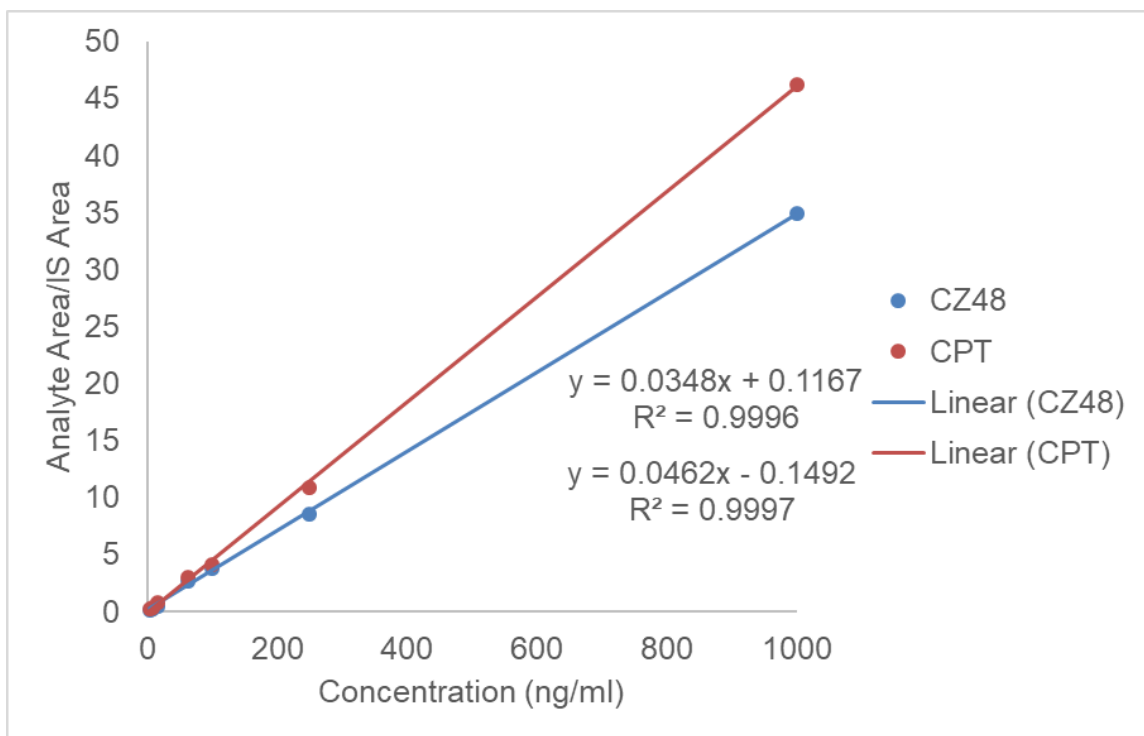
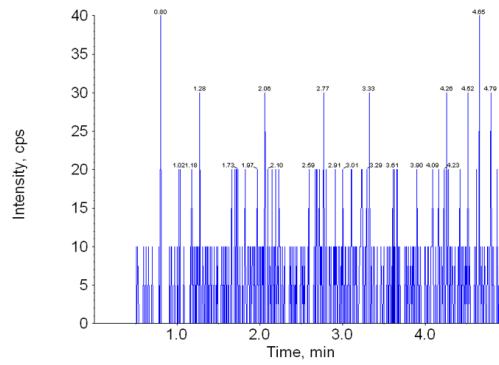
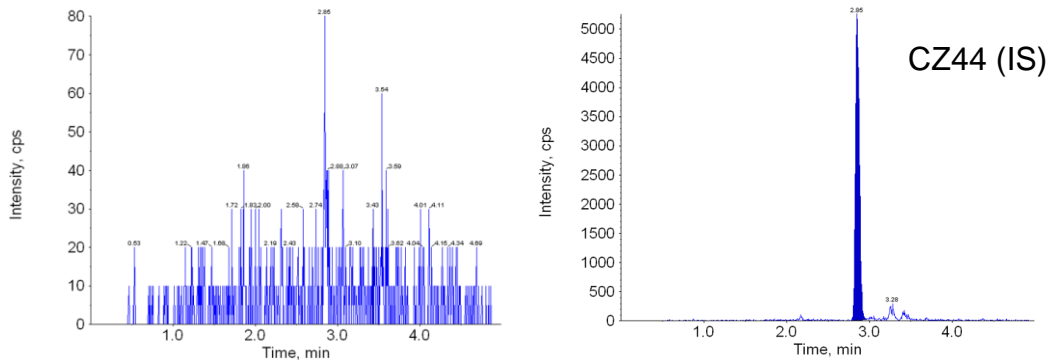


Figure 18. Representative MRM Chromatograms of (a) Blank, (b) Zero Blank, and (c) Spiked CZ48 at 15.6 ng/ml in Rat Plasma

(a)



(b)



(c)

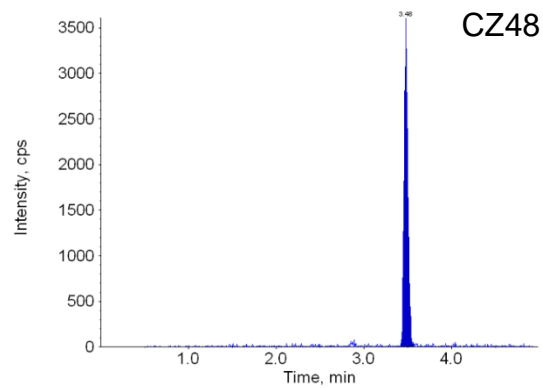
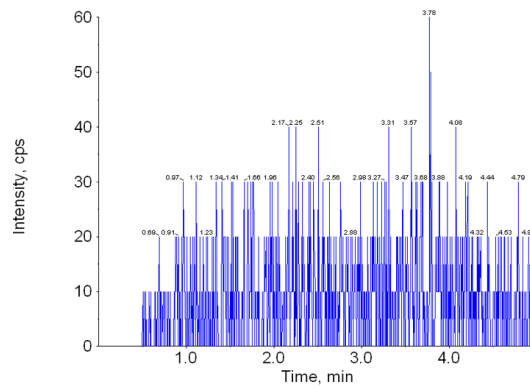
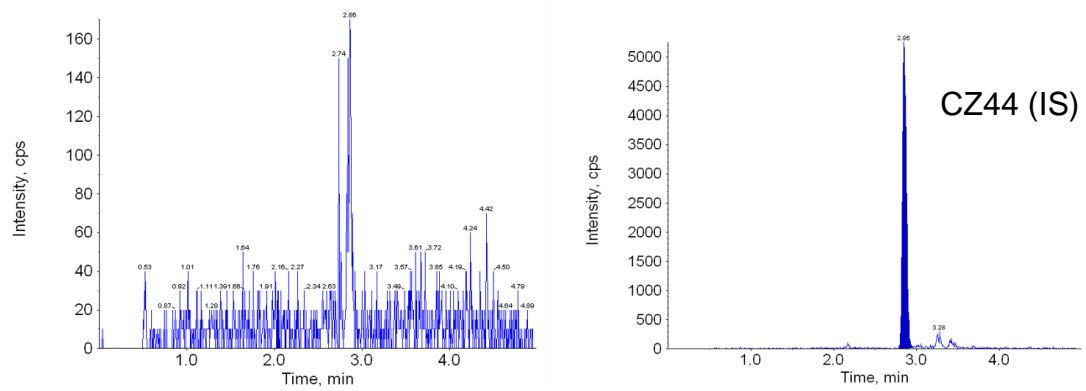


Figure 19. Representative MRM Chromatograms of (a) Blank, (b) Zero Blank, and (c) Spiked CPT at 15.6 ng/ml in Rat Plasma

(a)



(b)



(c)

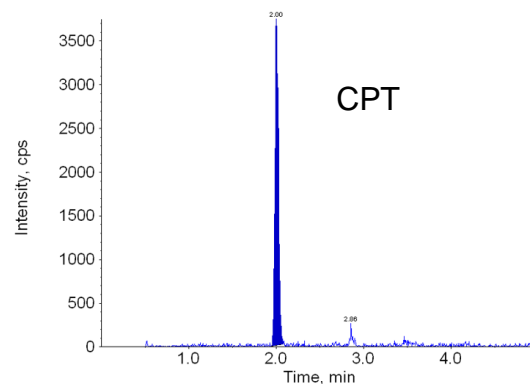
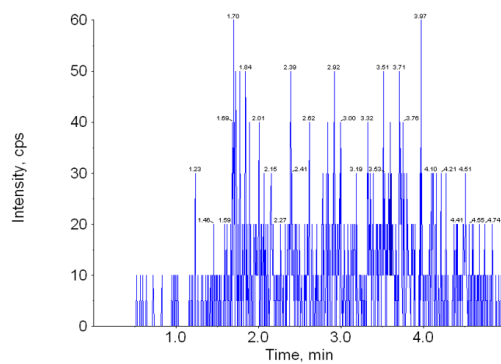
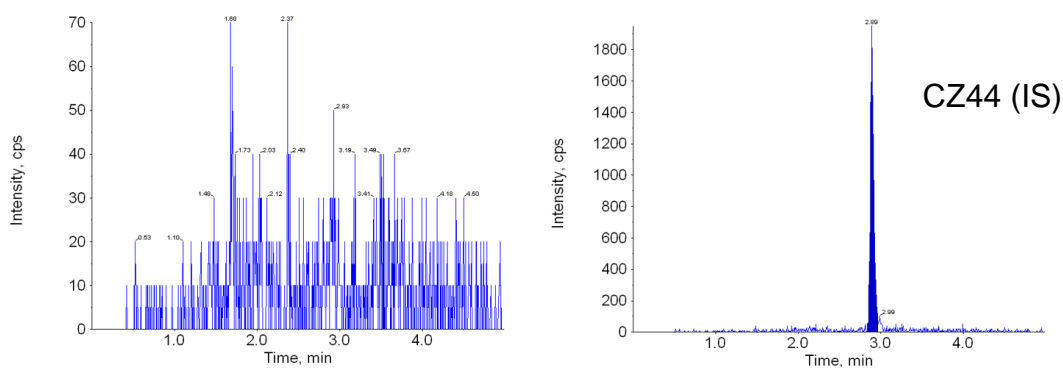


Figure 20. Representative MRM Chromatograms of (a) Blank, (b) Zero Blank, and (c) Spiked CZ48 at 15.6 ng/ml in Rat Bile

(a)



(b)



(c)

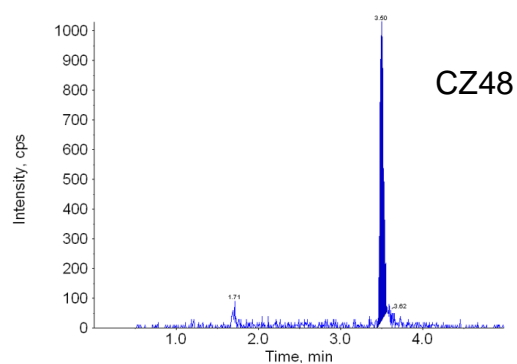
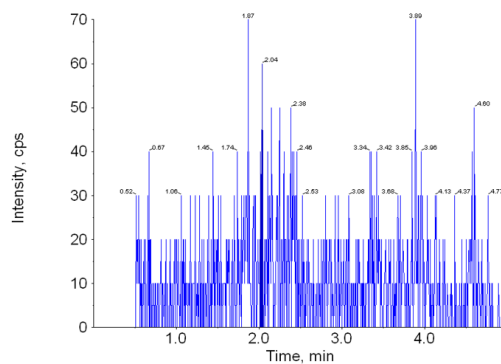
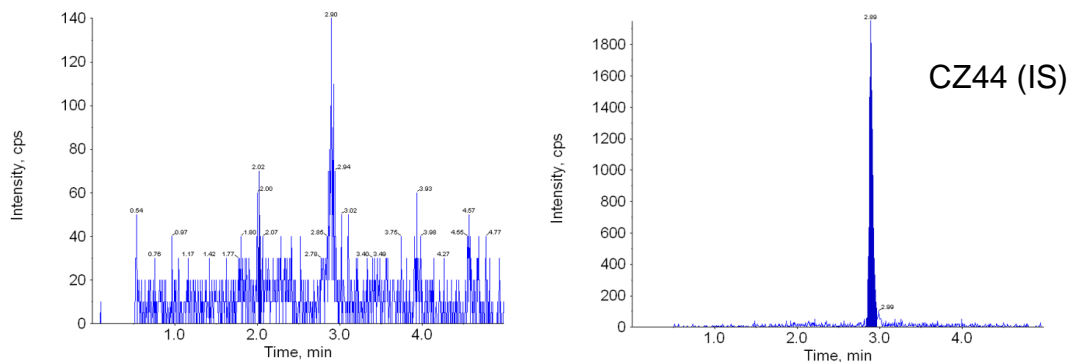


Figure 21. Representative MRM Chromatograms of (a) Blank, (b) Zero Blank, and (c) Spiked CPT at 15.6 ng/ml in Rat Bile

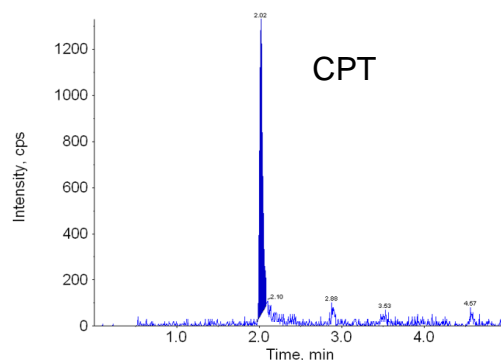
(a)



(b)



(c)



#### **4.2.2 Intra- and inter-day Accuracy and Precision**

The intra-day and inter-day accuracy and precision were evaluated at three QC concentrations (2, 40, and 800 ng/ml) in plasma (Table 7) and two QC concentrations (10 and 800 ng/ml) in bile (Table 8). The intra-day accuracy values of CZ48 and CPT in plasma were 97.99 – 106.24 % and 95.18 – 110.15 %, respectively. The inter-day accuracy values were 95.69 – 104.47 % and 96.24 – 106.30 % for CZ48 and CPT in plasma, respectively. The intra- and inter-day precisions in plasma were 8.27 % or below. In bile, the intra-day accuracy values were 88.36 – 96.85 % for CZ48 and 86.52 – 90.19 % for CPT. The inter-day accuracy in bile was 97.60 – 98.16 % for CZ48 and 88.80 – 97.09 % for CPT. The intra- and inter-day precisions were within 12.09 %. All accuracy and precision values were in the acceptable range (15% based on the FDA guideline) at different QC concentrations in plasma and bile.

Table 7. Intra- and Inter-day Accuracies and Precisions of CZ48 and CPT in Rat Plasma (Mean  $\pm$  SD)

Plasma				
	Intra-day		Inter-day	
Concentration (ng/ml)	Accuracy (%) n=6	Precision (%) n=6	Accuracy (%) n=18	Precision (%) n=18
CZ48				
2	97.99 $\pm$ 6.11	6.24	95.69 $\pm$ 6.29	6.57
40	106.24 $\pm$ 2.40	2.26	104.47 $\pm$ 3.67	3.52
800	102.12 $\pm$ 4.30	4.21	99.83 $\pm$ 4.17	4.18
CPT				
2	95.18 $\pm$ 5.89	6.19	96.24 $\pm$ 7.96	8.27
40	110.15 $\pm$ 2.73	2.48	106.30 $\pm$ 5.62	5.28
800	99.68 $\pm$ 3.88	3.90	97.70 $\pm$ 3.80	3.89

Table 8. Intra- and Inter-day Accuracies and Precisions of CZ48 and CPT in Rat Bile (Mean  $\pm$  SD)

Bile				
	Intra-day		Inter-day	
Concentration (ng/ml)	Accuracy (%) n=6	Precision (%) n=6	Accuracy (%) n=18	Precision (%) n=18
CZ48				
10	96.85 $\pm$ 5.09	5.26	98.16 $\pm$ 9.15	9.32
800	88.36 $\pm$ 4.90	5.55	97.60 $\pm$ 11.80	12.09
CPT				
10	86.52 $\pm$ 4.53	5.24	88.80 $\pm$ 7.83	8.81
800	90.19 $\pm$ 4.56	5.05	97.09 $\pm$ 9.70	9.99

### **4.2.3 Extraction Recovery and Matrix Effect**

The extraction recoveries and matrix effects of CZ48 and CPT were summarized in Table 9 for plasma and Table 10 for bile. The extraction recoveries were 90.18 – 95.42 % and 91.56 – 97.06 % for CZ48 and CPT, respectively, in plasma. The recoveries of CZ48 and CPT from bile were 86.51 – 91.66 % and 84.89 – 89.15 %, respectively. No significant matrix effects were observed for CZ48 and CPT in plasma, which were within 14 and 5.36 %, respectively.

To extract CZ48 and CPT from bile, an SPE method was employed, and the mixture of water and methanol (MeOH) was used as a washing solvent. In order to reduce matrix effects of CZ48 and CPT in bile, different ratios of water to methanol (MeOH) were tested. We tested 0, 10, 20, and 40 % of MeOH in water. The matrix effect of CZ48 was reduced with increasing percentages of MeOH. The combination of two washing solvents was finally selected to remove bile salts and interferences in the bile, which were 100 % water (for the first wash) and 40 % of MeOH in water (for the second wash). Matrix effects of CZ48 and CPT were within 5.31 and 16.19 % in bile, respectively.

Table 9. Extraction Recoveries and Matrix Effects of CZ48 and CPT in Rat Plasma (Mean  $\pm$  SD)

Plasma		
Concentration (ng/ml)	Recovery (%), n=6	Matrix effect (%), n=6
CZ48		
2	90.18 $\pm$ 8.65	86.00 $\pm$ 8.15
40	91.39 $\pm$ 5.55	92.84 $\pm$ 8.35
800	95.42 $\pm$ 4.48	90.18 $\pm$ 2.77
CPT		
2	95.48 $\pm$ 5.25	101.49 $\pm$ 3.96
40	91.56 $\pm$ 5.58	95.87 $\pm$ 4.22
800	97.06 $\pm$ 3.76	94.64 $\pm$ 3.24

Table 10. Extraction Recoveries and Matrix Effects of CZ48 and CPT in Rat Bile  
(Mean  $\pm$  SD)

Bile		
Concentration (ng/ml)	Recovery (%), n=3	Matrix effect (%), n=3
CZ48		
10	91.66 $\pm$ 1.13	95.22 $\pm$ 2.46
800	86.51 $\pm$ 0.60	94.69 $\pm$ 9.54
CPT		
10	84.89 $\pm$ 9.15	83.81 $\pm$ 9.68
800	89.15 $\pm$ 1.62	89.20 $\pm$ 7.45

#### **4.2.4 Stability Tests**

The stabilities of CZ48 and CPT in plasma were evaluated under different storage conditions in terms of processed stability, 3-cycle of freeze-thaw, short-term stability, and long-term stability (Table 11). Relative errors of CZ48 and CPT were within  $\pm 14.44\%$  at three QC concentrations after the treatment of different storage conditions, which indicated that CZ48 and CPT are stable during the extraction process, analysis and storage.

Table 11. Stability Tests for CZ48 and CPT in Rat Plasma (Mean ± SD)

Observed Concentration (ng/ml) [Relative error, %]					
Conditions	Processed Stability n=5	Freeze-thaw n=4	Short-term Stability (4 hr) n=4	Long-term Stability (3 month) n=3	
<b>CZ48</b>					
2	1.85 ± 0.09 [-8.28]	1.95 ± 0.14 [-2.37]	1.96 ± 0.24 [-2.27]	2.08 ± 0.06 [3.85]	
40	42.55 ± 1.74 [6.00]	39.36 ± 2.51 [-1.63]	36.56 ± 1.11 [-9.40]	41.69 ± 1.64 [4.05]	
800	769.73 ± 25.56 [-3.93]	770.22 ± 51.34 [-3.87]	729.40 ± 21.68 [-9.68]	750.58 ± 22.14 [-6.58]	
<b>CPT</b>					
2	2.06 ± 0.20 [2.82]	1.92 ± 0.15 [-4.38]	1.84 ± 0.08 [-8.44]	1.99 ± 0.20 [-0.69]	
40	43.79 ± 1.36 [8.66]	38.88 ± 3.86 [-2.87]	35.96 ± 1.59 [-11.25]	45.98 ± 0.17 [13.00]	
800	757.52 ± 18.78 [-5.61]	734.89 ± 46.86 [-8.86]	699.03 ± 13.30 [-14.44]	815.37 ± 26.80 [1.89]	

### **4.3 Phase 1 Metabolism**

Phase 1 metabolism of CPT was investigated by incubating CPT in rat liver microsomes (RLM) with a cofactor, UDPGA for 0, 2, and 4 hr. Testosterone was incubated in the same condition for 0, 5, and 30 min as a positive control. Phase 1 metabolites of CPT were not detected in chromatograms even after 4 hr incubation (Table 12). On the contrary, a phase 1 metabolite of testosterone was detected within 30 min of the incubation (Table 13).

### **4.4 Phase 2 Metabolism**

CPT was incubated in RLM or rat S9 fractions in the presence of cofactors, UDPGA or PAPS for glucuronidation or sulfation reaction, respectively. Genistein was incubated in the same condition as a positive control. No significant conjugations were observed for CPT. The peak area of CPT was not decreased after 2 hr or overnight incubation, and its glucuronides were not detected after UPLC or UPLC-MS/MS analyses (Table 14). CPT sulfates were not detected either in the chromatogram even after an overnight incubation (Figure 22). However, genistein was conjugated by UGTs or SULTs within 30 min of the incubation (Table 15).

Table 12. Phase 1 Metabolism of CPT in the *In Vitro* System

Time (hr)	Peak Area	
	CPT	CPT-Metabolites
0	89826.33 ± 4326.26	ND
2	146577.33 ± 3848.55	ND
4	117352.00 ± 10801.44	ND

Data presented as the Mean ± SD, n=3

ND: Not detectable

Table 13. Phase 1 Metabolism of Testosterone in the *In Vitro* System

Time (min)	Peak Area	
	Testosterone	Testosterone-Metabolites
0	13010.67 ± 212.06	ND
5	10286.33 ± 2180.42	14167.00 ± 443.50
30	2643.67 ± 2664.66	17245.00 ± 1513.20

Data presented as the Mean ± SD, n=3

ND: Not detectable

Table 14. Phase 2 Metabolism of CPT in the *In Vitro* System

Time (hr)	Peak Area	
	CPT	CPT-Glucuronides
0	35271.33 ± 5675.17	ND
2	38689.67 ± 212.68	ND
Overnight	37110.00 ± 441.47	ND

Data presented as the Mean ± SD, n=3

ND: Not detectable

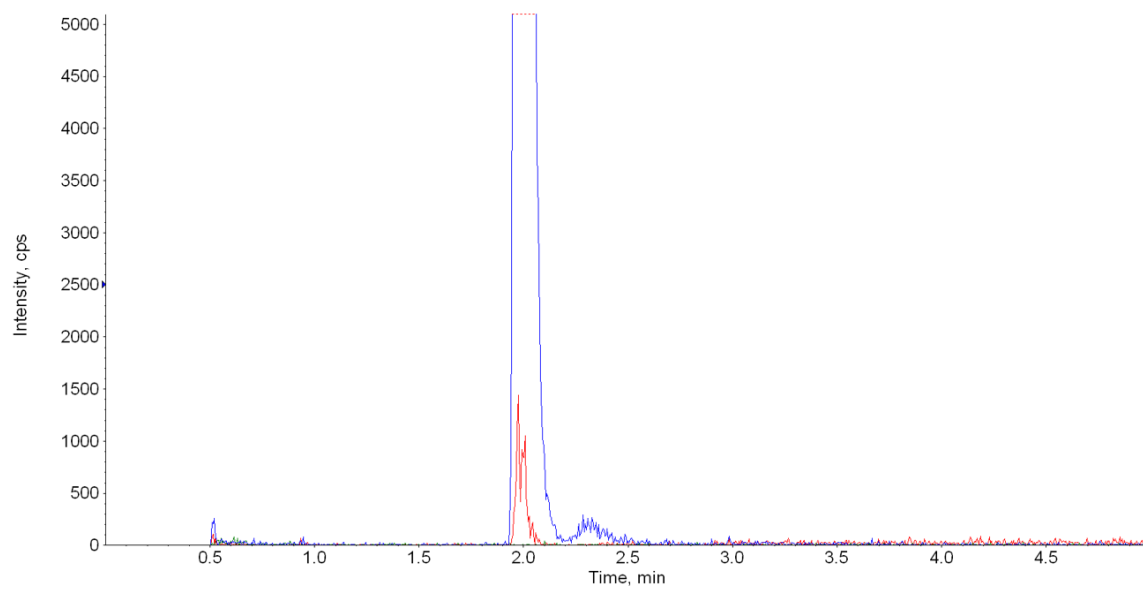
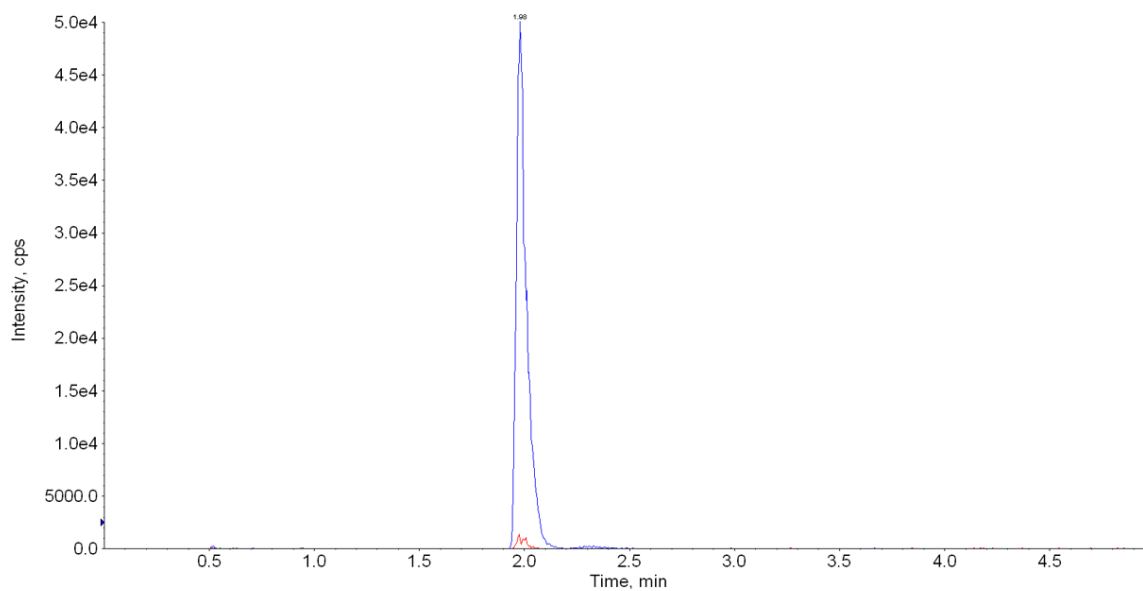
Table 15. Phase 2 Metabolism of Genistein in the *In Vitro* System

Time (min)	Peak Area	
	Genistein	Genistein-Glucuronides
0	32860.33 ± 4555.95	12200.67 ± 2420.67
15	ND	47013.67 ± 1830.70
30	ND	45109.67 ± 1373.20

Data presented as the Mean ± SD, n=3

ND: Not detectable

Figure 22. Chromatograms of CPT and CPT-Sulfate Scanned with  $m/z$  349.1/305.2 (Blue Peak) and  $m/z$  429.1/349.1 (Red Peak), Respectively, after an Overnight Incubation



#### 4.5 Biliary Excretions of CZ48 and CPT after an IV Dose of CZ48-CoS

The concentration-time profiles of CZ48 and CPT in plasma were established after an IV dose of CZ48-CoS at 5 mg/kg as shown in Figure 23. The cumulative amounts of CZ48 and CPT in bile for 6 hr post IV dose were established in Figure 24. Pharmacokinetic (PK) parameters of CZ48 and CPT in plasma and bile were summarized in Table 16. As shown in Figure 23, CZ48 was dominant than CPT in plasma.  $AUC_{0-6h}$  of CZ48 was  $3,203.03 \pm 1,785.24$  h\*ng/ml, which was approximately 4.4 times of that of CPT ( $722.13 \pm 397.72$  h\*ng/ml). On the contrary, CPT was dominant than CZ48 in bile as shown in Figure 24. The cumulative amount of CPT was  $38.11 \pm 14.03$   $\mu$ g for 6 hr post dose in bile, which was approximately 13.96-fold of that of CZ48 ( $2.73 \pm 1.45$   $\mu$ g). Biliary clearance of CPT ( $CL_b$ ) was  $56.38 \pm 15.37$  mL/h, which were 64.8 times of that of CZ48 ( $0.87 \pm 0.20$  mL/h). The  $CL_b$  of CPT was 2.74 % of its total clearance (CL),  $2,058.90 \pm 888.87$  mL/h. The study characterized the biliary secretions of CPT and CZ48, with CPT being more favorable than CZ48 in the secretion. The percent doses recovered in the bile were  $0.19 \pm 0.10$  for CZ48 and  $3.05 \pm 1.13$  % for CPT 6 hr post the IV dose of CZ48. Low percent recovery in bile indicated that biliary excretion was not a major elimination route for CZ48 after the IV dose.

Figure 23. Plasma Concentration-Time Profiles of CZ48 and CPT after an IV Dose of CZ48-CoS (Mean  $\pm$  SD, n=3)

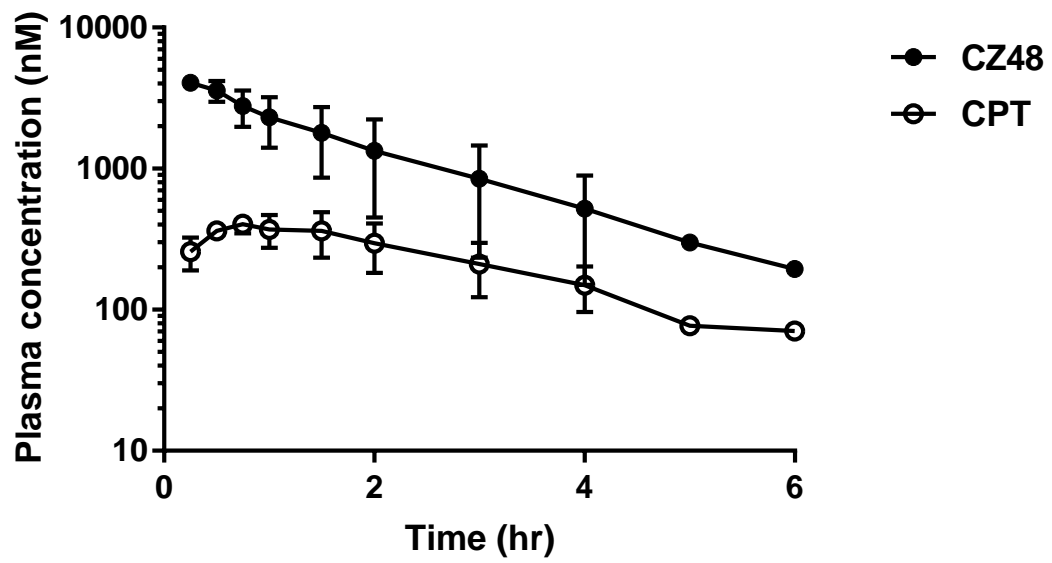


Figure 24. Cumulative Amounts of CZ48 and CPT in Bile after an IV Dose of CZ48-CoS (Mean  $\pm$  SD, n=3)

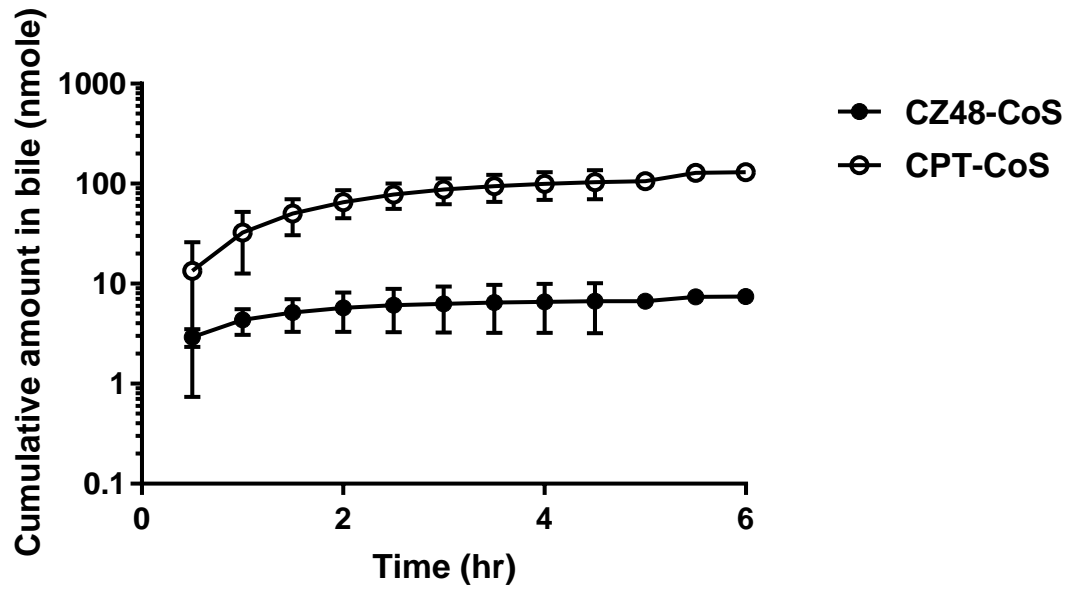


Table 16. Pharmacokinetic Parameters of CZ48 and CPT in Rat Plasma and Bile after an IV Dose of CZ48-CoS

		Plasma	
		CZ48	CPT
AUC <sub>0-6h</sub>	h*ng/mL	3,203.03 ± 1,785.24	722.13 ± 397.72
t <sub>1/2</sub>	h	1.12 ± 0.69	3.46 ± 1.80
CL	mL/h	540.61 ± 236.31	2,058.90 ± 888.87
		Bile	
		CZ48	CPT
Cumulative amount for 6 hr	µg	2.73 ± 1.45	38.11 ± 14.03
% Dose for 6 hr	%	0.19 ± 0.10	3.05 ± 1.13
CL <sub>bile</sub>	mL/h	0.87 ± 0.20	56.38 ± 15.37

Data presented as Mean ± SD, n=3

## **4.6 Biliary Excretions of CZ48 and CPT after an Oral Dose of CZ48-CoS or CZ48-NS**

### **4.6.1 Characterization of CZ48 Nanosuspension (CZ48-NS)**

CZ48-NS was prepared at the concentration of 5.9 % by wt, and diluted with double distilled water for an IV dose at 25 mg/kg. Before dosing, particle size, polydispersity index (PI), and zeta potential were characterized by Zetapals (Brookhaven Instruments, Holtsville, NY). NS used in biliary excretion studies had particle sizes of 204.1-276.9 nm, PI of 0.139-0.177, and zeta potential of (-32.22) – (-38.56).

### **4.6.2 Comparison of Biliary Excretions of CZ48 and CPT Between Oral and IV Doses of CZ48-CoS**

The plasma concentration-time profiles of CZ48 and CPT after a single IV dose or a single oral dose of CZ48-CoS were compared in Figure 25. The amounts of CZ48 and CPT in the bile were presented in Figure 26.

As shown in Figure 25 and Table 17, CZ48 was dominant than CPT in plasma after an oral or IV dose of CZ48-CoS. Dose adjusted  $AUC_{0-6h}$  of CZ48 after the IV dose ( $AUC_{0-6h,IV,plasma}$ ) was  $640.61 \pm 357.05$  (ng/ml\*h)/[mg/kg], which was 4.44

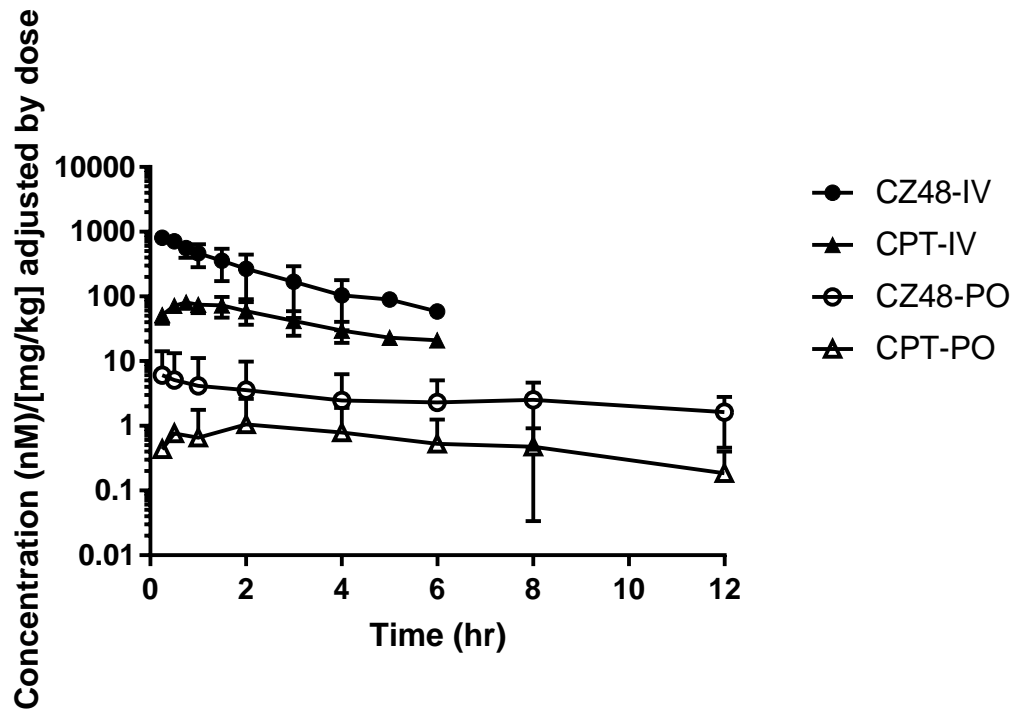
times of  $AUC_{0-6h,IV,plasma}$  of CPT ( $144.43 \pm 79.54$  (ng/ml\*h)/[mg/kg]). After an oral dose,  $AUC_{0-12h,PO,plasma}$  of CZ48 was  $12.66 \pm 15.65$  (ng/ml\*h)/[mg/kg], which was 4.65 times of  $AUC_{0-12h,PO,plasma}$  of CPT ( $2.73 \pm 2.41$  (ng/ml\*h)/[mg/kg]). Plasma concentrations of CZ48 and CPT were higher after an IV dose than those after an oral dose.  $AUC_{0-6h,IV,plasma}$  of CZ48 ( $640.61 \pm 357.05$  (ng/ml\*h)/[mg/kg]) was 50.60 times of  $AUC_{0-12h,PO,plasma}$  of CZ48 ( $12.66 \pm 15.65$  (ng/ml\*h)/[mg/kg]).  $AUC_{0-6h,IV,plasma}$  of CPT ( $144.43 \pm 79.54$  (ng/ml\*h)/[mg/kg]) was 52.99 times of  $AUC_{0-12h,PO,plasma}$  of CPT ( $2.73 \pm 2.41$  (ng/ml\*h)/[mg/kg]).

After the IV dose, plasma concentrations of CZ48 and CPT tended to decline rapidly within 6 hr post dose. However, sustained concentrations of CZ48 and CPT were observed after an oral dose for up to 12 hr post dose. These trends were similar in the bile profiles of CZ48 and CPT. The secretions of CZ48 and CPT into the bile were declined after 1 hr post IV dose, but their secretions were sustained for 12 hr post oral dose.

In bile, CPT was more abundant than CZ48 in both IV and oral groups (Figure 26). The concentration ratios of CZ48 (or CPT) in bile to plasma (B/P) were calculated for both IV and oral groups (Table 18). CPT-B/P ratios were 41.70 – 96.61 and 150.24 – 259.41 in IV and oral groups, respectively. CZ48-B/P ratios were lower

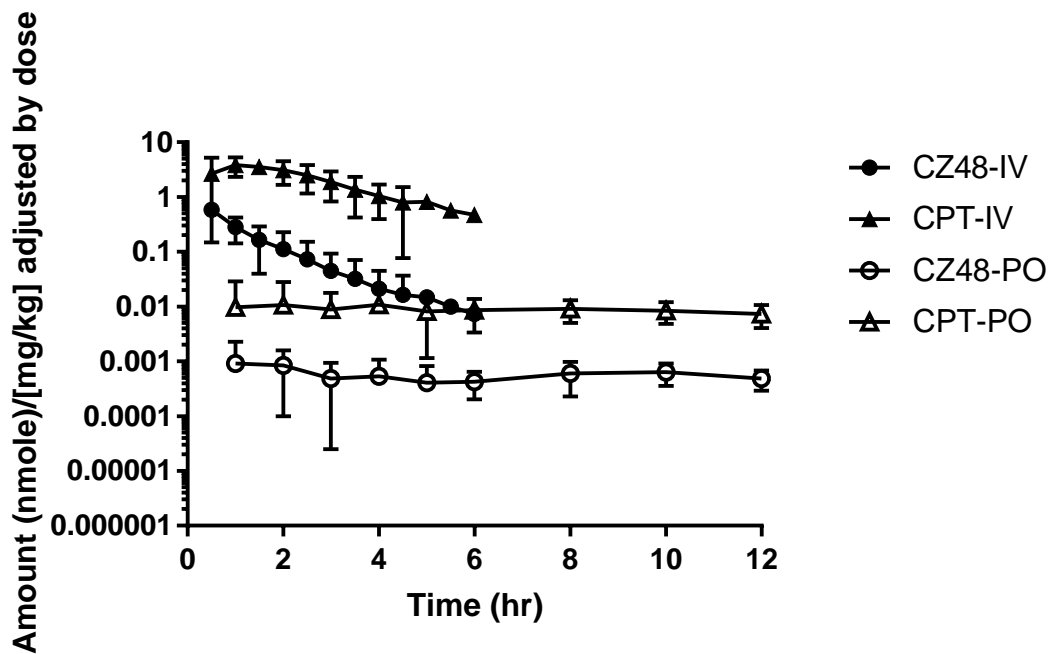
than CPT-B/P, which were 0.16 – 1.36 and 1.16 – 1.49 in IV and oral groups, respectively. When comparing CPT-B/P between two different dosing groups, oral administration of CZ48-CoS yielded 1.4 – 5.6 times higher CPT-B/P than IV administration.

Figure 25. Plasma Concentration-Time Profiles of CZ48 and CPT after a Single IV Dose or a Single Oral Dose of CZ48-CoS (Mean  $\pm$  SD, n=3-7)



CZ48-IV: n=3, CPT-IV: n=3, CZ48-PO: n=7, CPT-PO: n=4

Figure 26. Amounts of CZ48 and CPT Secreted into Bile after a Single IV Dose or a Single Oral Dose of CZ48-CoS (Mean  $\pm$  SD, n=3-7)



CZ48-IV: n=3, CPT-IV: n=3, CZ48-PO: n=7, CPT-PO: n=7

Table 17. AUC<sub>0-t</sub> of CZ48 and CPT in Plasma after an IV or Oral Dose of CZ48-CoS

Plasma, ng/ml*h/[mg/kg]			
AUC <sub>0-6h</sub> , IV		AUC <sub>0-12h</sub> , Oral	
CZ48	CPT	CZ48	CPT
640.61 ± 357.05	144.43 ± 79.54	12.66 ± 15.65	2.73 ± 2.41

Table 18. Concentration Ratios of CZ48 (or CPT) in Bile to Plasma (CZ48-B/P or CPT-B/P) after Single IV or Oral Dose of CZ48-CoS (Mean  $\pm$  SD)

Time (hr)	IV		Oral	
	CZ48-B/P	CPT-B/P	CZ48-B/P	CPT-B/P
0.5	1.36 $\pm$ 0.19	61.95 $\pm$ 57.43		
1	0.91 $\pm$ 0.08	89.51 $\pm$ 65.03	1.26 $\pm$ 0.66	150.24 $\pm$ 67.28
1.5	0.76 $\pm$ 0.08	96.61 $\pm$ 43.27		
2	0.61 $\pm$ 0.11	93.03 $\pm$ 28.79	1.44 $\pm$ 1.30	178.31 $\pm$ 122.06
3	0.41 $\pm$ 0.07	83.17 $\pm$ 11.89		
4	0.33 $\pm$ 0.09	66.29 $\pm$ 3.85	1.16 $\pm$ 0.47 *	181.18 $\pm$ 104.18
5	0.19, 0.31	55.97, 67.51		
6	0.16, 0.26	52.16, 41.70	1.19 $\pm$ 0.43	188.83 $\pm$ 95.80
8			1.20 $\pm$ 0.48	209.13 $\pm$ 175.02
12			1.49 $\pm$ 0.50	259.41 $\pm$ 117.53

IV: n=3

PO: n=7 for CZ48 in plasma and bile and for CPT in bile, n=4 for CPT in plasma

\* P<0.05, Mann-Whitney test, CZ48-B/P-IV versus CZ48-B/P-PO

#### **4.6.3 Comparison of Biliary Excretions of CZ48 and CPT after an Oral Dose of CZ48-CoS or CZ48-NS**

The plasma concentration-time profiles of CZ48 and CPT after a single oral dose of CZ48-CoS or CZ48-NS were shown in Figure 27. The amounts of CZ48 and CPT in the bile were presented in Figure 28.

The plasma concentration-time profiles of CZ48 and CPT were similar between CoS and NS groups (Figure 27). Sustained concentrations of CZ48 and CPT were observed in both formulation groups.  $AUC_{0-12h,plasma}$  values of CZ48 were  $12.19 \pm 15.89$  and  $7.28 \pm 3.74$  (ng/ml\*h/[mg/kg]) in the Co-S and NS groups, respectively.  $AUC_{0-12h,plasma}$  values of CPT were  $2.00 \pm 2.74$  and  $1.07 \pm 0.51$  (ng/ml\*h/[mg/kg]) in the Co-S and NS groups, respectively. The CPT amounts in bile were higher than that of CZ48 in both CoS and NS groups (Figure 28).  $AUC_{0-12,bile}$  values of CZ48 were  $11.61 \pm 7.99$  and  $7.33 \pm 2.22$  (ng/ml\*h/[mg/kg]) in the CoS and NS groups, respectively.  $AUC_{0-12,bile}$  values of CPT were  $213.45 \pm 232.09$  and  $250.40 \pm 134.84$  (ng/ml\*h/[mg/kg]) in two formulation groups.  $AUC_{0-12,bile}$  values of CPT were 18.39 and 34.16 times higher than those of CZ48 in the CoS and NS groups, respectively. The secretions of CZ48 and CPT into bile were sustained for up to 12 hr post an oral dose in both formulation groups.

When comparing concentration of CZ48 and CPT between plasma and bile in each oral formulation group (Table 19 and Figure 29),  $AUC_{0-12h}$  values of CPT in bile were  $213.45 \pm 232.09$  and  $250.40 \pm 134.83$  ng/ml\*h/[mg/kg], which were 106.73 and 234.02 times of those in plasma ( $2.00 \pm 2.74$  and  $1.07 \pm 0.51$  ng/ml\*h/[mg/kg]) in CoS and NS groups, respectively. However, the CZ48 concentrations in plasma and bile were comparable for both formulations. The  $AUC_{0-12h}$  ratio profiles of CZ48 (or CPT) in bile to plasma (B/P) are shown in Figure 30. CZ48-B/P ratios were  $1.34 \pm 0.44$  and  $1.13 \pm 0.52$  in CoS and NS groups, respectively. The ratios of CPT were  $191.96 \pm 128.83$  and  $339.33 \pm 336.71$  in CoS and NS groups, respectively. The B/P ratios were not significantly different between the two formulation groups for both CZ48 and CPT.

Table 19. AUC<sub>0-12</sub> of CZ48 and CPT in Plasma and Bile after an Oral Dose of CZ48-CoS or CZ48-NS  
(Mean ± SD, n=3-7)

	AUC <sub>0-12h</sub> (ng/ml*h/[mg/kg])					
	Plasma		Bile		Bile/Plasma (B/P)	
	CoS	NS	CoS	NS	CoS	NS
CZ48	12.19 ± 15.89	7.28 ± 3.74	11.61 ± 7.99	7.33 ± 2.22	1.34 ± 0.44	1.13 ± 0.52
CPT	2.00 ± 2.74	1.07 ± 0.51	213.45 ± 232.09	250.40 ± 134.83	191.96 ± 128.83	339.33 ± 336.71

Figure 27. Plasma Concentration-Time Profiles of CZ48 and CPT after Single Oral Dose of CZ48-CoS or CZ48-NS (Mean  $\pm$  SD, n=3-7)

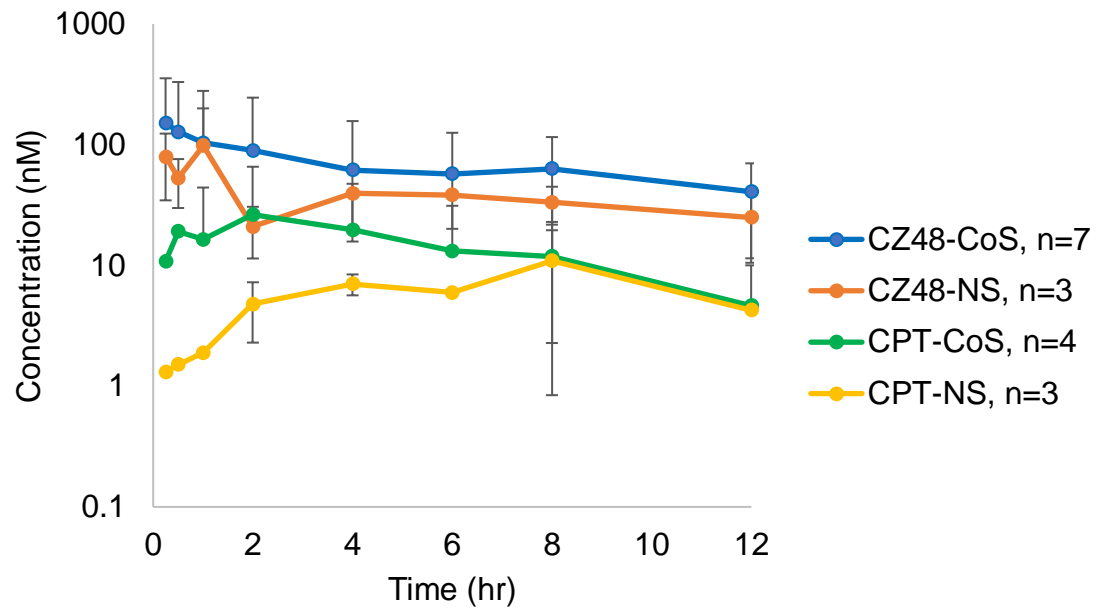


Figure 28. Amounts of CZ48 and CPT Secreted into Bile after Single Oral Dose of CZ48-CoS or CZ48-NS (Mean  $\pm$  SD, n=3-7)

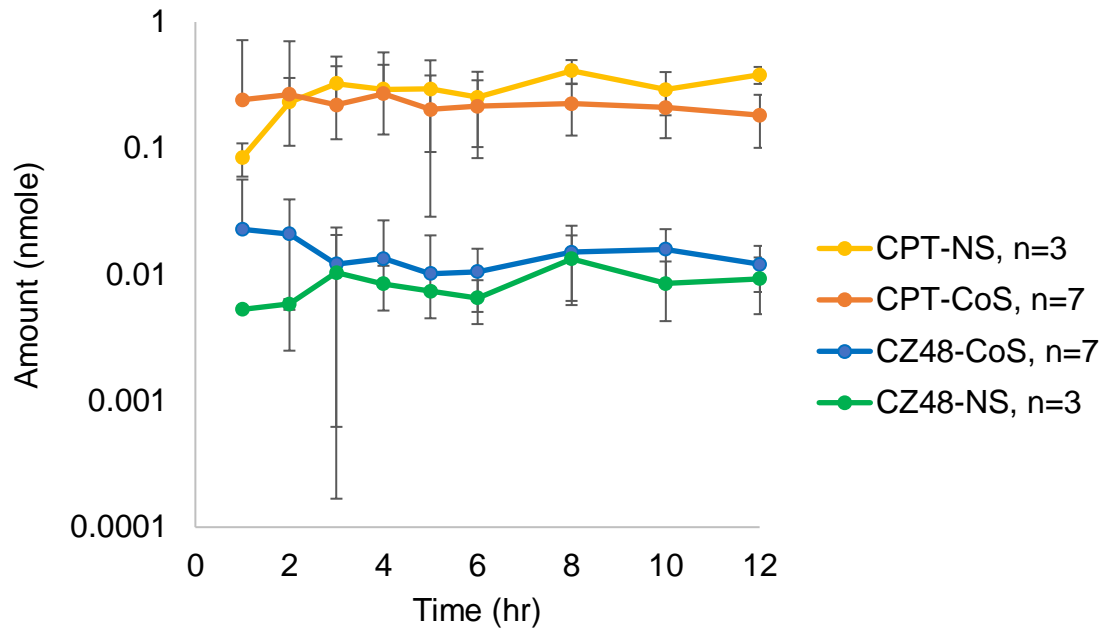


Figure 29. Concentrations of CZ48 and CPT in Plasma and Bile from CoS and NS Formulations (Mean  $\pm$  SD, n=3-7)

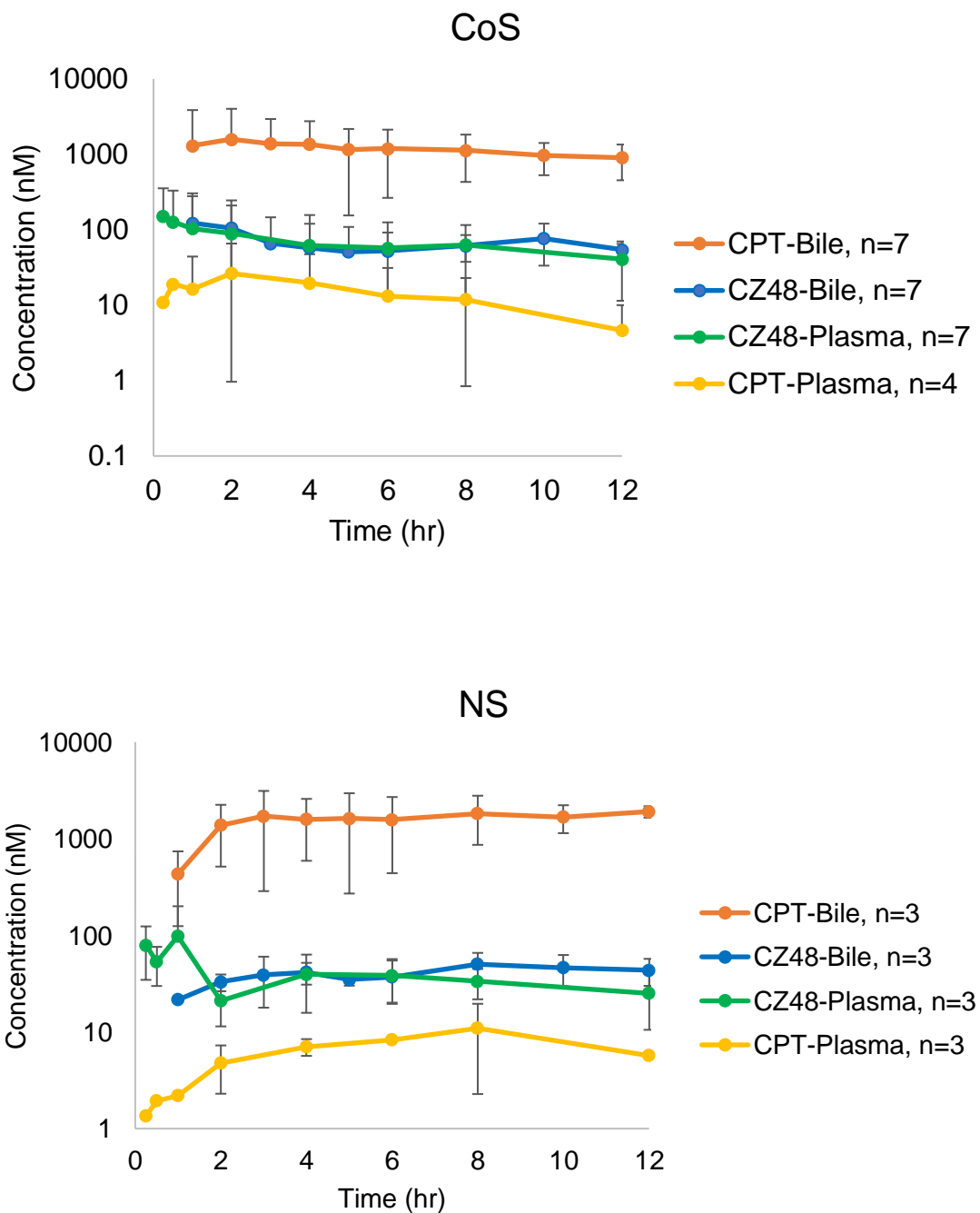
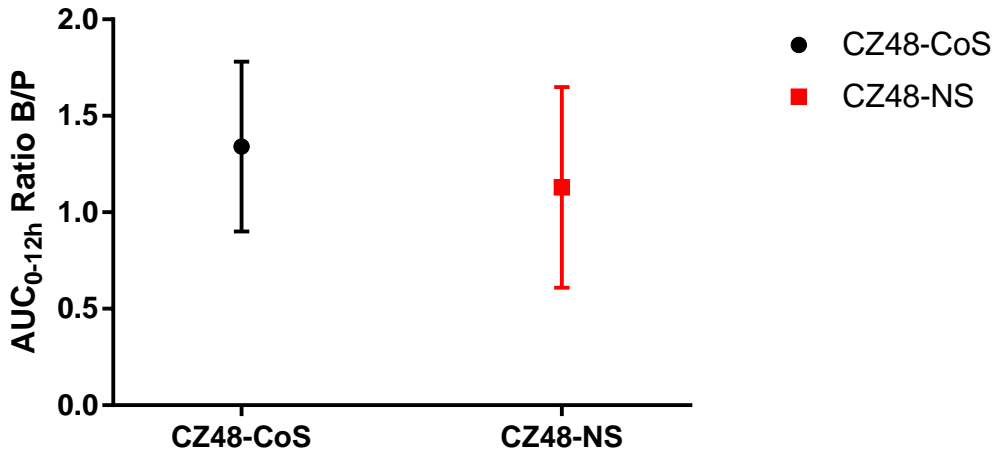


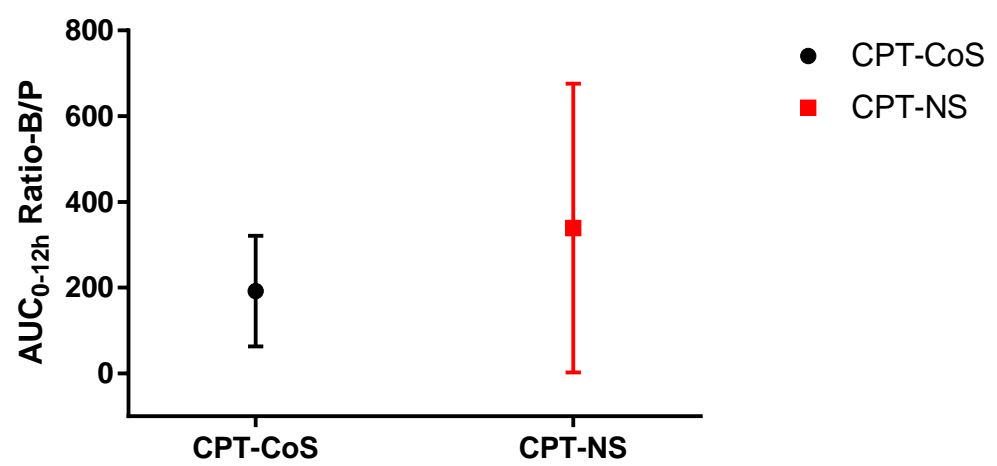
Figure 30. AUC<sub>0-12h</sub> Ratios (B/P) of CZ48 (a) and CPT (b) after a Single Oral Dose of CZ48-CoS or CZ48-NS (Mean ± SD)

(a)



NS-CZ48: n=3, CoS-CZ48: n=7

(b)



NS-CPT: n=3, CoS-CPT: n=4

## 4.7 Enterohepatic Recycling of CZ48 and CPT after an Oral Dose of CZ48-NS

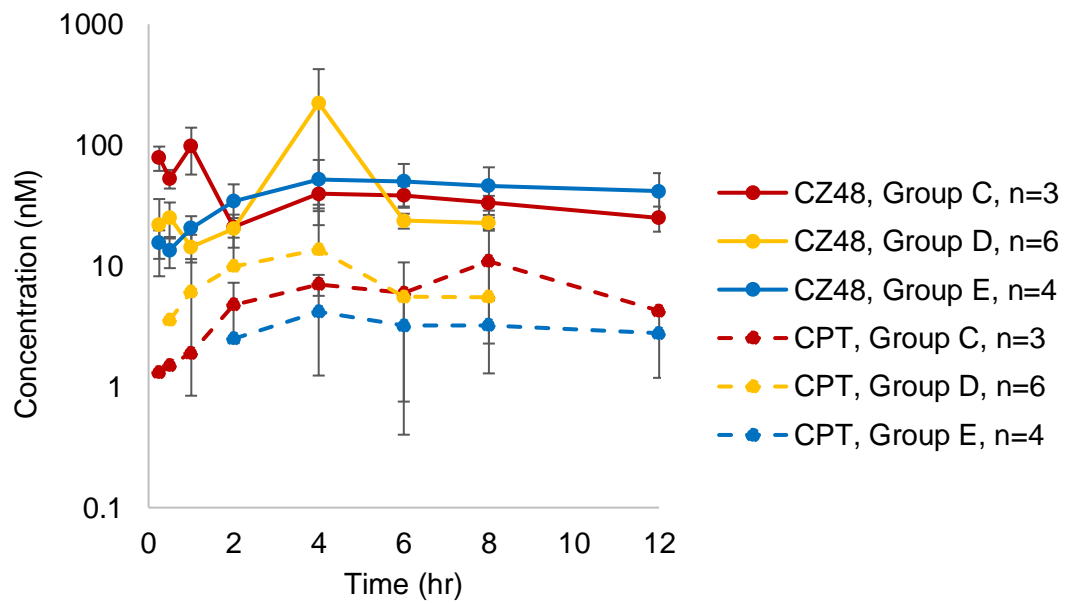
To characterize enterohepatic recycling of CZ48 and CPT, the recycling system was experimentally interrupted by using two different rat models, bile duct-cannulated and bile duct-intact rats. Animals were divided into three groups (Groups C, D, and E) as shown in Table 4. Plasma concentration-time profiles of CZ48 and CPT in three groups are represented in Figure 31. Amounts of CZ48 and CPT secreted into bile are shown in Figure 32.

Enterohepatic recycling of CZ48 and CPT was minor in this study. No significant differences were observed among three groups in plasma profiles of CZ48 and CPT (Figure 31). Double peaks were observed within 2 hr post oral dose and sustained concentrations of CZ48 and CPT were observed till 8 or 12 hr post oral dose.  $AUC_{0-t}$  of CZ48 and CPT were similar among groups with or without interrupting enterohepatic recycling.  $AUC_{0-12h}$  values of CZ48 in group C and E were  $7.28 \pm 3.74$  and  $8.06 \pm 8.13$  ng/ml\*h/[mg/kg], respectively.  $AUC_{0-12h}$  values of CPT were  $1.07 \pm 0.51$  and  $0.46 \pm 0.29$  ng/ml\*h/[mg/kg] in Group C and E, respectively. When the recycling was interrupted,  $AUC_{0-8h}$  values of CZ48 and CPT were  $9.24 \pm 16.07$  and  $0.82 \pm 0.89$  ng/ml\*h/[mg/kg], respectively, in Group D. In

the bile profiles shown in Figure 32, the secretions of CZ48 and CPT into bile were sustained until 8 or 12 hr post oral dose.

To evaluate the impact of the interruption of enterohepatic recycling on biliary secretions of CZ48 and CPT, the concentration ratios of CZ48 (or CPT) in bile to plasma (B/P) were calculated and presented in Figure 33. The trend of profiles implied the decline of ratios between 2 and 4 hr post oral dose by interrupting the enterohepatic recycling of CZ48 and CPT in Group D. However, the ratios were sustained after 4 hr post oral dose.

Figure 31. Plasma Concentration-Time Profiles of CZ48 and CPT after Single Oral Dose of CZ48-NS with or without Interrupting Enterohepatic Recycling (Mean  $\pm$  SD, n=3-6)



Group C: Recycling (intermittent bile collection)

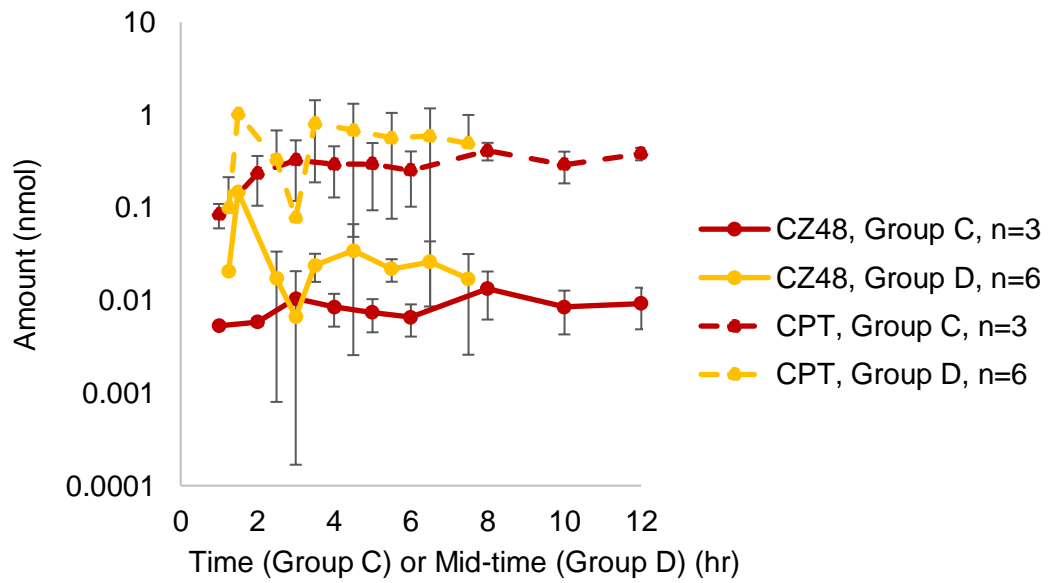
Group D: No recycling (continuous bile collection)

Group E: Recycling (no bile collection)

Table 20. AUC<sub>0-t</sub> of CZ48 and CPT in Plasma after an Oral Dose of CZ48-NS  
(Mean ± SD)

	Unit	Group C	Group D	Group E
CZ48	ng/ml*h/[mg/kg]	7.28 ± 3.74	9.24 ± 16.07	8.06 ± 8.13
CPT	ng/ml*h/[mg/kg]	1.07 ± 0.51	0.82 ± 0.89	0.46 ± 0.29

Figure 32. Amounts of CZ48 and CPT Secreted into Bile after Single Oral Dose of CZ48-NS with or without Interrupting Enterohepatic Recycling (Mean  $\pm$  SD, n=3-6)

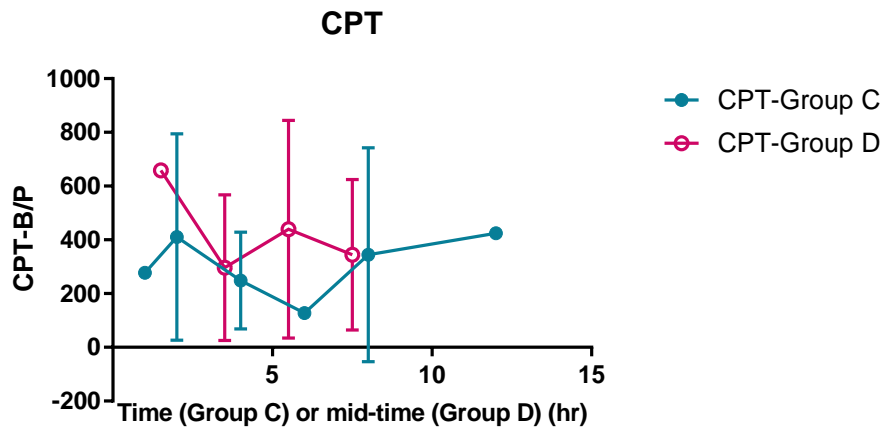
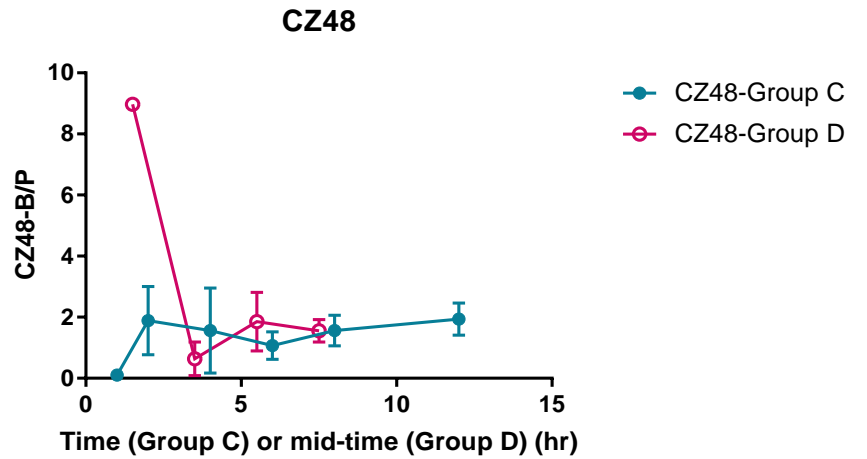


Group C: Recycling (intermittent bile collection)

Group D: No recycling (continuous bile collection)

Figure 33. Concentration Ratios (B/P) of CZ48 and CPT after Single Oral Dose of CZ48-NS with or without Interrupting Enterohepatic Recycling

(Mean  $\pm$  SD, n=3-6)



Group C: Recycling (intermittent bile collection), n=3

Group D: No recycling (continuous bile collection), n=6

#### 4.8 Development of a Population Pharmacokinetic (PK) Model

A population PK model was developed to describe PK of CZ48 and CPT and biliary excretion of CPT as shown in Figure 34. The following components were considered to establish the PK model: (1) oral absorption of CZ48-CoS or CZ48-NS, (2) plasma concentrations of CZ48 and CPT, (3) biliary excretion of CPT, (4) clearance of CPT in other routes (metabolism, urine, and feces), (5) total clearance of CZ48 (conversion to CPT, metabolism, urine, bile, and feces), and (6) enterohepatic recycling of CZ48 and CPT. Based on our *in vivo* results, biliary excretion of CPT was dominant than that of CZ48, and % dose recovered in bile as CZ48 was only about 0.19 % after an IV dose of CZ48-CoS. Thus, biliary excretion of CZ48 was assumed to be minor when establishing the PK model. The estimated PK parameters of CZ48 and CPT after an oral dose of CZ48-CoS or CZ48-NS are presented in Tables 21 and 22. DV versus IPRED, DV versus PRED, CWRES versus TAD, and QQ IWRES scatterplots for each formulation group, CoS and NS, are shown in Figures 35 and 36, respectively.

The developed population PK model adequately described PK and biliary excretions of CZ48 and CPT in all compartments in CoS and NS groups. The CV % of population PK estimates was within 101 % in both formulation groups. The comparisons of observed values with the corresponding individual-specific

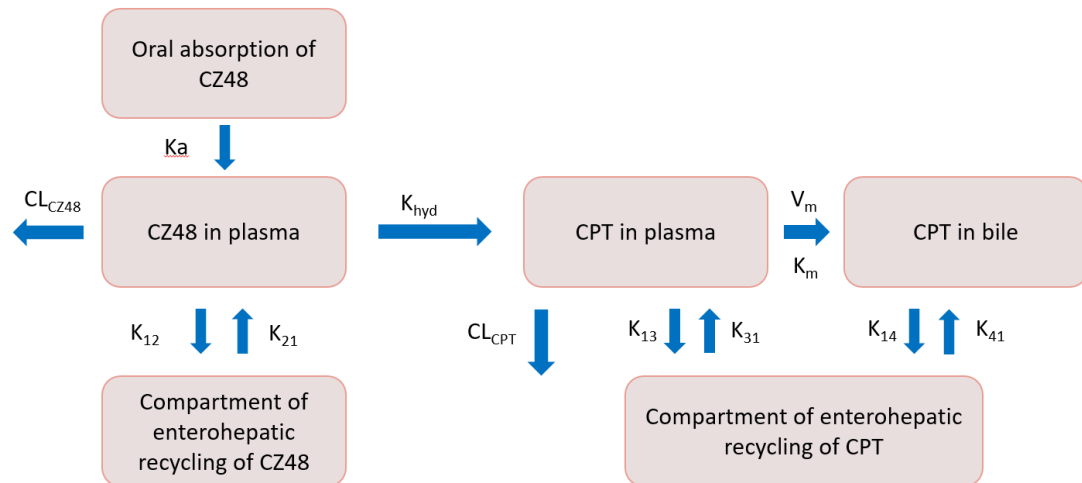
predicted values or population predicted values are shown in the scatterplots of DV versus IPRED or DV versus PRED. The plot showed the good model fit with good correspondences between individual predicted (or population predicted) and observed values almost falling on a slope line for CZ48 concentrations in plasma and CPT concentrations in plasma and bile for both formulation groups (Figures 35a, 35b, 36a, and 36b). In the CoS group, CZ48 concentrations in plasma were slightly underestimated at earlier time points and overestimated at later time points, and CPT concentrations in plasma were slightly overestimated with one outlier over the time (Figure 35c). However, the model fit for CPT concentrations in bile was good by showing all points were distributed around CWRES=0. In the NS group, Figure 36c showed the good model fit, since almost all points were distributed around CWRES=0, especially for CPT concentrations in plasma and bile.

When comparing estimated PK parameters in compartments between CoS and NS groups, the absorption rate constant ( $K_a$ ) was greater in the CoS group than in the NS group. The rate constants for hydrolysis of CZ48 to CPT were comparable between the two formulation groups (0.591 and 0.781  $\text{hr}^{-1}$  for CoS and NS groups, respectively). Interestingly, there was a clear increase in the rate constant from the compartment representing CPT concentrations in bile to the

compartment representing enterohepatic recycling of CPT ( $K_{14}$ ) in the NS group, as compared to that in the CoS group.

The population PK model was validated by employing two validation methods, bootstrapping and Visual Predictive Check (VPC) approaches. For the bootstrap analysis, multiple datasets (number of datasets: 145-200) were created from the original dataset. Tables 23 and 24 showed population PK estimates, and bootstrap median, 2.5% and 97.5% percentiles of the distributions in the CoS and NS groups, respectively. The population PK estimates were within 95% prediction intervals, and were close to median values of bootstrap estimates for both formulation groups. The VPC plots were obtained with 1,000 simulated concentration values and observed values at each time point as shown in Figures 37 and 38. The observed concentrations of CZ48 in plasma and CPT in plasma and bile were within 90% prediction intervals for both formulation groups, except one outlier of CPT concentration in plasma in the CoS group (Figure 37b). VPC plots for CPT concentrations in bile of the CoS and NS groups might imply overestimation of predictions by presenting a wider range of 90% prediction intervals than the observed concentration ranges.

Figure 34. The Population PK Model Structure Describing Pharmacokinetics of CZ48 and CPT in Plasma and Bile



$K_a$ : Absorption rate constant of CZ48

$K_{hyd}$ : Rate constant of hydrolysis of CZ48 to CPT

$CL_{CZ48}$ : Total clearance of CZ48 (metabolism, bile, urine, and feces)

$CL_{CPT}$ : Clearance of CPT (metabolism, urine, and feces)

$V_m$  and  $K_m$ : Nonlinear biliary excretion of CPT

$K_{12}$  and  $K_{21}$ : Rate constants for enterohepatic recycling of CZ48

$K_{13}$ ,  $K_{31}$ ,  $K_{14}$ , and  $K_{41}$ : Rate constants for enterohepatic recycling of CPT

Table 21. Estimated Population PK Parameters of CZ48 and CPT after an Oral Dose of CZ48-CoS for Each Compartment in the PK Model Shown in Figure 34

Population Parameter	Units	Population Estimate	Standard Error	CV%	2.5% CI	97.5% CI
V1	mg*ml/ng	0.02	0.01	24.80	0.01	0.03
CL <sub>CZ48</sub>	mg*ml/(ng*hr)	0.005	0.001	16.34	0.003	0.007
K <sub>a</sub>	1/hr	1.67	0.38	22.86	0.91	2.43
V2	mg*ml/ng	0.01	0.001	18.73	0.01	0.01
K <sub>hyd</sub>	1/hr	0.59	0.39	66.62	-0.19	1.37
CL <sub>CPT</sub>	mg*ml/(ng*hr)	0.177	0.178	101.02	-0.18	0.53
K <sub>12</sub>	1/hr	16.83	4.47	26.56	7.94	25.72
K <sub>21</sub>	1/hr	1.52	0.85	55.90	-0.17	3.21
V <sub>m</sub>	mg/hr	1.59	0.04	2.72	1.51	1.68
K <sub>m</sub>	ng/ml	19.64	0.28	1.41	19.09	20.19
K <sub>13</sub>	1/hr	0.23	0.01	6.18	0.20	0.26
K <sub>31</sub>	1/hr	4.48	0.12	2.61	4.25	4.71
K <sub>14</sub>	1/hr	0.69	0.08	11.06	0.54	0.84
K <sub>41</sub>	1/hr	0.97	0.002	0.16	0.97	0.97

V1: Volume of distribution of the compartment for CZ48 concentrations in plasma

V2: Volume of distribution of the compartment for CPT concentrations in plasma

Figure 35. Diagnostic Plots for CZ48 and CPT after an Oral Dose of CZ48-CoS

(a) DV versus IPRED:

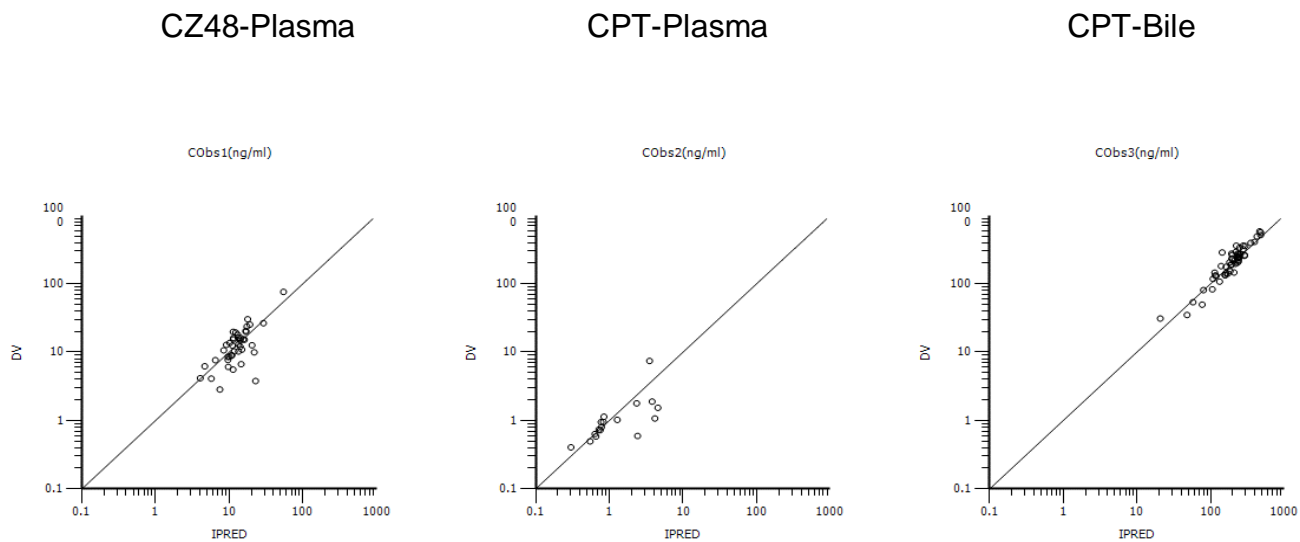


Figure 35 (Cont). Diagnostic Plots for CZ48 and CPT after an Oral Dose of CZ48-CoS

(b) DV versus PRED:

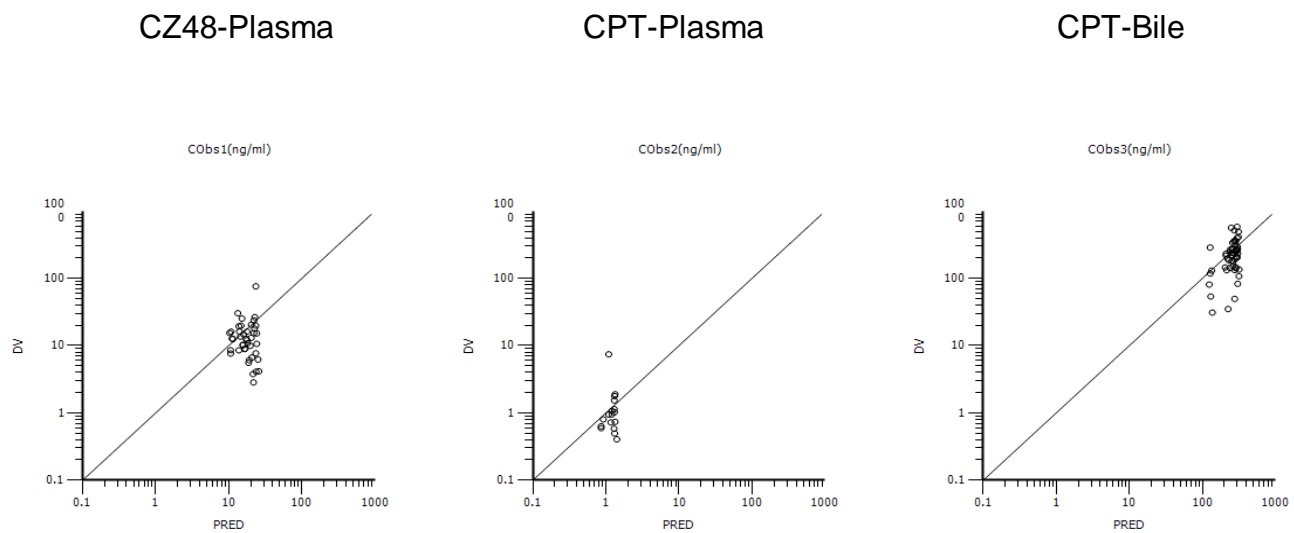


Figure 35 (Cont). Diagnostic Plots for CZ48 and CPT after an Oral Dose of CZ48-CoS

(c) CWRES versus TAD

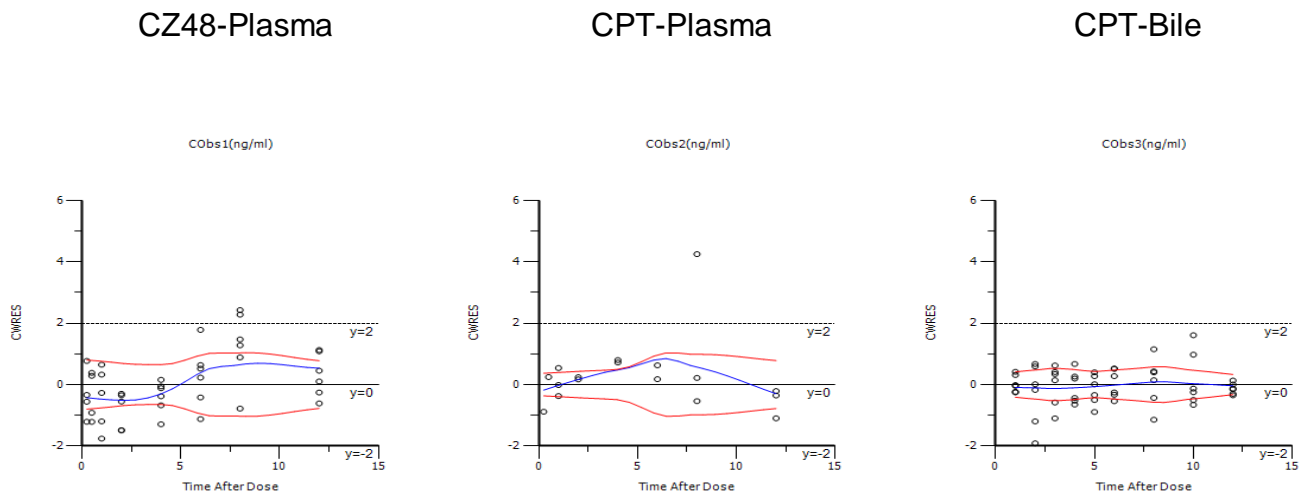


Figure 35 (Cont). Diagnostic Plots for CZ48 and CPT after an Oral Dose of CZ48-CoS

(d) QQ IWRES

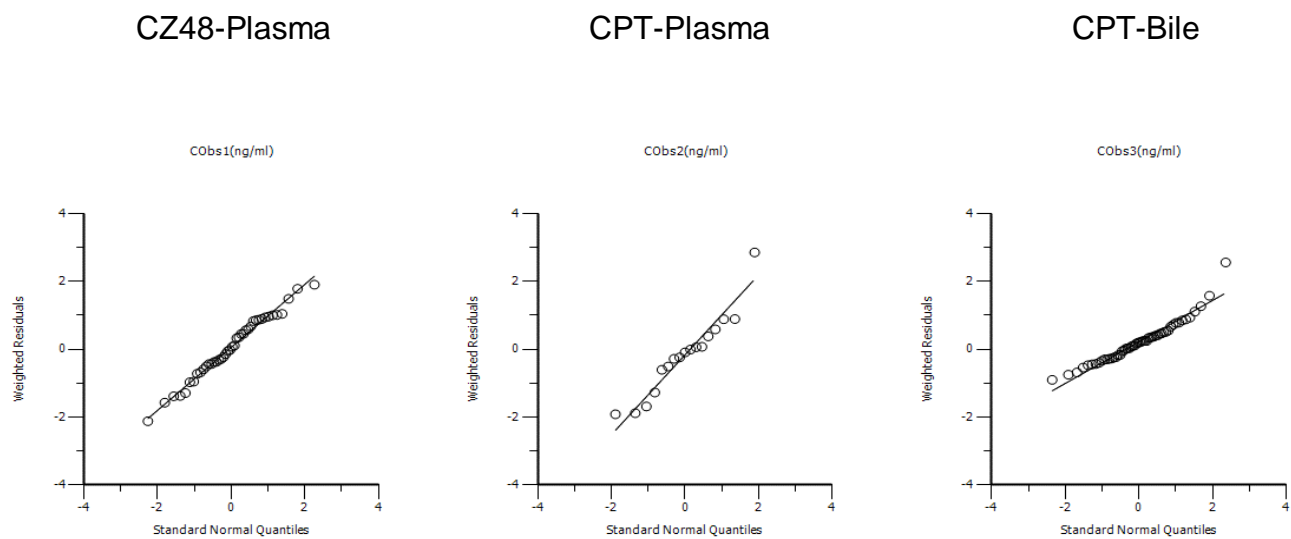


Table 22. Estimated Population PK Parameters of CZ48 and CPT after an Oral Dose of CZ48-NS for Each Compartment in the PK Model Shown in Figure 34

Population Parameter	Units	Population Estimate	Standard Error	CV%	2.5% CI	97.5% CI
V1	mg*ml/ng	0.004	0.001	28.88	0.002	0.01
CL <sub>CZ48</sub>	mg*ml/(ng*hr)	0.014	0.002	11.86	0.01	0.02
K <sub>a</sub>	1/hr	0.69	0.07	9.77	0.55	0.82
V2	mg*ml/ng	0.04	0.001	2.63	0.04	0.04
K <sub>hyd</sub>	1/hr	0.78	0.03	3.47	0.73	0.84
CL <sub>CPT</sub>	mg*ml/(ng*hr)	0.01	0.0001	2.47	0.01	0.01
K <sub>12</sub>	1/hr	29.85	1.09	3.64	27.66	32.05
K <sub>21</sub>	1/hr	0.43	0.01	2.88	0.41	0.46
V <sub>m</sub>	mg/hr	3.25	0.09	2.66	3.07	3.42
K <sub>m</sub>	ng/ml	18.16	0.40	2.22	17.35	18.98
K <sub>13</sub>	1/hr	0.42	0.01	1.87	0.40	0.43
K <sub>31</sub>	1/hr	3.06	0.09	3.10	2.87	3.25
K <sub>14</sub>	1/hr	56.15	0.75	1.34	54.63	57.67
K <sub>41</sub>	1/hr	0.16	0.002	1.02	0.15	0.16

V1: Volume of distribution of the compartment for CZ48 concentrations in plasma

V2: Volume of distribution of the compartment for CPT concentrations in plasma

Figure 36. Diagnostic Plots for CZ48 and CPT after an Oral Dose of CZ48-NS

(a) DV versus IPRED

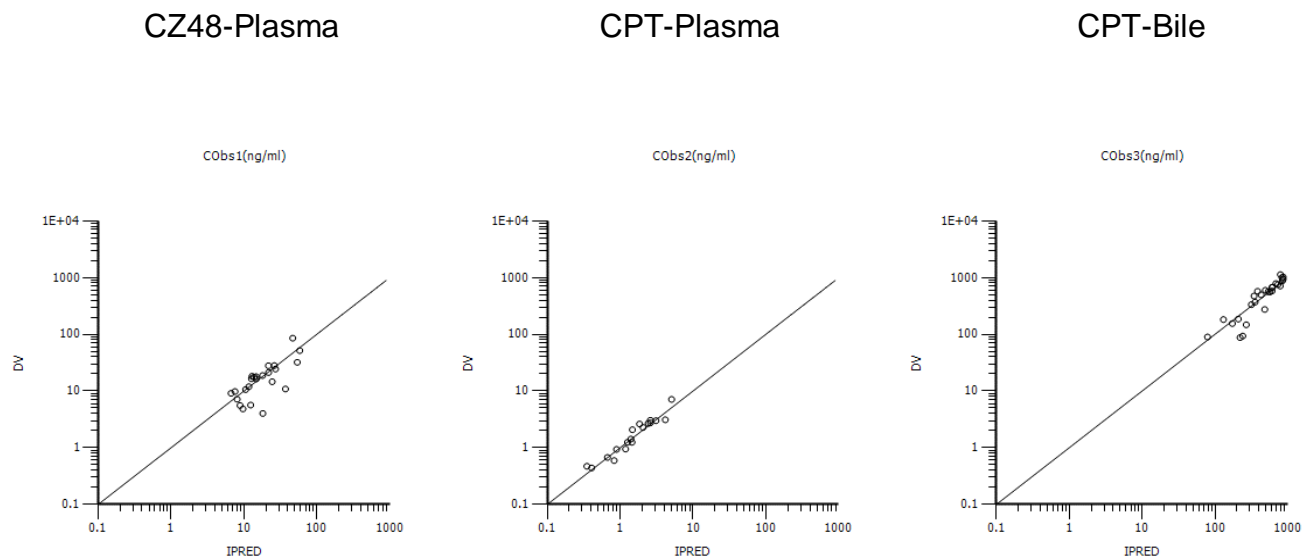


Figure 36 (Cont). Diagnostic Plots for CZ48 and CPT after an Oral Dose of CZ48-NS

(b) DV versus PRED

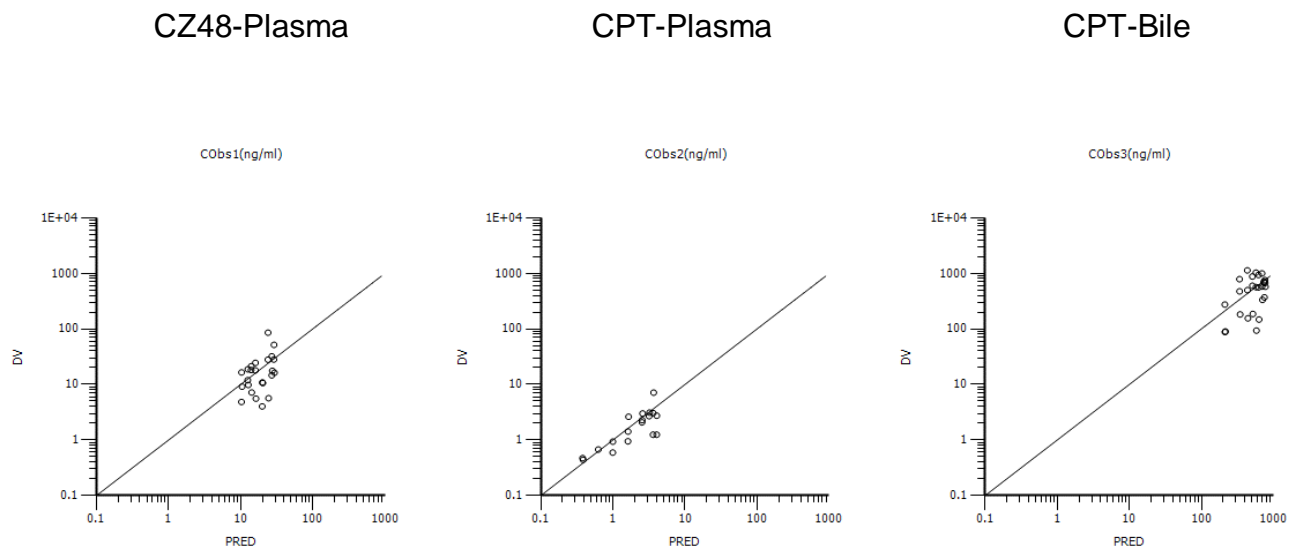


Figure 36 (Cont). Diagnostic Plots for CZ48 and CPT after an Oral Dose of CZ48-NS

(c) CWRES versus TAD

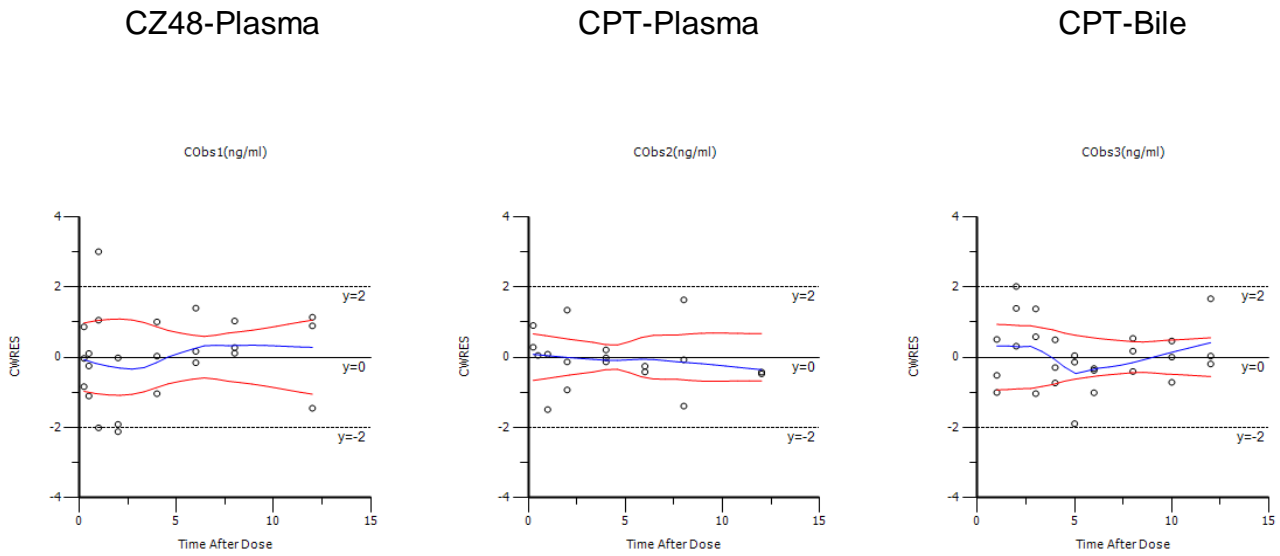


Figure 36 (Cont). Diagnostic Plots for CZ48 and CPT after an Oral Dose of CZ48-NS

(d) QQ IWRES

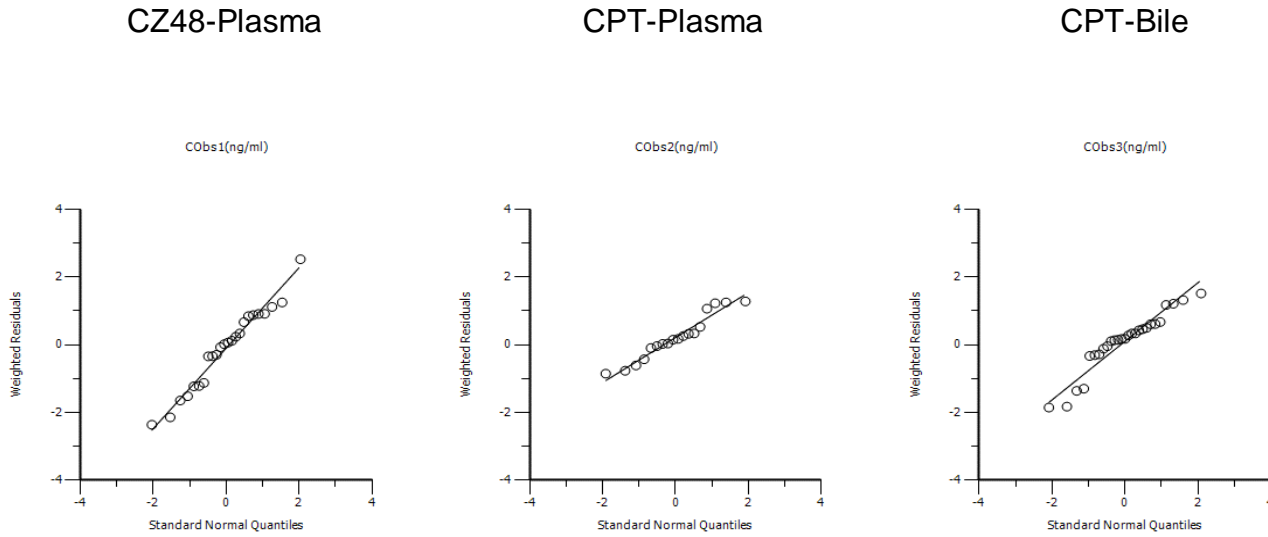


Table 23. Final Population Parameter Estimates and the Results of Bootstrap for the CoS Group

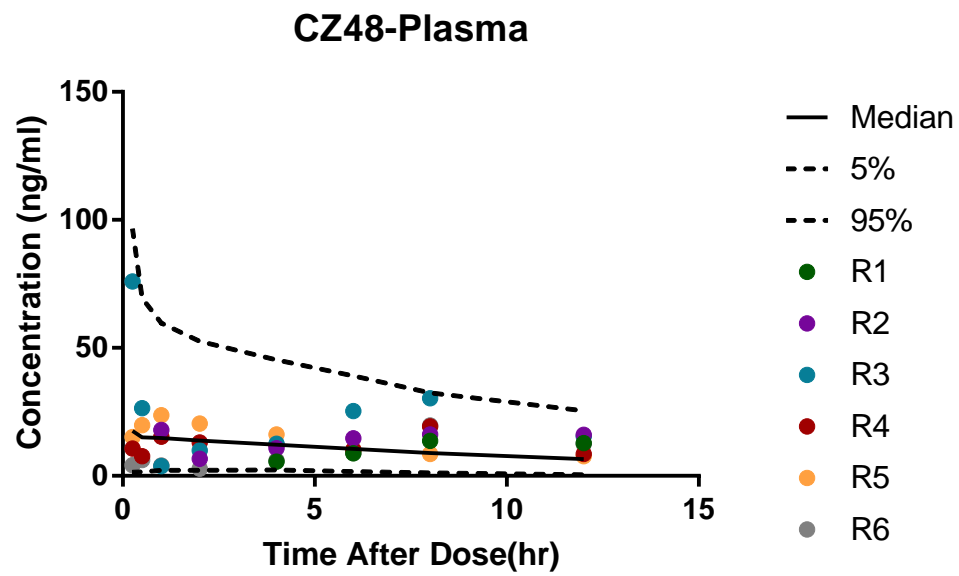
Population Parameter	Units	Population Estimate	CV%	Median	2.5%	97.5%
V1	mg*ml/ng	0.02	24.80	0.01	0.003	0.04
CL <sub>CZ48</sub>	mg*ml/(ng*hr)	0.005	16.34	0.0001	-0.007	0.014
K <sub>a</sub>	1/hr	1.67	22.86	1.32	0.20	8.64
V2	mg*ml/ng	0.01	18.73	0.01	0.002	0.18
K <sub>hyd</sub>	1/hr	0.59	66.62	0.65	0.04	4.35
CL <sub>CPT</sub>	mg*ml/(ng*hr)	0.18	101.02	0.07	0.01	0.22
K <sub>12</sub>	1/hr	16.83	26.56	22.98	9.23	82.03
K <sub>21</sub>	1/hr	1.52	55.90	0.75	0.42	2.87
V <sub>m</sub>	mg/hr	1.59	2.72	0.31	0.003	4.47
K <sub>m</sub>	ng/ml	19.64	1.41	3.91	0.03	175.80
K <sub>13</sub>	1/hr	0.23	6.18	0.20	0.02	1.32
K <sub>31</sub>	1/hr	4.48	2.61	14.63	3.43	98.33
K <sub>14</sub>	1/hr	0.69	11.06	0.69	0.24	4.55
K <sub>41</sub>	1/hr	0.97	0.16	0.86	0.02	4.31

Table 24. Final Population Parameter Estimates and the Results of Bootstrap for the NS Group

Population Parameter	Units	Population Estimate	CV%	Median	2.5%	97.5%
V1	mg*ml/ng	0.004	28.88	0.005	0.002	0.023
CL <sub>CZ48</sub>	mg*ml/(ng*hr)	0.014	11.86	0.012	-0.053	0.031
K <sub>a</sub>	1/hr	0.69	9.77	0.65	0.14	1.25
V2	mg*ml/ng	0.04	2.63	0.04	0.01	0.16
K <sub>hyd</sub>	1/hr	0.78	3.47	0.76	0.50	5.00
CL <sub>CPT</sub>	mg*ml/(ng*hr)	0.008	2.47	0.009	-0.003	0.088
K <sub>12</sub>	1/hr	29.86	3.64	23.97	4.82	42.38
K <sub>21</sub>	1/hr	0.43	2.88	0.41	0.003	0.64
V <sub>m</sub>	mg/hr	3.25	2.66	3.25	1.50	7.71
K <sub>m</sub>	ng/ml	18.16	2.22	16.43	0.97	28.48
K <sub>13</sub>	1/hr	0.42	1.87	0.44	0.26	1.10
K <sub>31</sub>	1/hr	3.06	3.10	2.97	1.68	9.17
K <sub>14</sub>	1/hr	56.15	1.34	52.34	1.72	87.03
K <sub>41</sub>	1/hr	0.16	1.02	0.15	0.12	0.51

Figure 37. Visual Predictive Check Plots for CZ48 and CPT from the CoS Group

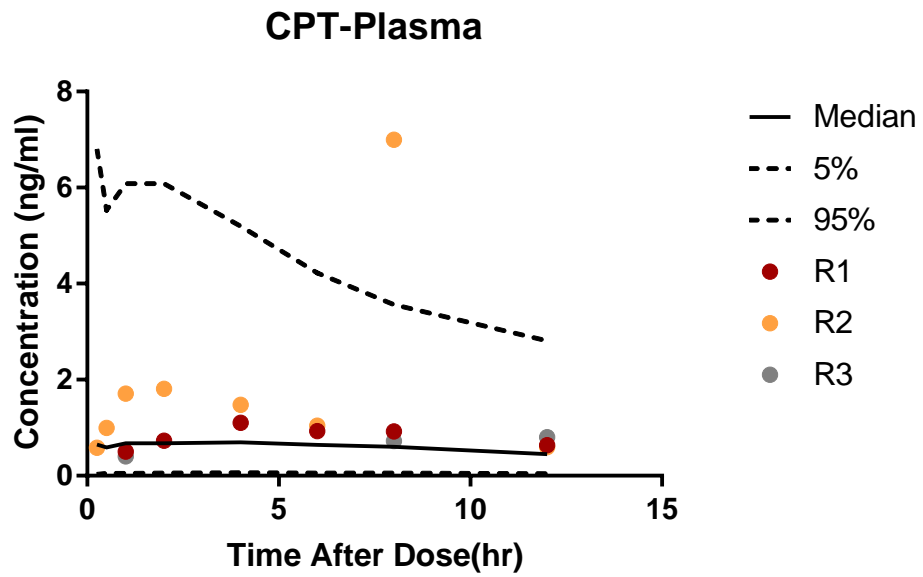
(a) CZ48 Concentrations in Plasma



R1-6: Individual observed data

Figure 37 (Cont). Visual Predictive Check Plots for CZ48 and CPT from the CoS Group

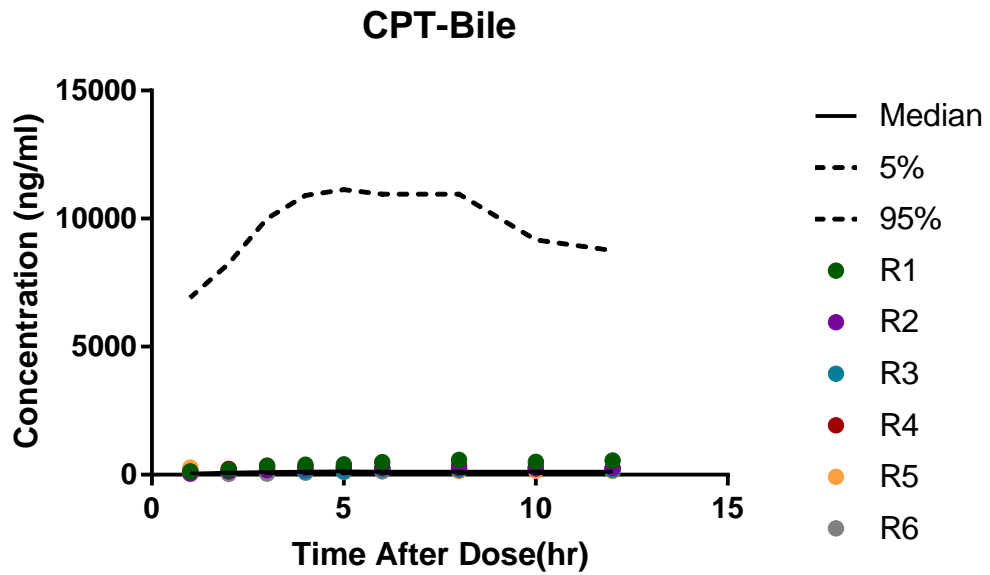
(b) CPT Concentrations in Plasma



R1-3: Individual observed data

Figure 37 (Cont). Visual Predictive Check Plots for CZ48 and CPT from the CoS Group

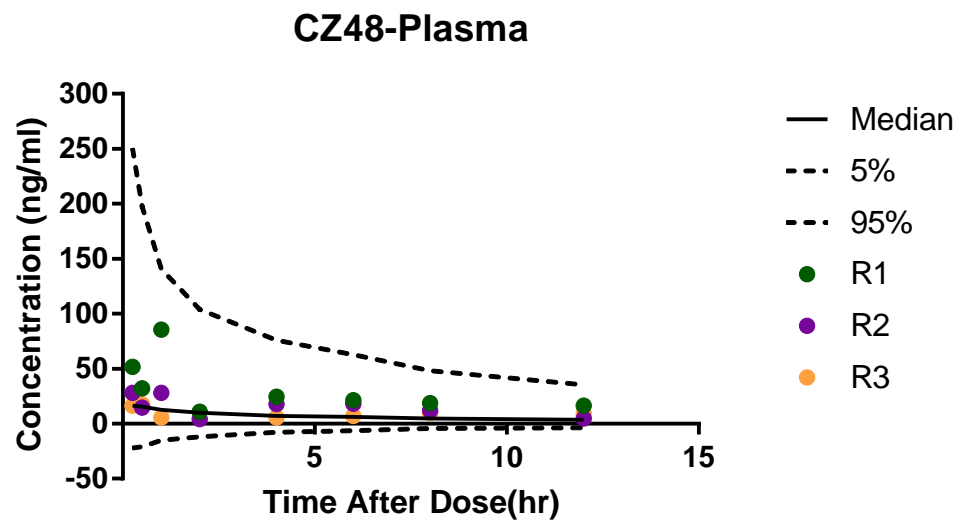
(c) CPT Concentrations in Bile



R1-6: Individual observed data

Figure 38. Visual Predictive Check Plots for CZ48 and CPT from the NS Group

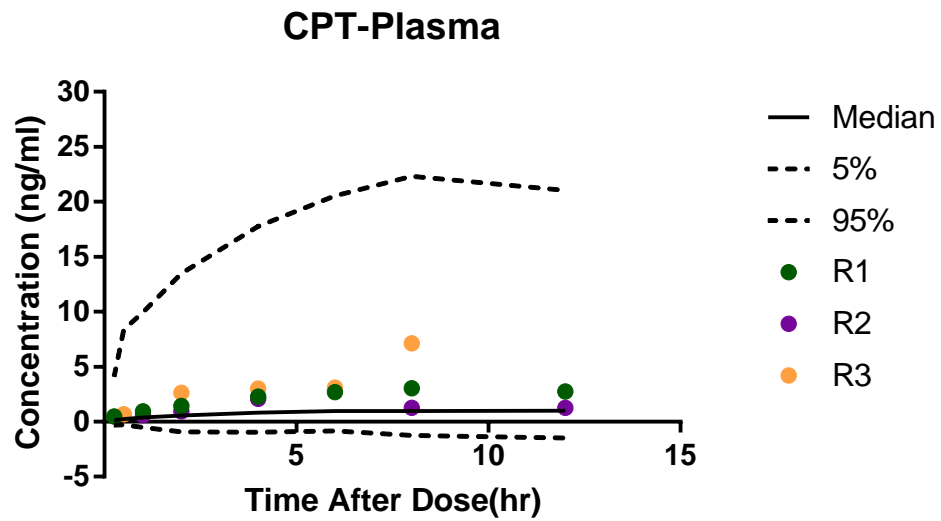
(a) CZ48 Concentrations in Plasma



R1-3: Individual observed data

Figure 38 (Cont). Visual Predictive Check Plots for CZ48 and CPT from the NS Group

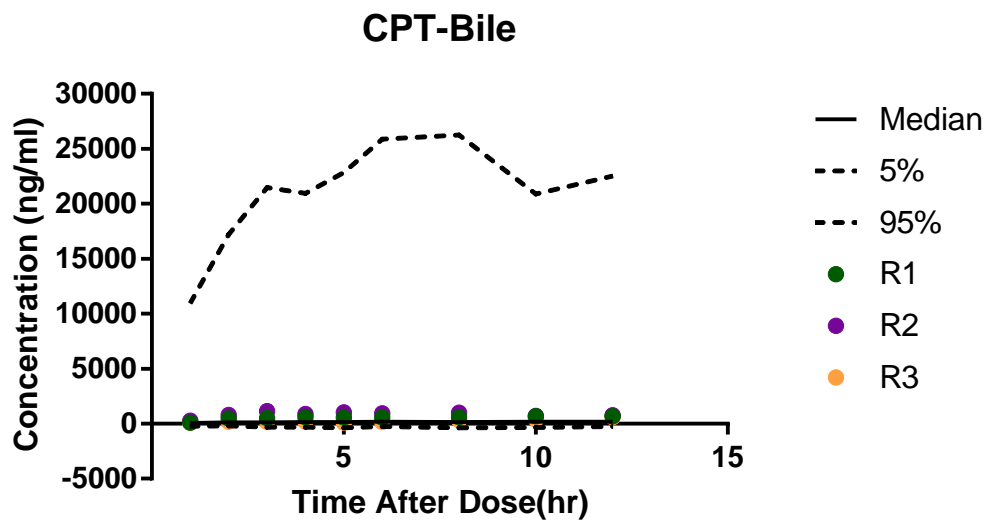
(b) CPT Concentrations in Plasma



R1-3: Individual observed data

Figure 38 (Cont). Visual Predictive Check Plots for CZ48 and CPT from the NS Group

(c) CPT Concentrations in Bile



R1-3: Individual observed data

## Chapter 5. Discussion

CZ48 is a promising anticancer agent, which showed remarkable tumor suppression against various types of human tumors with a lack of toxicity in nude mice (63). A merit of CZ48 over CPT, topotecan, and irinotecan is its lactone stability. Due to the stability, the majority of CZ48 stays as a lactone form in the blood circulation (23), and CZ48 is cleaved by esterase and converted to the active form once it is distributed into tumor cells or other targeted organs. However, during the phase 1 clinical trials, it was revealed that the concentration of CZ48 in the blood circulation was lower than expected. Later, studies demonstrated that it was because the formation rate of CPT in human liver was significantly higher than that in mouse liver (25). We believe nanosuspension formulation (NS) can be one potential approach to overcome the relatively rapid metabolic conversion of CZ48 to CPT in human liver. Based on *in vitro* and *in vivo* studies, NS provided the sustained release of CZ48 in plasma, tumor, and all tested organs, including liver, spleen, kidneys, lung, heart, and brain. The sustained release of CZ48 from NS may prevent the rapid biotransformation to CPT, which results in a prolonged exposure of the active moiety, CPT, in tissues. The efficacy of NS with the particle size of 200 nm was previously demonstrated in tumor-xenografted mice with subcutaneous inoculation of NSCLC H460 cells (29). Significant tumor growth suppression and prolonged duration of median survival (the period when half of

the animals are alive) without significant body weight loss were observed with the treatment of NS at 25 mg/kg.

Even though CZ48 has shown strong potential as an anticancer agent, studies are still scarce to fully understand its absorption, metabolism, and excretions. Especially, a unique observation was revealed in the oral plasma pharmacokinetic profiles of CZ48 and its active moiety, CPT (35). The profiles showed sustained elimination phases after an oral dose of CZ48, which may imply enterohepatic recycling of CZ48 and CPT. To characterize the enterohepatic recycling, it is the prerequisite to thoroughly investigate their hepatic metabolisms and biliary excretions. In particular, NS may impact biliary excretions and enterohepatic recycling of CZ48 and CPT, since NS significantly increased the exposure of CZ48 in the liver in both healthy (29) and tumor-xenografted mice; the liver is a major organ associated with biliary excretion and enterohepatic recycling of a drug. Thus, the effects of NS on biliary excretions and potential enterohepatic recycling of CZ48 and CPT were significantly addressed in this project.

## 5.1 Biodistributions of CZ48 and CPT in Tumor-Xenografted Mice

The impacts of nanosuspension (NS) on the biodistributions of CZ48 and CPT were evaluated in human tumor-xenografted Swiss nude mice. Swiss nude male mice were selected because it is well-established animal model to xenograft human tumor cells and to study pharmacokinetics of anticancer agents. NSCLC was selected for investigation using the tumor-xenografted mice based on the following rationales: (a) CZ48 from NS was highly exposed in the liver, lung, and spleen of healthy mice, and particularly CZ48 from both CoS and NS was highly exposed in the lung of healthy mice (29), and (b) lung cancer is the leading cause of cancer death, and approximately 80 to 85 % of lung cancers are NSCLS. To characterize the biodistribution, organ exposures ( $AUC_{0-4h}$ ) and half-lives of CZ48 and CPT after a single IV dose of CZ48 nanosuspension (CZ48-NS) were compared with those after a single IV dose of CZ48 co-solvent (CZ48-CoS) in six organs, including liver, kidneys, lung, spleen, heart, and brain, as well as tumor. In addition, the biodistributions of CZ48 and CPT were compared between healthy and tumor-xenografted mice.

### **5.1.1 Biodistributions of CZ48 and CPT from CoS or NS in Tumor-Xenografted Mice**

Biodistribution patterns were different between CoS and NS groups. After a CZ48-CoS dosing, CZ48 was highly distributed in the lung. However, after a CZ48-NS dosing, CZ48 was highly accumulated in the liver, spleen, and lung. On the contrary, the biodistribution patterns of CPT were comparable between CoS and NS groups, which showed the highest exposure in the liver and the lowest exposure in the brain.

The CZ48 exposure ( $AUC_{0-4h}/Dose$ ) was significantly increased by NS in the reticuloendothelial system (RES) rich cell organs, liver and spleen. It has been well known that the RES cells recognize nanoparticles as foreign particles and uptake them to clear while they are circulating in the blood. *In vitro* release studies have been conducted to characterize the release of CZ48 from NS in human plasma for 48 hr (29). CZ48-NS showed sustained release characteristics in human plasma, 10.6-fold longer than that of CoS. Therefore, CZ48-NS was expected to circulate in the blood for a prolonged period of time and to have more chances to be exposed to RES cells. As a result, CZ48 exposures in the liver and spleen were significantly higher, as compared to those in other organs. In particular, liver is a key organ responsible for biliary excretion, metabolism, and enterohepatic

recycling of a drug. Thus, a significant increase of CZ48 exposure in the liver by NS may affect the biliary excretion and enterohepatic recycling of CZ48 and its active moiety, CPT. These effects were evaluated in Specific Aims 2 and 3. On the other hand, the CZ48 exposure was significantly decreased in kidneys, heart, brain, and tumor. More sustained concentrations of CZ48 were observed by NS in the organs and tumor, with approximately 1.5 – 2.8 times longer half-lives of CZ48, as compared to those in the CoS group. This sustained concentration characteristic of CZ48 was also appeared in all tested organs including the RES organs.

NS did not increase the exposure ( $AUC_{0-4h}$ ) of CPT in tumor and six tested organs, compared to that in the CoS group. CPT from CoS or NS was high in the liver. Based on *in vitro* metabolism studies (1), the highest metabolic conversion and esterase activity of CZ48 to CPT were observed in the hepatic tissue. Due to high exposure of CZ48 and active conversion from CZ48 to CPT in the liver, the CPT exposure was the highest in the liver as compared to other organs. The CPT exposure was intermediately in tumor, spleen, lung, and kidneys. The off-target effect of CPT by NS may be relatively less in the brain due to the lowest exposure of CZ48 and CPT. Like CZ48, concentration-time profiles showed sustained concentrations of CPT by NS in tumor and all tested organs, as compared to those in the CoS group.

In particular, the exposures of CZ48 and CPT were significantly decreased by NS in tumor. However, the residence times (half-lives) of CZ48 and CPT were approximately 2.7 and 3.5 times longer, respectively, with NS. Since CZ48 and CPT are S-phase cell-cycle specific agents, a sustained drug exposure to the tumor at a moderate concentration exceeding a minimum threshold is more effective for its antitumor activity than a short-term exposure at a high concentration (30). The prolonged exposures of CZ48 and CPT by NS without a remarkable increase in their concentrations in tumor will be beneficial for the treatment of cancer.

### **5.1.2 Biodistributions of CZ48 and CPT from Co-S or NS in Healthy or Tumor-Xenografted Mice**

The biodistribution patterns of CZ48 and CPT from CoS or NS were compared between healthy and tumor-xenografted mice. The biodistribution patterns using healthy Swiss nude mice were previously studied (29). The same IV dose and dosing formulations (CoS and NS) were given to both healthy and tumor-xenografted Swiss nude male mice (25 – 30 g). For tumor-xenograft mouse model, the NSCLC H460 cells were subcutaneously injected and the mice were considered to be ready for the biodistribution study when the tumor volume was approximately 100 mm<sup>3</sup> (approximately 8-10 days after injection). Organ samples

were collected from healthy mice for up to 12 hr and from tumor-xenografted mice for up to 4 hr. In tumor-xenograft mice, samples were collected for the shorter period of time (4 hr), due to the limited availability of tumor mouse model. The rapid decrease in concentrations of CZ48 and CPT was observed with the half-lives of 0.58 – 2 hr in all tested organs after the administration of CZ48-CoS. However, the concentrations were sustained with the prolonged half-lives, 1.03 – 38.21 hr, after the administration of CZ48-NS (data from the healthy mice (29)).

No remarkable differences in  $AUC_{0-\infty}/Dose$  values of CZ48 and CPT were observed in most tested organs between healthy and tumor-xenografted mice except in lung. The CZ48 exposure was highly increased by NS in the RES organs, liver and spleen. The CPT exposure was the highest in the liver and the lowest in the brain. The extent of CPT exposures was comparable between CoS and NS groups as well as between healthy and tumor-xenografted mice. Half-life values of CZ48 and CPT were prolonged by NS in all tested organs in both healthy and tumor-xenografted mice, as compared to those by CoS.

Two differences were observed in biodistributions of CZ48 and CPT between healthy and tumor-xenografted mice. First,  $AUC_{0-\infty}/Dose$  of CZ48 was approximately 13.2 times increased by NS in the lung of healthy mice, although

$AUC_{0-\infty}/Dose$  was comparable between CoS and NS in the lung of tumor-xenografted mice. Second, half-life values of CZ48 and CPT were more highly increased in healthy mice than those in tumor-xenografted mice. Half-life values of CZ48 and CPT were approximately 1.8-19.1 and 2.8-9.5 times extended by NS in six tested organs of healthy mice, but 1.5-2.8 and 2.3-3.6 times increased, respectively, by NS in tumor-xenografted mice. There is no clear explanation for these observations at this time, and the phenomenon of tumor-induced changes in drug distribution warrants future investigation.

Advantages and limitations of using immunosuppressed mice subcutaneously implanted with human tumors for the anticancer drug development have been discussed in many previous reports (64-67). The main advantage of this model is its convenience to evaluate antitumor activities of antitumor agents in a preclinical stage, including simple implantation, reproducibility, and homogeneity in tumor characteristics (68). However, an analysis by the National Cancer Institute (NCI) using the data of 39 cytotoxic agents showed that a xenografted model provided moderate prediction of clinical responses for the agents that showed at least one-third of activity in xenografted models (64-67). Furthermore, NSCLS xenografted mice provided the most prediction of clinical responses for the agents in the same disease, and breast cancer xenografts provided the most prediction of clinical

responses in any diseases (69). In addition, there are studies characterizing drug metabolism and pharmacokinetics (DMPK)-related gene expression profiles and responses to typical cytochrome P450 inducers in monolayer carcinoma cells grown in tissue culture versus those subcutaneously inoculated into xenograft nude mice (70). Their observations indicated that the expression of drug metabolizing enzymes and transporters increased after inoculation of tumor cells into mice, and these observations were primarily due to the up-regulation of the DMPK-related gene regulation pathway resulting from up-regulated nuclear receptor expression. This study is an important report showing the changes in expression levels of metabolizing enzymes and transporters in tumor cells, which may significantly affect the antitumor activity of anticancer compounds in tumor cells.

## **5.2 Method Development and Validation Using UPLC-MS/MS**

It is critical to develop a sensitive and reliable analytical method for the evaluation of drug pharmacokinetics in preclinical and clinical studies. After the administration of CZ48, it is converted to CPT by esterase, and CPT is an active moiety for its antitumor activity. Thus, it is prerequisite to develop an analytical method for the simultaneous quantifications of CZ48 and CPT in various biological matrices, such as bile and urine, in order to fully evaluate pharmacokinetics of CZ48.

To date, an analytical method was developed for the simultaneous quantifications of CZ48 and CPT in plasma using high-performance liquid chromatography (HPLC) with a fluorescence detector (62). To our knowledge, no analytical method was reported for the simultaneous quantifications of CZ48 and CPT in different matrices, such as bile. In this study, we speculated enterohepatic recycling of CZ48 and CPT. Based on our previous pharmacokinetic studies, sustained concentrations of CZ48 and CPT were observed up to 6 hr after an oral dose of CZ48, even though their concentrations rapidly declined after an IV dose (35). In particular, biliary excretion is one of the important elimination pathways for many drugs and/or their conjugated metabolites, and a critical factor that affects enterohepatic recycling of drugs and/or metabolites. To characterize potential enterohepatic recycling of CZ48 and CPT, it was the prerequisite to develop a reliable analytical method that simultaneously quantifies CZ48 and CPT in both plasma and bile. Moreover, it is widely known that ultra-performance liquid chromatography with mass spectrometry (UPLC-MS/MS) system provides more rapid, selective, and sensitive methods to generate drug pharmacokinetics than the HPLC system. Hence, the UPLC-MS/MS system was selected to simultaneously quantify CZ48 and CPT in plasma and bile.

The developed analytical method in our study provided higher sensitivity than a previous method using the HPLC-fluorescence system. LLOQ values of CZ48 and CPT using the HPLC-fluorescence system were 10 and 5 ng/ml, respectively, in mouse plasma (62). However, the developed method using UPLC-MS/MS in this study provides higher sensitivity with the LLOQ of 0.98 ng/ml and 3.9 ng/ml in rat plasma and bile, respectively, for both CZ48 and CPT. The higher sensitivity enabled us to quantify low concentrations of CZ48 and CPT in rat plasma for up to 12 hr after an oral dose of CZ48.

The solid phase extraction (SPE) method was employed to extract CZ48 and CPT from rat bile. It is an efficient method to remove bile salts and interferences in bile before injecting it into mass spectrometry, as compared to protein precipitation and liquid-liquid extraction methods.

### **5.3 Phase 1 and 2 Metabolisms of CPT**

Hepatic metabolism is one of the major elimination routes of many drugs. Liver is a major organ for phase 1 and 2 metabolisms of drugs. Based on the biodistribution study in healthy and tumor-xenografted Swiss nude mice, CZ48 and CPT were highly distributed into the liver after an IV dose of CZ48-CoS or CZ48-NS.

Moreover, the CZ48 exposure was remarkably increased by NS in the liver. Since the exposures of CZ48 and CPT were high in the liver, it is critical to evaluate their phase 1 and 2 metabolisms. Furthermore, hepatic metabolism is a key factor that may influence enterohepatic recycling of drugs. We initially hypothesized that CPT and/or phase 1 metabolites of CPT are conjugated by phase 2 metabolizing enzymes such as UGTs and SULTs in the liver, and then CPT conjugates may be secreted into the bile and undergo enterohepatic recycling with its parent form, CPT. Based on chemical structures of CZ48 and CPT, CPT contains a hydroxyl group, but CZ48 does not. Thus, we hypothesized that CPT may be metabolized after the biotransformation from CZ48 to CPT in the liver. With these hypotheses, we examined the phase 1 and 2 metabolisms of CPT by conducting *in vitro* metabolism studies.

Our *in vitro* phase 2 metabolism study indicated that CPT was not conjugated by UGTs or SULTs even after overnight incubation in rat liver microsomes or S9 fractions with cofactors, UDPGA for glucuronidation or PAPS for sulfation. Phase 1 metabolism study was additionally conducted in order to investigate whether CPT is conjugated after its phase 1 metabolism in the liver. However, no significant phase 1 metabolites were identified even after 4 hr incubation of CPT in rat liver microsomes with NADPH.

Even though *in vitro* studies did not show significant phase 1 and 2 metabolisms of CPT, there is a study showing the phase 1 metabolism of CPT by employing the isolated perfused rat liver system (71). In their study, three phase 1 metabolites, one monohydroxylation and two dihydroxylation, were identified in bile and a monohydroxylation was identified in perfusate. No phase 2 conjugations with glucuronic acid or sulfuric acid were identified in this *ex vitro* metabolism study. Even though phase 1 metabolites of CPT were identified in their study, the formation of three phase 1 metabolites in the liver was low, which was 2.8% of total cleared CPT. Hence, phase 1 metabolism may not significantly contribute to the hepato-biliary excretion and enterohepatic recycling of CPT *in vivo*.

#### **5.4 Biliary Excretions of CZ48 and CPT in SD Rats**

Biliary excretion is one of the major elimination routes for drugs and/or their conjugates. However, it is experimentally difficult to evaluate biliary excretion of a drug in the clinical stage. It is important to examine biliary excretion of a drug using preclinical animal model in the drug discovery and development process. In addition, biliary excretion is an important factor related to enterohepatic recycling of a drug. In particular, plasma concentration-time profiles of CZ48 and CPT implied potential enterohepatic recycling of CZ48 and CPT *in vivo* (35). A sustained concentration (extended half-life) and double/multiple peaks of a drug in its oral

PK profile are common observations when the drug undergoes enterohepatic recycling. In this study, biliary excretions were thoroughly investigated using bile duct-cannulated SD rats by administering a CZ48 dose in two major dosing routes, IV and oral, and in two different types of formulations, CoS and NS.

#### **5.4.1 Biliary Excretions of CZ48 and CPT after an IV Dose of CZ48-CoS**

Biliary excretions of CZ48 and CPT were initially examined after an IV administration of CZ48-CoS to bile duct-cannulated rats. The purpose of this study was to evaluate whether CZ48 and CPT are highly excreted into the bile. With this purpose, key biliary PK parameters, such as cumulative amounts in bile, biliary clearances, and dose recoveries (%) in bile were determined. A one-compartment pharmacokinetic model best described pharmacokinetics of CZ48 and CPT after an IV dose of CZ48-CoS. Key results from this study were that: (1) CPT was more favorably secreted into the bile than CZ48, and (2) % dose recovery of CPT, active moiety of CZ48, in bile was minor.

Based on plasma concentration-time profiles of CZ48 and CPT, the concentration of CZ48 was higher than that of CPT in plasma.  $AUC_{0-6h}$  of CZ48 ( $3203.03 \pm 1785.24 \text{ hr} \cdot \text{ng/ml}$ ) was approximately 4.4 times higher than that of CPT ( $722.13 \pm$

397.72 hr\*ng/ml). On the contrary, biliary clearance ( $CL_b$ ) of CZ48 was  $0.87 \pm 0.20$  ml/hr, which was approximately 64.8 times lower than that of CPT ( $56.38 \pm 15.37$  ml/hr). There are two potential reasons regarding more favorable biliary secretion of CPT than CZ48. First, CPT is secreted into the bile after its conversion from CZ48 by esterase in the liver. Active metabolic conversion and esterase activity of CZ48 to CPT in hepatic tissue have been previously demonstrated (1). Second, CPT might have more favorable binding affinity to transporters than CZ48 for biliary excretion. In general, it is more appropriate for biliary secretion when a parent compound is altered to a metabolite that is more hydrophilic, large, and charged (34). However, no remarkable CPT conjugations by UGTs and SULTs enzymes were observed in our *in vitro* studies, and CZ48 and CPT were secreted into the bile as their parent forms. Hence, the biliary secretions of CZ48 and CPT might be mediated by transporters. To date, there is no report showing the association of CZ48 with influx/efflux transporters. The associations of CPT with human P-glycoprotein (P-gp, ABCB1) and human MRP2 (ABCC2) were studied (72). In the study, they demonstrated that CPT is a substrate of P-gp and MRP2 by using Caco-2 cells, MDCK2 wild-type cells, and MDCK2 cells transfected with human P-gp or human MRP2. It has been known that P-gp and MRP2 located on the canalicular membrane of hepatocytes contribute to biliary excretions of xenobiotics (47, 73). Hence, those two transporters might play roles in the transporter-mediated secretion of CPT into bile.

The percent (%) recoveries of CZ48 and CPT in bile were about  $0.19 \pm 0.10$  and  $3.05 \pm 1.13$  %, respectively, which indicated that biliary excretion is not a major elimination route after an IV dose of CZ48. This is the first study evaluating biliary excretions of CZ48 and CPT after a CZ48 dosing. In the previous studies, biliary and urinary excretions of CPT were evaluated after a CPT (lactone) or sodium form of CPT (Na-CPT) dosing (74). In the study, CPT (lactone) or Na-CPT was administered via IV infusion into the left external jugular vein of SD rats. After an IV dose of CPT (lactone),  $10.1 \pm 4.2$  % of the dose was excreted into the urine and  $7.5 \pm 4.2$  % of the dose was excreted into the bile. After an IV dose of Na-CPT,  $39.5 \pm 10.4$  % and  $26.4 \pm 8.9$  % of the dose were excreted into the urine and bile, respectively. Based on their studies, CPT was more favorably excreted via the urine than the bile. CPT was highly excreted via the bile after a Na-CPT dosing (26.4 %). However, the amount of CPT excreted via the bile was relatively low after a CPT dosing (7.5 %).

#### **5.4.2 Biliary Excretions of CZ48 and CPT after an Oral Dose of CZ48-CoS**

In the study of biliary excretions of CZ48 and CPT after an oral dose of CZ48-CoS, bile was collected intermittently to examine whether biliary secretions of CZ48 and CPT are sustained. We hypothesized that the biliary secretions of CZ48 and CPT may be sustained if they undergo enterohepatic recycling.

Similar to the CZ48 and CPT profiles in plasma and bile after an IV dose of CZ48-CoS, the concentration of CZ48 was higher than that of CPT in plasma. On the contrary, biliary secretion of CPT was dominant than CZ48, so that the amount of CPT observed in bile was remarkably higher than that of CZ48. As shown in the plasma concentration-time profiles of CZ48 and CPT for 6 hr after an oral dose of CZ48-CoS (35), our plasma profiles also showed sustained concentrations of CZ48 and CPT in plasma till 12 hr after the oral dose of CZ48 prepared in the same CoS formulation. Double/multiple peaks were observed within 2 hr post oral dose of CZ48 in both oral plasma profiles of CZ48 and CPT. The sustained characteristics were also observed in their bile profiles. The biliary secretions of CZ48 and CPT were sustained up to 12 hr without a decline after an oral dose of CZ48-CoS. The sustained biliary secretions of CZ48 and CPT might support their enterohepatic recycling.

#### **5.4.3 Comparison of Biliary Excretions of CZ48 and CPT Between IV and Oral Doses of CZ48-CoS**

The characteristics of biliary excretions of CZ48 and CPT were compared by administering a CZ48-CoS dose in two different dosing routes, IV and oral. The plasma concentration-time profiles and drug amount profiles in bile showed distinct trends between IV and oral groups. After an IV dose of CZ48-CoS, CZ48 and CPT

concentrations in plasma rapidly declined within 6 hr post dose, and their amounts in bile were also decreased after 1 hr post dose. On the contrary, CZ48 and CPT concentrations in plasma and their amounts secreted in bile were sustained for 12 hr after an oral dose of CZ48-CoS. A potential reason of the sustained concentrations in plasma and biliary secretions of CZ48 and CPT after an oral dose might be their circulations in the liver, bile, and intestine by enterohepatic recycling.

The amounts of CZ48 and CPT secreted in bile were lower after an oral dose than those after an IV dose. However, their concentrations were also lower in plasma after an oral dose. Lower amounts of CZ48 and CPT in bile after an oral dose were due to incomplete oral absorption of CZ48-CoS. Based on our pharmacokinetic study, oral bioavailability of CZ48-CoS was approximately 1.98%.

Due to the low concentrations of CZ48 and CPT in the systemic circulation after an oral dose, the concentration ratio of CZ48 (or CPT) in bile to plasma (B/P) was calculated to more reasonably compare their biliary excretions between IV and oral groups. Although actual amounts of CZ48 and CPT in bile were lower after an oral dose, the concentration ratios of CZ48 (or CPT) of B/P were higher after an oral dose than an IV dose. The ratios were approximately 1.4 – 5.6 times increased

after the oral dose. Hence, we concluded that increased amounts of CZ48 and CPT were secreted into bile when a dose was orally administered.

#### **5.4.4 Impact of NS on the Biliary Excretions of CZ48 and CPT after an Oral Dose of CZ48**

Biliary excretions of CZ48 and CPT were compared after an oral dose of CZ48 in two different types of formulations, CoS and NS, in order to evaluate the impact of NS on the biliary excretions of CZ48 and CPT. Bile was intermittently collected from bile duct-cannulated SD rats for 12 hr after an oral dose of CZ48-CoS or CZ48-NS.

The plasma concentration-time profiles of CZ48 and CPT were similar between two different formulation groups. After an oral dose of CZ48-CoS or CZ48-NS, sustained concentrations of CZ48 and CPT were observed till 12 hr post dose in their plasma profiles. The bile profiles showed similar trends between two formulation groups. First, CPT amounts were remarkably higher than CZ48 amounts, which was a consistent result from the biliary excretion study after an IV dose of CZ48. It supported that CPT is more favorable for biliary excretion than CZ48. Second, the amounts of CZ48 or CPT secreted in bile were similar between

two formulation groups. Third, CZ48 and CPT secretions were sustained till 12 hr post oral dose in both groups.

The effect of NS on the biliary excretions of CZ48 and CPT were evaluated by comparing  $AUC_{0-12h}$  ratios of CZ48 (or CPT)-B/P. The ratios of B/P did not exhibit significant differences between the two formulation groups. The ratios of CZ48 were  $1.34 \pm 0.44$  and  $1.13 \pm 0.52$  in CoS and NS groups, respectively. Those of CPT were  $191.96 \pm 128.83$  and  $339.33 \pm 336.71$  in CoS and NS groups, respectively. These results indicated there was no significant effect of NS on the biliary excretions of CZ48 and CPT for 12 hr post dose with the given doses with CoS and NS, respectively.

### **5.5 Enterohepatic recycling of CZ48 and CPT after an oral dose of CZ48-NS**

Enterohepatic recycling of CZ48 and CPT was characterized by using two different types of SD rats, bile duct-cannulated and bile duct-intact SD rats. In this study, enterohepatic recycling of CZ48 and CPT was completely interrupted by continuously collecting bile from bile duct-cannulated rats for 8 hr (Group D in Table 4). In bile duct-intact rats, complete enterohepatic recycling was existed

during experiments (Group E in Table 4). Bile was also collected intermittently at designated time points for 12 hr from bile duct-cannulated SD rats (Group C in Table 4). In the Group C, recycling was existed, but only interrupted when collecting bile samples. Group C was included in this study for two purposes. First, biliary secretions of CZ48 and CPT were compared with or without the presence of enterohepatic recycling. Second, plasma pharmacokinetics of CZ48 and CPT were compared between bile duct-cannulated and bile duct-intact rats, in the presence of enterohepatic recycling, since bile duct-cannulation may impact drug PK in plasma.

The plasma concentration-time profiles of CZ48 and CPT were similar in all three groups. We observed sustained drug concentrations for 8 or 12 hr with or without the presence of enterohepatic recycling of CZ48 and CPT. The bile profiles showed the sustained biliary secretions of CZ48 and CPT up to 8 or 12 hr post oral dose. The concentration ratios of CZ48 (or CPT)-B/P were compared between Group C and D, with or without the presence of enterohepatic recycling. The trend of ratio profiles showed a slight decline between 2 and 4 hr post dose. But the ratios were sustained at later time points. These results indicated that the enterohepatic recycling of CZ48 and CPT was minor in this study. However, the duration of sample collection time for Group D (for continuous bile collection) was

shorter (8 hr) than other groups, and might not be sufficient to conclude the enterohepatic recycling of CZ48 and CPT. Thus, continuous studies are recommended to confirm their recycling. There are multiple factors including enterohepatic recycling that might induce the sustained concentrations of CZ48 and CPT after an oral dose. Other possible reasons might be continuous absorption of CZ48 into the different segments in the gut at different absorption rates, different dissolution characteristics of CZ48 by pH variations in the gut, and/or the depot of CZ48 in the liver (75).

In the enterohepatic recycling study, bile duct-intact rats were employed for the complete enterohepatic recycling model in Group E (Table 4). However, the use of bile duct-cannulated rats without collecting bile may be a more proper control model, since bile duct cannulation may impact PK of CZ48 and CPT in rats. Previous studies evaluated the effect of bile duct-cannulation on the health conditions of SD male and female rats, and demonstrated limited and short-term alterations of the liver function (76). In their study, a catheter was inserted into the bile duct, with one extremity towards the liver and the other towards the duodenum. The bile flow was diverted via an exteriorized loop on the neck of rats. When collecting bile, the loop was sectioned into two portions. One section of catheter was used for bile collection and the other section was connected to an infusion

pump to deliver an artificial bile salt solution. The results showed that approximately 70 % of the surviving animals had normal serum liver enzyme levels, such as bilirubin, alkaline phosphatase, alanine aminotransferase, and aspartate aminotransferase, 2 days after surgery. There were slight to moderate focal/hemorrhagic hepatocytic necrosis and minimal peri-biliary fibrosis on days 8 and 22 after surgery, and slight to moderate epithelial hyperplasia in the major bile duct mainly on day 22.

Although enterohepatic recycling of CZ48 and CPT was minor in rats, the extent of enterohepatic recycling of CPT may be significant in Humans. The difference between humans and animals may be due to anatomical, physiological, and biochemical differences among species. In animals that do not possess a gallbladder (e.g. rats), bile fluid is secreted continuously. However, in humans, a drug is accumulated in gallbladder during fasted state, and released at meal time over some period of time, which may cause re-entry of compounds into enterohepatic recycling at a high concentration and secondary peak after the specific time intervals. Hydrolysis of conjugates in the intestine is another factor responsible for enterohepatic recycling of compounds (77). There are interspecies differences with  $\beta$ -glucuronidase activities between the upper and distal small intestines of humans and rodents. The estimated  $\beta$ -glucuronidase activities in the

proximal and distal small intestine of humans are considerably lower in humans than those in rats and mice (78). Species differences with fluid capacities, pH, bile flow, and pancreatic juice in various sections of the GI tract are other components affecting dissolutions, solubility, transit times, and membrane transport of compounds, which can cause variations in oral drug absorption (78, 79) and eventually enterohepatic recycling in humans and animals. Moreover, biotransformation of CZ48 to CPT was more rapid in humans than that in mice (25), which may be another potential factor for the differences of enterohepatic recycling among different species.

## **5.6 Development of a Population PK Model**

A population PK model was used to estimate PK parameters that describe plasma concentrations of CZ48 and CPT and biliary excretion of CPT after an oral dose of CZ48-CoS or CZ48-NS. There are previous reports developing a population PK model to describe biliary excretion and enterohepatic recycling of drugs. A population PK model was constructed to describe enterohepatic recycling of mycophenolate mofetil using clinical plasma data (80) and enterohepatic recycling of diclofenac and rofecoxib in rats (81). In another study, PK models were established to describe plasma concentration-time profiles of pyrrole-imidazole polyamides 1035 and 1666 using their urinary and biliary excretion data (82). This

study is unique because urinary and biliary excretion data were used to construct PK models to predict plasma concentration-time profiles, especially when plasma or serum concentrations of the compounds are under LLOQ after analysis. In addition, there is a study establishing a PK model to compare plasma concentrations of docetaxel and to predict its biliary metabolites when a dose was given by a nanoscale micellar docetaxel prodrug or commercial docetaxel formulation, Taxotere (83).

In our study, the PK parameters, such as clearances, volume of distribution values, and rate constants indicating biliary excretion, were estimated by using *in vivo* data collected from both plasma and bile. The model was used to evaluate the effect of NS on the PK of CZ48 and CPT. Based on *in vivo* data, the concentration of CPT in bile was remarkably higher than that in plasma. Moreover, biliary excretion is generally associated with activities of various transporters, which may cause competitive binding of drugs to transporters and saturation of the transporter-mediated biliary excretion process. Thus, the biliary excretion of CPT was considered to be a nonlinear saturable process when developing the PK model. Although *in vivo* data supported minor enterohepatic recycling of CZ48 and CPT, our PK model was more adequately described when adopting compartments for

the recycling of CZ48 and CPT that may explain the sustained concentrations of CZ48 and CPT in plasma after an oral dose of CZ48-CoS or CZ48-NS.

Diagnostic goodness of fit plots and CV % of estimates were used to assess the model fit when optimizing a population PK model. The scatterplots of DV versus IPRED and DV versus PRED were used to compare observed values with corresponding individual predicted and population predicted values, respectively. In the CoS group, the scatterplots showed good correspondences between observed and predicted values for CZ48 concentrations in plasma and CPT concentrations in bile. Most predicted values were identical to observed values and they fell on slopes in the scatterplots. CPT concentrations in plasma exhibited over-estimation for some data points. The model showed good fitting in the NS group as in the CoS group. The DV versus IPRED and DV versus PRED scatterplots exhibited good correspondences between observed and predicted values, and most data points were distributed around CWRES=0 at different time points.

When comparing the estimated PK parameters between CoS and NS groups, the absorption rate constant of CZ48 to its central compartment ( $K_a$ ) was greater in the CoS group than that in the NS group, which may indicate the sustained release

of CZ48 into the systemic circulation by NS. Total clearance of CZ48 ( $CL_{CZ48}$ ) that contains all elimination pathways, such as bile, urine, feces, and metabolism, was higher in the NS group. On the other hand, total clearance of CPT ( $CL_{CPT}$ ) excluding biliary excretion was lower in the NS group. These may indicate increased extent of biliary excretions of CZ48 and CPT by NS. The conversion rate constant (hydrolysis) from CZ48 to CPT ( $K_{hyd}$ ) was comparable between CoS and NS groups, which may depict that there was no significant depot effect by NS in the liver. If CZ48-NS was accumulated in the liver as a depot for a prolonged time, the hydrolysis of CZ48 to CPT was expected to delay, yielding a slower hydrolysis rate constant. The rate constant representing hydrolysis of CZ48 was comparable between the two formulation groups. Nonlinear kinetic values ( $V_m$  and  $K_m$ ) for biliary secretion of CPT were comparable between the two formulation groups. However, the rate constant of CPT from its bile compartment to the compartment representing enterohepatic recycling (responsible for sustained CPT concentrations) was remarkably greater in the NS group, which might imply potential impact of NS on enterohepatic recycling of CPT due to a prolonged exposure of CPT as a consequence of the sustained release of CZ48 from NS.

The population PK model was validated by bootstrapping and VPC approaches. With the bootstrapping technique, 145-200 bootstrap replicates were re-sampled

from the original data, and median and 95 % intervals of the bootstrap replicates were obtained. The final population estimates and bootstrap median values of replicates were similar, and those estimates were within 95 % intervals for the CoS and NS groups. The 95 % intervals of bootstrap estimates for  $CL_{CZ48}$  in the CoS and NS groups and  $CL_{CPT}$  in the NS group included zero. One potential reason might be due to interindividual variability in bootstrap estimates for those clearance parameters. Large standard errors of bootstrap clearance estimates were observed with high CV % (> 179 %). In this population PK model, population PK parameters were predicted using small original sample size (n=6 and n=3 for the CoS and NS groups, respectively), but the model was relatively complicated including five compartments to describe PK of CZ48 and CPT, biliary excretion of CPT, and compartments responsible for sustained concentrations of CZ48 and CPT in plasma and bile. Larger size of original data may improve the predictability of population PK parameters and provide a more reliable validation for clearance estimates of CZ48 and CPT using the bootstrap technique. To avoid negative predictive values for  $CL_{CZ48}$  and  $CL_{CPT}$ , changes in the types of residual error or initial estimates of error values for the compartments associated with  $CL_{CZ48}$  and  $CL_{CPT}$  may improve the prediction of those parameters. With the VPC procedure, 90 % prediction intervals from 1,000 simulated concentrations and observed concentration values were presented in the VPC plots. Most observed data were within 90 % prediction intervals. For CPT concentrations in bile of the CoS and NS

groups, the observed data were in a narrow range within the prediction intervals (close to 5 % percentile predicted line), which might result in the overestimation of some estimates in the population PK model.

## Chapter 6. Summary

### 6.1 Biodistributions of CZ48 and CPT in Tumor-Xenografted Mice

The Biodistribution pattern of CZ48 was different between CoS and NS groups in tumor-xenografted mice. CZ48 was highly distributed in the lung in the CoS group, and in the liver, spleen, and lung in the NS group. The highest exposure of CPT was observed in the liver and the lowest exposure was observed in the brain. The extent of CPT exposure in tumor was comparable with those in kidney, spleen, and lung. NS significantly increased the exposure of CZ48 in the RES organs, liver and spleen. In other tested organs, the biodistribution patterns of CZ48 and CPT were significantly decreased in NS groups. Half-lives of CZ48 and CPT were significantly decreased in NS groups. Half-lives of CZ48 and CPT were approximately 1.5 – 3.6 times increased in all tested organs and tumor. The prolonged exposure of CPT will be a merit of NS for its antitumor activity as a topoisomerase 1 enzyme inhibitor.

The biodistribution patterns of CZ48 and CPT were similar between healthy and tumor-xenografted mice except in lung. NS increased the exposure of CZ48 in the liver and spleen in both mouse models. The exposure of CZ48 was highly increased by NS in the lung of healthy mice, but decreased in tumor-xenografted mice. The exposure of CPT was the highest in the liver and lowest in the brain.

The extent of CPT exposures was comparable in kidney, spleen, and lung between two models. Half-lives of CZ48 and CPT were extended by NS in all tested organs, approximately 1.8 – 19.1 times in healthy mice and 1.5 – 3.6 times in tumor-xenografted mice.

## **6.2 Method Development and Validation Using UPLC-MS/MS**

Development of a reliable analytical method is a prerequisite to fully characterize the absorption, distribution, metabolism, and excretion of a drug in preclinical and clinical studies. In this study, a sensitive, accurate, and reproducible UPLC-MS/MS method was developed for simultaneous quantifications of CZ48 and CPT in rat plasma and bile. Especially, this is the first report developing an assay for the simultaneous analyses of CZ48 and CPT in bile. By employing the UPLC system, the method provides rapid sample analyses of CZ48 and CPT, 7 min, as compared to the HPLC system, 18 min (62). Sample extraction procedures for both plasma and bile were carefully developed to preserve the lactone stability of CPT during the extraction and analysis processes. In the previous method using HPLC, LLOQ values were 10 and 5 ng/ml for CZ48 and CPT, respectively, in mouse plasma (62). However, our method using UPLC-MS/MS provides higher sensitivity for both CZ48 and CPT, with the LLOQ values of 0.98 ng/ml for plasma and 3.9 ng/ml for bile samples. Extraction recoveries of CZ48 and CPT were over 90 and 85 % from

plasma and bile, respectively. No significant matrix effects were observed, within 14 and 16 % in plasma and bile, respectively.

### **6.3 Phase 1 and 2 Metabolisms of CPT**

Hepatic metabolism is one of the components related to enterohepatic recycling of a drug. In this study, phase 1 and 2 metabolisms of CPT were examined using *in vitro* system. The results did not show significant phase 1 metabolism of CPT. Also, there were no glucuronidation or sulfation reactions of CPT. Thus, hepatic metabolism of CPT may not significantly influence biliary excretions and enterohepatic recycling of CZ48 and CPT *in vivo*.

### **6.4 Biliary Excretions of CZ48 and CPT**

After an IV dose of CZ48-CoS, both CZ48 and CPT were secreted into the bile as their parent forms. Higher concentrations of CZ48 than CPT were observed at all time points in plasma. However, the amounts of CPT secreted in bile were remarkably higher than those of CZ48 at various time intervals. The percentages of the dose recovered in bile were approximately 0.19 and 3.05 % for CZ48 and CPT, respectively. Biliary clearance ( $CL_b$ ) of CPT was  $56.38 \pm 15.37$  ml/h, 64.8 times higher than that of CZ48,  $0.87 \pm 0.20$  ml/h. The concentration ratios of CPT

in bile to plasma (CPT-B/P) were 41.70 – 96.61, higher than those of CZ48 (CZ48-B/P), 0.16 – 1.36, at various time intervals. These results supported the more favorable biliary secretion of CPT than CZ48.

Similar to the results with IV administration of CZ48-CoS, biliary secretion of CPT was more favorable than that of CZ48 after an oral dose of CZ48-CoS. CPT-B/P were 150.24 – 259.41, higher than CZ48-B/P, 1.26 – 1.49. However, there was a distinct difference in plasma and bile profiles of CZ48 and CPT between IV and oral administrations of CZ48-CoS. After an oral dose, the sustained plasma concentrations and biliary secretions of CZ48 and CPT up to 12 hr were observed. On the contrary, the plasma concentrations and biliary secretions declined significantly 1 hr post IV dose.

To evaluate the impacts of NS on biliary excretions of CZ48 and CPT, plasma and bile profiles were established after an oral dose of CZ48-NS. The profiles showed similar trends exhibiting the sustained plasma concentrations and biliary secretions of CZ48 and CPT for 12 hr. The actual amounts of CZ48 and CPT observed in the bile were respectively comparable between CoS and NS groups. The AUC<sub>0-12h</sub> ratios of CZ48 (or CPT)-B/P were not significantly different between

the two formulation groups, which suggested that NS did not significantly impact the biliary excretions of CZ48 and CPT.

### **6.5 Enterohepatic Recycling of CZ48 and CPT**

The plasma concentration-time profiles and biliary excretions of CZ48 and CPT were compared to characterize the enterohepatic recycling with or without the interruption of their recycling in bile duct-cannulated and -intact rats, respectively. The plasma and bile profiles of CZ48 and CPT exhibited similar trends by showing sustained plasma concentrations and biliary secretions for 8 or 12 hr with or without the interruption of the recycling, respectively. The profiles of CZ48-B/P and CPT-B/P slightly declined between 2-4 hr post oral dose when the recycling was interrupted, but remained sustained at later time points. These results indicated that the enterohepatic recycling of CZ48 and CPT was a minor process in rats.

### **6.6 PK Model for Biliary Excretions and Enterohepatic Recycling of CZ48 and CPT**

A population PK model was employed to describe and characterize the multiple factors that affect the PK of CZ48 and CPT including (a) the hydrolysis of CZ48 to CPT after a CZ48 dosing, (b) sustained concentrations of CZ48 and CPT in plasma

concentration-time profiles after an oral administration, (c) the biliary excretions of CZ48 and CPT, and (d) the effect of NS on their PK. The developed PK model in this study contains two central compartments for CZ48 and CPT, respectively, one compartment for a nonlinear saturable biliary excretion of CPT, with total clearances of CZ48 and CPT, and two compartments for the enterohepatic recycling of CZ48 and CPT, respectively. The CV % of population estimates within 101 % and the scatterplots including DV versus IPRED, DV versus PRED, CWRES versus TAD, and QQ IWRES supported reliable prediction of the PK parameters of CZ48 and CPT using the model. Our population PK model described the sustained release of CZ48 from NS, comparable conversion rate constants of CZ48 to CPT by hydrolysis between CoS and NS groups, and similar nonlinear saturation biliary excretion of CPT between the formulation groups. The model was validated by employing bootstrapping and VPC approaches. Most population estimates were similar to bootstrap median values of 145-200 sample replicates for the CoS and NS group, and the estimates were within 95 % intervals. The VPC plots might indicate appropriate predictions for CZ48 in plasma in the CoS and NS groups. However, the plots might imply the overestimation of CPT concentrations in bile in the formulation groups.

Overall, this project has five significant findings:

First, the impacts of NS on the biodistribution patterns of CZ48 and CPT were investigated in human tumor-xenografted nude mice, and the prolonged exposure of CPT was achieved by the sustained release of CZ48 in all tested organs and tumor. Furthermore, the biodistribution patterns of CZ48 and CPT were similar between healthy and tumor-xenografted mice except in lung.

Second, the phase 1 and 2 metabolisms of CPT were evaluated using *in vitro* systems, and no significant metabolism reactions were observed. It suggested that the hepatic metabolism of CPT may not be a critical factor influencing the biliary excretions and enterohepatic recycling of CZ48 and CPT *in vivo*.

Third, biliary excretions of CZ48 and CPT were evaluated as an important factor affecting enterohepatic recycling. The evaluation was performed after a single CZ48 dose via two major dosing routes, oral and IV, and after a single CZ48 dose prepared in two different types of formulations, CoS and NS. This study suggested biliary excretion of CPT was increased when a dose was administered orally, but was not significantly increased by NS as compared to CoS.

Fourth, the enterohepatic recycling of CZ48 and CPT was characterized after an oral dose of CZ48-NS with or without interrupting the recycling system *in vivo*. The extent of enterohepatic recycling of CZ48 and CPT was minor in the preclinical rat model.

Fifth, a population PK model was developed and validated to describe PK characteristics of CZ48 and CPT, as well as biliary excretion of CPT, which provided the comparison of estimated PK parameters from an oral dose between CZ48-NS and CZ48-CoS.

## Reference

1. Liehr JG, Harris NJ, Mendoza J, Ahmed AE, Giovanella BC. Pharmacology of camptothecin esters. *Annals of the New York Academy of Sciences*. 2000;922(1):216-23.
2. Cao Z, Kozielski A, Vardeman D, Giovanella B. Sulfuric Acid Catalyzed Preparation of Alkyl and Alkenyl Camptothecin Ester Derivatives and Antitumor Activity against Human Xenografts Grown in Nude Mice. *Open Journal of Medicinal Chemistry*. 2012;2(1):10.
3. Wall ME, Wani MC. Camptothecin and taxol: discovery to clinic—thirteenth Bruce F. Cain Memorial Award Lecture. *Cancer research*. 1995;55(4):753-60.
4. Creaven P, Allen L. Renal clearance of camptothecin (NSC-100880): effect of urine volume. *Cancer chemotherapy reports*. 1973;57(2):175-84.
5. Gottlieb JA, Guarino AM, Call JB, Oliverio VT, Block JB. Preliminary pharmacologic and clinical evaluation of camptothecin sodium (NSC-100880). *Cancer chemotherapy reports*. 1970;54(6):461.
6. Fassberg J, Stella VJ. A kinetic and mechanistic study of the hydrolysis of camptothecin and some analogues. *Journal of pharmaceutical sciences*. 1992;81(7):676-84.
7. Giovanella BC, Hinz HR, Kozielski AJ, Stehlin JS, Silber R, Potmesil M. Complete growth inhibition of human cancer xenografts in nude mice by treatment with 20-(S)-camptothecin. *Cancer Research*. 1991;51(11):3052-5.
8. van Warmerdam LJ, Creemers G-J, Rodenhuis S, Rosing H, de Boer-Dennert M, Schellens JH, et al. Pharmacokinetics and pharmacodynamics of topotecan given on a daily-times-five schedule in phase II clinical trials using a limited-sampling procedure. *Cancer chemotherapy and pharmacology*. 1996;38(3):254-60.
9. Garcia-Carbonero R, Supko JG. Current perspectives on the clinical experience, pharmacology, and continued development of the camptothecins. *Clinical Cancer Research*. 2002;8(3):641-61.

10. van Warmerdam LJ, Verweij J, Schellens JH, Rosing H, Davies BE, de Boer-Dennert M, et al. Pharmacokinetics and pharmacodynamics of topotecan administered daily for 5 days every 3 weeks. *Cancer chemotherapy and pharmacology*. 1995;35(3):237-45.
11. Wall JG, Burris III HA, Von Hoff DD, Rodriguez G, Kneuper-Hall R, Shaffer D, et al. A phase I clinical and pharmacokinetic study of the topoisomerase I inhibitor topotecan (SK&F 104864) given as an intravenous bolus every 21 days. *Anti-cancer drugs*. 1992;3(4):337-46.
12. Rosing H, van Zomeren DM, Doyle E, Bult A, Beijnen JH. O-glucuronidation, a newly identified metabolic pathway for topotecan and N-desmethyl topotecan. *Anti-cancer drugs*. 1998;9(7):587-92.
13. Schellens J, Creemers G, Beijnen J, Rosing H, de Boer-Dennert M, McDonald M, et al. Bioavailability and pharmacokinetics of oral topotecan: a new topoisomerase I inhibitor. *British journal of cancer*. 1996;73(10):1268.
14. Herben V, Rosing H, ten Bokkel Huinink W, Van Zomeren D, Batchelor D, Doyle E, et al. Oral topotecan: bioavailability and effect of food co-administration. *British journal of cancer*. 1999;80(9):1380.
15. Ormrod D, Spencer CM. Topotecan. *Drugs*. 1999;58(3):533-51.
16. Rothenberg ML, Kuhn JG, Burris 3rd H, Nelson J, Eckardt JR, Tristan-Morales M, et al. Phase I and pharmacokinetic trial of weekly CPT-11. *Journal of Clinical Oncology*. 1993;11(11):2194-204.
17. Rothenberg ML, Cox JV, DeVore RF, Hainsworth JD, Pazdur R, Rivkin SE, et al. A multicenter, Phase II trial of weekly irinotecan (CPT-11) in patients with previously treated colorectal carcinoma. *Cancer*. 1999;85(4):786-95.
18. Rougier P, Bugat R, Douillard J, Culine S, Suc E, Brunet P, et al. Phase II study of irinotecan in the treatment of advanced colorectal cancer in chemotherapy-naive patients and patients pretreated with fluorouracil-based chemotherapy. *Journal of Clinical Oncology*. 1997;15(1):251-60.
19. Hsiang Y-H, Hertzberg R, Hecht S, Liu L. Camptothecin induces protein-linked DNA breaks via mammalian DNA topoisomerase I. *Journal of Biological Chemistry*. 1985;260(27):14873-8.

20. Hsiang Y-H, Liu LF. Identification of mammalian DNA topoisomerase I as an intracellular target of the anticancer drug camptothecin. *Cancer research*. 1988;48(7):1722-6.
21. Svejstrup JQ, Christiansen K, Gromova II, Andersen AH, Westergaard O. New technique for uncoupling the cleavage and religation reactions of Eukaryotic Topoisomerase I.: The mode of action of camptothecin at a specific recognition site. *Journal of molecular biology*. 1991;222(3):669-78.
22. Liu LF, Desai SD, LI TK, Mao Y, Sun M, SIM SP. Mechanism of action of camptothecin. *Annals of the New York Academy of Sciences*. 2000;922(1):1-10.
23. Liu X, Wang Y, Cao Z, Zhan M, Vardeman D, Giovanella B. Enhanced Lactone Stability of CZ48 in Blood Correlates to its Lack of Toxicity in Mice. *Journal of Pharmacy & Pharmaceutical Sciences*. 2013;16(1):115-24.
24. Cao Z, Kozielski A, Liu X, Wang Y, Vardeman D, Giovanella B. Crystalline camptothecin-20 (S)-O-propionate hydrate: A novel anticancer agent with strong activity against 19 human tumor xenografts. *Cancer research*. 2009;69(11):4742-9.
25. Liu X, DeJesus A, Cao Z, Vardeman D, Giovanella B. Metabolic difference of CZ48 in human and mouse liver microsomes. *International journal of molecular sciences*. 2012;13(5):5498-505.
26. Zhang M. Study on the fabrication of CZ48 loaded cerasomes and its freeze-drying technology [Thesis]: Northeast Forestry University, China; 2016.
27. Müller R, Jacobs C, Kayser O. Nanosuspensions as particulate drug formulations in therapy: rationale for development and what we can expect for the future. *Advanced drug delivery reviews*. 2001;47(1):3-19.
28. Patravale V, Kulkarni R. Nanosuspensions: a promising drug delivery strategy. *Journal of pharmacy and pharmacology*. 2004;56(7):827-40.
29. Dong D. Sustained delivery of CZ48, a lactone-stabilized camptothecin, by nanosuspensions [Dissertation]: University of Houston; 2012.

30. Gerrits C, De Jonge M, Schellens J, Stoter G, Verweij J. Topoisomerase I inhibitors: the relevance of prolonged exposure for present clinical development. *British journal of cancer*. 1997;76(7):952.
31. Yang S, Zhu J, Lu Y, Liang B, Yang C. Body distribution of camptothecin solid lipid nanoparticles after oral administration. *Pharmaceutical research*. 1999;16(5):751-7.
32. Min KH, Park K, Kim Y-S, Bae SM, Lee S, Jo HG, et al. Hydrophobically modified glycol chitosan nanoparticles-encapsulated camptothecin enhance the drug stability and tumor targeting in cancer therapy. *Journal of Controlled Release*. 2008;127(3):208-18.
33. Çirpanli Y, Bilensoy E, Doğan AL, Çalış S. Comparative evaluation of polymeric and amphiphilic cyclodextrin nanoparticles for effective camptothecin delivery. *European Journal of Pharmaceutics and Biopharmaceutics*. 2009;73(1):82-9.
34. Roberts MS, Magnusson BM, Burczynski FJ, Weiss M. Enterohepatic circulation. *Clinical pharmacokinetics*. 2002;41(10):751-90.
35. Li X. Comparative preclinical pharmacokinetics of CZ48, lactone-stabilized camptothecin, and camptothecin in rats and potential routes of administration for therapy [Dissertation]: University of Houston; 2004.
36. Malik MY, Jaiswal S, Sharma A, Shukla M, Lal J. Role of enterohepatic recirculation in drug disposition: cooperation and complications. *Drug Metab Rev*. 2016;48(2):281-327.
37. Charman WN, Porter CJ, Mithani S, Dressman JB. Physicochemical and physiological mechanisms for the effects of food on drug absorption: the role of lipids and pH. *Journal of pharmaceutical sciences*. 1997;86(3):269-82.
38. Ilett KF, Tee LB, Reeves PT, Minchin RF. Metabolism of drugs and other xenobiotics in the gut lumen and wall. *Pharmacology & therapeutics*. 1990;46(1):67-93.
39. Gao Y, Shao J, Jiang Z, Chen J, Gu S, Yu S, et al. Drug enterohepatic circulation and disposition: constituents of systems pharmacokinetics. *Drug discovery today*. 2014;19(3):326-40.

40. Levine WG. Biliary excretion of drugs and other xenobiotics. Annual review of pharmacology and toxicology. 1978;18(1):81-96.
41. Lecureur V, Courtois A, Payen L, Verhnet L, Guillouzo A, Fardel O. Expression and regulation of hepatic drug and bile acid transporters. Toxicology. 2000;153(1):203-19.
42. Tirona RG, Tan E, Meier G, Pang KS. Uptake and glutathione conjugation of ethacrynic acid and efflux of the glutathione adduct by periportal and perivenous rat hepatocytes. Journal of Pharmacology and Experimental Therapeutics. 1999;291(3):1210-9.
43. Sugiyama Y, Kato Y, Chu X-y. Multiplicity of biliary excretion mechanisms for the camptothecin derivative irinotecan (CPT-11), its metabolite SN-38, and its glucuronide: role of canalicular multispecific organic anion transporter and P-glycoprotein. Cancer chemotherapy and pharmacology. 1998;42:S44-S9.
44. Chu X-Y, Kato Y, Ueda K, Suzuki H, Niinuma K, Tyson CA, et al. Biliary excretion mechanism of CPT-11 and its metabolites in humans: involvement of primary active transporters. Cancer research. 1998;58(22):5137-43.
45. Köck K, Brouwer K. A perspective on efflux transport proteins in the liver. Clinical Pharmacology & Therapeutics. 2012;92(5):599-612.
46. Suzuki H, Sugiyama Y, editors. Transport of drugs across the hepatic sinusoidal membrane: sinusoidal drug influx and efflux in the liver. Seminars in liver disease; 2000: Copyright© 2000 by Thieme Medical Publishers, Inc., 333 Seventh Avenue, New York, NY 10001, USA. Tel.:+ 1 (212) 584-4662.
47. Chandra P, Brouwer KL. The complexities of hepatic drug transport: current knowledge and emerging concepts. Pharmaceutical research. 2004;21(5):719-35.
48. Li K, Tang Y, Fawcett JP, Gu J, Zhong D. Characterization of the pharmacokinetics of dioscin in rat. Steroids. 2005;70(8):525-30.
49. Zhang D, Frost CE, He K, Rodrigues AD, Wang X, Wang L, et al. Investigating the enteroenteric recirculation of apixaban, a factor Xa inhibitor: administration of activated charcoal to bile duct-cannulated rats

and dogs receiving an intravenous dose and use of drug transporter knockout rats. *Drug Metabolism and Disposition*. 2013;dmd. 112.050575.

50. Brewster D, Jones RS, Symons AM. Effects of neomycin on the biliary excretion and enterohepatic circulation of mestranol and 17 $\beta$ -oestradiol. *Biochemical pharmacology*. 1977;26(10):943-6.
51. Marier J-F, Vachon P, Gritsas A, Zhang J, Moreau J-P, Ducharme MP. Metabolism and disposition of resveratrol in rats: extent of absorption, glucuronidation, and enterohepatic recirculation evidenced by a linked-rat model. *Journal of Pharmacology and Experimental Therapeutics*. 2002;302(1):369-73.
52. Xing J, Chen X, Zhong D. Absorption and enterohepatic circulation of baicalin in rats. *Life Sci*. 2005;78(2):140-6.
53. Chen YJ, Huang SM, Liu CY, Yeh PH, Tsai TH. Hepatobiliary excretion and enterohepatic circulation of colchicine in rats. *Int J Pharm*. 2008;350(1-2):230-9.
54. Deng J, Zhuang X, Shen G, Li H, Gong Z. Biliary excretion and enterohepatic circulation of thienorphine and its glucuronide conjugate in rats. *Acta Pharmaceutica Sinica B*. 2012;2(2):174-80.
55. Ouellet D, Pollack GM. Biliary excretion and enterohepatic recirculation of morphine-3-glucuronide in rats. *Drug metabolism and disposition*. 1995;23(4):478-84.
56. Kuchimanchi KR, Udata C, Johnston TP, Mitra AK. Pharmacokinetics, biliary excretion, and tissue distribution of novel anti-HIV agents, cosalane and dihydrocosalane, in Sprague-Dawley rats. *Drug metabolism and disposition*. 2000;28(4):403-8.
57. Kocbek P, Baumgartner S, Kristl J. Preparation and evaluation of nanosuspensions for enhancing the dissolution of poorly soluble drugs. *International journal of pharmaceutics*. 2006;312(1):179-86.
58. Bailer AJ. Testing for the equality of area under the curves when using destructive measurement techniques. *Journal of pharmacokinetics and biopharmaceutics*. 1988;16(3):303-9.

59. Ackley DC, Rockich KT, Baker TR. Metabolic stability assessed by liver microsomes and hepatocytes. Optimization in Drug Discovery: In Vitro Methods. 2004:151-62.
60. Yang Z, Zhu W, Gao S, Yin T, Jiang W, Hu M. Breast cancer resistance protein (ABCG2) determines distribution of genistein phase II metabolites: reevaluation of the roles of ABCG2 in the disposition of genistein. Drug Metabolism and Disposition. 2012;40(10):1883-93.
61. Guidance for Industry Bioanalytical Method Validation, U.S. Department of Health and Human Services Food and Drug Administration Center for Drug Evaluation and Research (CDER) Center for Veterinary Medicine (CVM), 2013, <https://www.fda.gov/downloads/drugs/guidances/ucm368107.pdf>.
62. Liu X, Wang Y, Vardeman D, Cao Z, Giovanella B. Development and validation of a reverse-phase HPLC with fluorescence detector method for simultaneous determination of CZ48 and its active metabolite camptothecin in mouse plasma. Journal of Chromatography B. 2008;867(1):84-9.
63. Cao Z, Fantazis P, Mendoza J, Early J, Kozielski A, Harris N, et al. Structure-Activity Relationship of Alkyl Camptothecin Esters. Annals of the New York Academy of Sciences. 2000;922(1):122-35.
64. Kelland LR. Of mice and men: values and liabilities of the athymic nude mouse model in anticancer drug development. Eur J Cancer. 2004;40(6):827-36.
65. Peterson JK, Houghton PJ. Integrating pharmacology and in vivo cancer models in preclinical and clinical drug development. Eur J Cancer. 2004;40(6):837-44.
66. Hollingshead MG. Antitumor efficacy testing in rodents. J Natl Cancer Inst. 2008;100(21):1500-10.
67. Wong H, Choo EF, Alicke B, Ding X, La H, McNamara E, et al. Anti-tumor activity of targeted and cytotoxic agents in murine subcutaneous tumor models correlates with clinical response. Clinical Cancer Research. 2012:clincanres. 0738.2012.

68. De Jong M, Maina T. Of mice and humans: are they the same?— Implications in cancer translational research. *Journal of Nuclear Medicine*. 2010;51(4):501-4.
69. Johnson J, Decker S, Zaharevitz D, Rubinstein L, Venditti J, Schepartz S, et al. Relationships between drug activity in NCI preclinical in vitro and in vivo models and early clinical trials. *British journal of cancer*. 2001;84(10):1424.
70. Sugawara M, Okamoto K, Kadowaki T, Kusano K, Fukamizu A, Yoshimura T. Expressions of cytochrome P450, UDP-glucuronosyltransferase, and transporter genes in monolayer carcinoma cells change in subcutaneous tumors grown as xenografts in immunodeficient nude mice. *Drug Metab Dispos*. 2010;38(3):526-33.
71. Platzer P, Thalhammer T, Hamilton G, Ulsperger E, Rosenberg E, Wissiack R, et al. Metabolism of camptothecin, a potent topoisomerase I inhibitor, in the isolated perfused rat liver. *Cancer chemotherapy and pharmacology*. 2000;45(1):50-4.
72. Lalloo AK, Luo FR, Guo A, Paranjpe PV, Lee S-H, Vyas V, et al. Membrane transport of camptothecin: facilitation by human P-glycoprotein (ABCB1) and multidrug resistance protein 2 (ABCC2). *BMC medicine*. 2004;2(1):16.
73. Tian X, Li J, Zamek-Gliszczynski MJ, Bridges AS, Zhang P, Patel NJ, et al. Roles of P-glycoprotein, Bcrp, and Mrp2 in biliary excretion of spiramycin in mice. *Antimicrobial agents and chemotherapy*. 2007;51(9):3230-4.
74. Scott DO, Bindra DS, Sutton SC, Stella VJ. Urinary and biliary disposition of the lactone and carboxylate forms of 20 (S)-camptothecin in rats. *Drug metabolism and disposition*. 1994;22(3):438-42.
75. Davies NM, Takemoto JK, Brocks DR, Yáñez JA. Multiple peaking phenomena in pharmacokinetic disposition. *Clinical pharmacokinetics*. 2010;49(6):351-77.
76. Faure L, Vignand P, Raynard A, Pasello-Legrand F, Descotes J. Evaluation of a surgical procedure to measure drug biliary excretion of rats in regulatory safety studies. *Fundamental & clinical pharmacology*. 2006;20(6):587-93.

77. Scheline RR. Metabolism of foreign compounds by gastrointestinal microorganisms. *Pharmacological reviews*. 1973;25(4):451-523.
78. Kararli TT. Comparison of the gastrointestinal anatomy, physiology, and biochemistry of humans and commonly used laboratory animals. *Biopharmaceutics & drug disposition*. 1995;16(5):351-80.
79. McConnell EL, Basit AW, Murdan S. Measurements of rat and mouse gastrointestinal pH, fluid and lymphoid tissue, and implications for in-vivo experiments. *J Pharm Pharmacol*. 2008;60(1):63-70.
80. FUNAKI T. Enterohepatic circulation model for population pharmacokinetic analysis. *Journal of pharmacy and pharmacology*. 1999;51(10):1143-8.
81. Huntjens D, Strougo A, Chain A, Metcalf A, Summerfield S, Spalding D, et al. Population pharmacokinetic modelling of the enterohepatic recirculation of diclofenac and rofecoxib in rats. *British journal of pharmacology*. 2008;153(5):1072-84.
82. Nagashima T, Aoyama T, Yokoe T, Fukasawa A, Fukuda N, Ueno T, et al. Pharmacokinetic modeling and prediction of plasma pyrrole-imidazole polyamide concentration in rats using simultaneous urinary and biliary excretion data. *Biological and Pharmaceutical Bulletin*. 2009;32(5):921-7.
83. Stern ST, Zou P, Skoczen S, Xie S, Liboiron B, Harasym T, et al. Prediction of nanoparticle prodrug metabolism by pharmacokinetic modeling of biliary excretion. *Journal of controlled release*. 2013;172(2):558-67.